Pharmacology and Pore-Forming Domains of the Cystic Fibrosis Transmembrane Conductance Regulator

Thesis by

Stefan I. McDonough

In Partial Fulfillment of the Requirements for

the Degree of Doctor of Philosophy

California Institute of Technology

Pasadena, California

1994

(Submitted May 24, 1994)

Acknowledgments

I thank my thesis committee, professors Lester, Davidson, Kennedy, Laurent, and Revel, especially GL for vicious, cathartic squash games;

Special thanks to the wonderful postdocs of the Lester Lab, who always took the time to teach me and to joke around, especially Nancy Lim, Bruce Cohen, Xian-Cheng Yang, and Nael McCarty;

Thanks to Bruce and Xian-Cheng for teaching me electrophysiology, and to Nael for teaching me molecular biology;

Thanks to Henry Lester, for three-plus years of support, grace, and gentle good humor (often in the face of undeserved teasing), and for his initial rescue of me from the Applied Physics department;

Most of all, thanks to Nael. We worked together very closely and efficiently, learned a lot from each other, and laughed our heads off into the bargain.

Thesis harmful if swallowed. If ingested, induce vomiting and call a physician.

Abstract

The cystic fibrosis transmembrane conductance regulator (CFTR) is a chloride channel member of the ATP-binding cassette (ABC) superfamily of membrane proteins. CFTR has two homologous halves, each consisting of six transmembrane spanning domains (TM) followed by a nucleotide binding fold, connected by a regulatory (R) domain. This thesis addresses the question of which domains are responsible for Cl^- selectivity, i.e., which domains line the channel pore.

To address this question, novel blockers of CFTR were characterized. CFTR was heterologously expressed in Xenopus oocytes to study the mechanism of block by two closely related arylaminobenzoates, diphenylamine-2-carboxylic acid (DPC) and flufenamic acid (FFA). Block by both is voltage-dependent, with a binding site $\approx$ 40% through the electric field of the membrane. DPC and FFA can both reach their binding site from either side of the membrane to produce a flickering block of CFTR single channels. In addition, DPC block is influenced by Cl^- concentration, and DPC blocks with a bimolecular forward binding rate and a unimolecular dissociation rate. Therefore, DPC and FFA are open-channel blockers of CFTR, and a residue of CFTR whose mutation affects their binding must line the pore.

Screening of site-directed mutants for altered DPC binding affinity reveals that TM-6 and TM-12 line the pore. Mutation of residue S341 in TM-6 abolishes most DPC block, greatly reduces single-channel conductance, and

alters the direction of current rectification. Additional residues are found in TM-6 (K335) and TM-12 (T1134) whose mutations weaken or strengthen DPC block; other mutations move the DPC binding site from TM-6 to TM-12. The strengthened block and lower conductance due to mutation T1134F is quantitated at the single-channel level. The geometry of DPC and of the residues mutated suggest α-helical structures for TM-6 and TM-12. Evidence is presented that the effects of the mutations are due to direct side-chain interaction, and not to allosteric effects propagated through the protein. Mutations are also made in TM-11, including mutation S1118F, which gives voltage-dependent current relaxations. The results may guide future studies on permeation through ABC transporters and through other Cl^- channels.

Table of Contents

Introduction

Background

Cystic fibrosis is the most common lethal inherited disease among Caucasian populations. The carrier frequency is approximately one out of twenty. Clinical manifestations of CF include salty skin, pancreatic insufficiency, infertility, and the accumulation of thick mucus in respiratory tracts (Boat et al., 1989). Mortality is usually due to bacterial infection of the respiratory mucus. The various symptoms of cystic fibrosis were first recognized as a unified syndrome in the 1930s, although European folklore from as early as the seventeenth century associates salty skin with premature death (Taussig, 1984).

Work in the early 1980s linked cystic fibrosis to defects in epithelial chloride permeability. First, in vivo experiments found an abnormally hyperpolarized transepithelial potential difference of nasal respiratory tissue in patients with cystic fibrosis as compared to controls (Knowles et al., 1981). Soon afterward, this abnormal hyperpolarization was also observed in sweat glands and was traced to a defect in Cl^-, rather than sodium, permeability (Quinton, 1983; Quinton and Bijman, 1983). Single-channel physiology identified several Cl^- channels prominent in secretory epithelia. Most work focused on an outwardly-rectifying Cl- channel (ORCC) abundant in both normal and cystic fibrosis epithelia. The activation of this channel by the protein kinase A pathway was found defective in cystic fibrosis epithelia

(Welsh and Liedtke, 1986; Welsh, 1986; Frizzell et al., 1986). Most concluded that the gene defective in cystic fibrosis was either this Cl^- channel or a controller of Cl^- channels in epithelial cells.

In 1989, the gene defective in cystic fibrosis was cloned (Riordan et al., 1989; Rommens et al., 1989). Surprisingly, the gene product was not homologous to known ion channels, but was identified as a member of the ATP-binding cassette (ABC) superfamily. The gene product was named the cystic fibrosis transmembrane conductance regulator, or CFTR. From the primary sequence, CFTR was predicted to have two homologous halves, each consisting of six transmembrane domains followed by a consensus ATP-binding motif. The two halves are connected by a highly charged regulatory ("R") domain, a domain also containing multiple consensus protein kinase A and C phosphorylation sites (see chapter 3, figure 1). The CFTR expression pattern agreed with expectations: it was localized to the apical membrane of secretory epithelial cells (Denning et al., 1992; Crawford et al., 1991). CFTR has also been found in pancreatic ducts and intestinal tract, and in reproductive tissue (Trezise et al., 1992). CFTR also exists in cardiac tissue, likely as an alternatively-spliced isoform (Horowitz et al., 1993; Nagel et al., 1992).

Approximately 70% of cystic fibrosis mutations are due to the deletion of a single phenylalanine residue in the first nucleotide binding fold (Riordan, 1993); it was later found that the CFTRΔF508 protein fails to reach the apical membrane in mammalian cells (Cheng et al., 1990). Heterologous expression of

wildtype CFTR, but not CFTRΔF508, in cystic fibrosis cells corrects the defect in Cl^- permeability (Rich et al., 1990). The question remained, however, whether CFTR was a Cl^- channel or a regulator of other Cl^- channels.

Since the cloning of CFTR, many experiments have shown unequivocally that the CFTR gene product is itself a Cl^- channel. Expression of CFTR in a variety of cell types results in a channel different from that initially expected, a low conductance ($\approx$ 10 picosiemens) Cl^- channel with a linear current-voltage relation (Tabcharani et al., 1991; Kartner et al., 1991). A channel with the same properties is found in untransfected, cultured epithelial cell lines (Tabcharani et al., 1990). Point mutations of charged residues in CFTR give slight changes in anion selectivity (Anderson et al., 1991). Most significantly, when purified and reconstituted in lipid bilayers, CFTR forms a Cl^- channel with conductance, kinetics, and regulation identical to those described in expression studies (Bear et al., 1992). For a comprehensive review of CFTR, see Riordan, 1993.

Although CFTR forms a Cl^- channel, its topology, homologous not to other channels but to the ABC superfamily, presents a major paradox. Many members of the ABC superfamily proteins form ATP-dependent transporters that pump diverse organic substrates. One such member is MDR, the multidrug resistance P-glycoprotein, which hydrolyzes ATP to pump hydrophobic drugs out of a variety of tumor cells. Another ABC superfamily member is the dimeric peptide transporter, with subunits TAP-1 and TAP-2, which pumps cytoplasmically produced antigen fragments into the

endoplasmic reticulum for association with the gene products of the major histocompatability locus. Other ABC transporters include the bacterial histidine permease, the yeast **a** mating factor transporter, and the genes whose mutations cause Zellweger syndrome or adrenoleukodystrophy. For a review of the ABC superfamily, see Higgins, 1992.

Goals

The goal of this research is to localize the permeation pathway of CFTR. Put another way, the goal is to determine what residues line the pore of CFTR, and thus how CFTR can function as a Cl^- channel. Defining the pore-lining domains responsible for Cl^- selectivity would (1) have bearing on the mechanisms for substrate specificity of other ABC transporters, with corresponding medical implications for cancer treatment, immunological specificity, and diabetes, among other diseases; and (2) guide future structure-function and biophysical work on other cloned Cl^- channels, a field that has lagged far behind cation channels.

The strategy to localize the permeation pathway of CFTR involved the discovery and characterization of blockers of CFTR, itself a novel conclusion. In brief, the strategy involved: (1) developing an open-channel blocker of CFTR; and (2) using site-directed mutagenesis to find residues that, when mutated, alter or abolish the open-channel block. Such residues must line the pore.

Chapter one is a review of structure-function work done to date on ion channels, and it places the following work on CFTR into context. Chapter two is devoted to the expression of CFTR channels in *Xenopus* oocytes and the characterization of two closely related blockers of CFTR, diphenylamine-2-carboxylic acid (DPC) and flufenamic acid (FFA). Chapter three presents further proof of the mechanism of DPC block, describes the effects of site-directed mutagenesis of CFTR on DPC block, and presents the resulting concept of the channel pore. Chapter four describes further mutations.

Data Summary and Conclusions

(1) DPC is an open-channel blocker of CFTR. DPC block of CFTR is voltage-dependent, and at the single-channel level, DPC produces brief, flickery closures with voltage-dependence and kinetics consistent with whole-cell measurements. In addition, the DPC block is changed by reduced Cl^- concentration, evidence that DPC and Cl^- interact within the pore. Experiments done on a mutant CFTR with more resolvable kinetics show that the rate of DPC block increases linearly with DPC concentration, while the rate constant for unblocking is concentration-independent. This is in agreement with classical kinetic models for open-channel blockers. Moreover, mutations within putative transmembrane domains are found that weaken or strengthen DPC block, further evidence that DPC binds within the pore. *(2) Flufenamic acid is also an open-channel blocker of CFTR.* FFA is identical to DPC, but with the

addition of a single trifluoromethyl group. Its block is flickery, with the same voltage-dependence as that of DPC. Its on-rate is similar to that of DPC, yet its off-rate is lower, resulting in a residence time on the channel double that of DPC.

(3) Residues in transmembrane domains (TM) six and twelve line the pore. Residue serine 341, at a position in TM-6 corresponding to the electrical position of the DPC binding site, is vital for DPC binding and Cl^- permeation. Mutation of S341 to alanine eliminates most DPC block, reduces single-channel conductance almost tenfold, and alters rectification. Once the binding site in TM-6 is eliminated, however, it can be reconstructed in TM-12, showing that TM-12 also lines the pore. Another mutation in TM-12 (T1134F) strengthens the block, and another residue in TM-6 (K335) is found that affects block and rectification. The T1134F mutation also lowers single-channel conductance by $\approx$ 25%; single-channel measurements of block correlate quantitatively with whole-cell measurements. Other mutations have no effects; these and other arguments discount the possibility that the mutations are having allosteric effects. Analysis of the geometry of the DPC molecule and the residues mutated shows that *(4) Transmembrane domains six and twelve are* α*-helical,* at least in the span around the DPC binding site. In this respect, CFTR is like the members of the ligand-gated channel superfamily, and unlike K^+ channels.

The results described here are in accordance with work done on other ABC transporters, and with previous studies on CFTR and on other ion

channels. As discussed more fully in chapter 3, these results represent a step towards bridging the gap between transporters and channels.

M. P. Anderson, R. J. Gregory, S. Thompson, D. W. Souza, S. Paul, R. C. Mulligan, A. E. Smith and M. J. Welsh (1991): Demonstration that CFTR is a chloride channel by alteration of its anion selectivity. Science 253:202-205.

C. E. Bear, C. Li, N. Kartner, R. J. Bridges, T. J. Jensen, M. Ramjeesingh and J. R. Riordan (1992): Purification and functional reconstitution of the cystic fibrosis transmembrane conductance regulator (CFTR). Cell 68:809-818.

T. F. Boat, M. J. Welsh and A. L. Beaudet (1989): Cystic Fibrosis. In W. S. Sly and D. Valle, eds., The Metabolic Basis of Inherited Disease. New York: McGraw-Hill, pp 2649-2680.

S. H. Cheng, R. J. Gregory, J. Marshall, S. Paul, D. W. Souza, G. A. White, C. R. O'Riordan and A. E. Smith (1990): Defective intracellular transport and processing of CFTR is the molecular basis of most cystic fibrosis. Cell 63:827-834.

I. Crawford, P. C. Maloney, P. L. Zeitlin, W. B. Guggino, S. C. Hyde, H. Turley, K. C. Gatter, A. Harris and C. F. Higgins (1991): Immunocytochemical localization of the cystic fibrosis gene product CFTR. Proc. Natl. Acad. Sci. USA 88:9262-9266.

G. M. Denning, L. S. Ostedgaard, S. H. Cheng, A. E. Smith and M. J. Welsh (1992): Localization of cystic fibrosis transmembrane conductance regulator in chloride secretory epithelia. J. Clin. Invest. 89:339-349.

R. A. Frizzell, G. Rechkemmer and R. Shoemaker (1986): Altered regulation of airway epithelial cell chloride channels in cystic fibrosis. Science 233:558-560.

L. M. Greenberger (1993): Major photoaffinity drug labeling sites for iodoaryl azidoprazosin in P-glycoprotein are within, or immediately C-terminal to, transmembrane domains 6 and 12. J. Biol. Chem. 268, 11417-11425.

C. F. Higgins (1992): ABC transporters--from microorganisms to man. Annu. Rev. Cell Biol. 8:67-113.

B. Horowitz, S. S. Tsung, P. Hart, P. C. Levesque and J. R. Hume (1993): Alternative splicing of CFTR Cl channels in heart. Am. J. Physiol. 264:H2214-H2220.

N. Kartner, J. W. Hanrahan, T. J. Jensen, A. L. Naismith, S. Sun, C. A. Ackerly, E. F. Reyes, L.-C. Tsui, J. M. Rommens, C. E. Bear and J. R. Riordan (1991): Expression of the cystic fibrosis gene in non-epithelial invertebrate cells produces a regulated anion conductance. Cell 94:681-691.

M. Knowles, J. Gatzy and R. Boucher (1981): Increased bioelectric potential difference across respiratory epithelia in cystic fibrosis. N. Engl. J. Med. 305:1489-1495.

G. Nagel, T.-C. Hwang, K. L. Nastiuk, A. C. Nairn and D. C. Gadsby (1992): The protein kinase A-regulated cardiac Cl channel resembles the cystic fibrosis transmembrane conductance regulator. Nature 360:81-84.

P. M. Quinton (1983): Chloride impermeability in cystic fibrosis. Nature 301:421-422.

P. M. Quinton and J. Bijman (1983): Higher bioelectric potentials due to decreased chloride absorption in the sweat glands of patients with cystic fibrosis. N. Engl. J. Med. 308:1185-1189.

D. P. Rich, M. P. Anderson, R. J. Gregory, S. H. Cheng, S. Paul, D. M. Jefferson, J. D. McCann, K. W. Klinger, A. E. Smith and M. J. Welsh (1990): Expression of cystic fibrosis transmembrane conductance regulator corrects defective chloride channel regulation in cystic fibrosis airway epithelial cells. Nature 347:358-363.

J. R. Riordan (1993): The cystic fibrosis transmembrane conductance regulator.

Annu. Rev. Physiol. 55:609-630.

J. R. Riordan, J. M. Rommens, B. Kerem, N. Alon, R. Rozmahel, Z. Grzelczak, J. Zielenski, S. Lok, N. Plasvic, J.-L. Chou, M. L. Drumm, M. C. Iannuzzi, F. S. Collins and L.-C. Tsui (1989): Identification of the cystic fibrosis gene: Cloning and characterization of complementary DNA. Science 245:1066-1072.

J. M. Rommens, M. C. Iannuzzi, S. Kerem, M. L. Drumm, G. Melmer, M. Dean, R. Rozmahel, J. L. Cole, D. Kennedy, N. Hidaka, M. Zsiga, M. Buchwald, J. R. Riordan, L.-C. Tsui and F. S. Collins (1989): Identification of the cystic fibrosis gene: Chromosome walking and jumping. Science 245:1059-1065.

J. A. Tabcharani, X.-B. Chang, J. R. Riordan and J. W. Hanrahan (1991): Phosphorylation-regulated Cl channel in CHO cells stably expressing the cystic fibrosis gene. Nature 352:628-631.

J. A. Tabcharani, W. Low, D. Elie and J. W. Hanrahan (1990): Low-conductance chloride channel activated by cAMP in the epithelial cell line T84. FEBS 270:157-164.

L. M. Taussig (1984): Cystic fibrosis: an overview. In L. M. Taussig, ed., Cystic Fibrosis. New York, Thieme-Stratton, pp 1-9.

A. Trezise, P. R. Romano, D. R. Gill, S. C. Hyde, F. V. Sepulveda, M. Buchwald and C. F. Higgins (1992): The multidrug resistance and cystic fibrosis genes have complementary patterns of epithelial expression. EMBO J. 11:4291-4303.

M. J. Welsh (1986): An apical membrane chloride channel in human tracheal epithelium. Science 232:1648-1650.

M. J. Welsh and C. M. Liedtke (1986): Chloride and potassium channels in cystic fibrosis airway epithelia. Nature 322:467-470.

An Overview of the Relationship Between Structure and Function in Ion Channels

Stefan McDonough and Henry A. Lester

Division of Biology

California Institute of Technology

Pasadena, California 91125

This review briefly introduces the known classes of ion channels, describes conceptual insights gained from structure-function work, and discusses the limitations of the techniques used. Finally, unresolved issues and promising future directions are highlighted.

"Structure- function" studies are ultimately aimed at explaining the various functional properties of ion channels, such as permeation and gating, at the level of 3-dimensional structures and motions. At present, structure-function studies have the interim goal of evaluating the role played by individual residues in the protein sequence. Such studies are most often accomplished by in vitro mutagenesis of one or more codons in a cloned complementary DNA. The experimenter then compares the electrophysiology or pharmacology of the mutant protein with wild-type protein. At the present state of the field, determination of the function of a domain in the primary protein sequence rarely gives unambiguous information about the actual "structure" of the domain. Mutagenesis and expression has provided actual structural data in only a handful of cases, including the conclusion that the pore-lining transmembrane domains of the acetylcholine receptor are α-helical (Lester, 1992), and that the transmembrane domains of the pore region of the *Shaker* potassium channel are β-strands (Yellen et al., 1991). Mutagenesis and expression does, however, localize functions of a protein to particular domains, or, in some cases, to particular residues.

Mutagenesis and expression are preceded by careful inspection of the predicted primary amino acid sequence. In many cases, such study reveals consensus functional motifs. Consecutive stretches of hydrophobic residues may signify transmembrane domains, while presence of an N-terminal signal sequence indicates an extracellular N-terminal. Other well-known protein

motifs include phosphorylation target sequences, ATP binding domains (Walker et al., 1982), and calcium binding domains (Tufty and Kretsinger, 1975).

Channel families

Such methods applied to the sequences of cloned channels reveal a number of distinct families. For a review of the evolution of channel families, see Jan and Jan, 1992b. The well-known **voltage-gated channel family** encompasses voltage-gated sodium, potassium, and calcium channels, reviewed extensively in later chapters. The basic subunit for this family is a polypeptide with cytoplasmic N- and C- termini and six membrane spanning domains, termed S1-S6. For Na^+ and Ca^{2+} channels, four subunits are linked in an internal repeat to form a presumed monomeric channel; for K^+ channels, four subunits coassemble to form a tetrameric channel (MacKinnon, 1991).

One common feature of voltage-gated channels is the pattern $(R/K\text{-}X\text{-}X)_n$ in S4, where X is a residue with a hydrophobic side chain, and n is 6-7. The S4 region is thought to play a major role in sensing changes in the membrane potential, as discussed below. A second common feature is a domain (termed SS1-SS2, S5-S6, H5, or, most commonly, the P region) between S5 and S6 that forms at least part of the pore for voltage-gated channels (Hartman et al., 1991; Yool and Schwartz, 1991; MacKinnon and Miller, 1989; Heinemann et al., 1992). This family also includes a subfamily of Ca^{2+}-activated K^+ channels (Atkinson

et al., 1991; Adelman et al., 1992; Butler et al., 1993) and a plant K^+ channel (Anderson et al., 1992). The recently cloned amiloride-sensitive epithelial Na^+ channel is apparently unrelated (Lingueglia et al., 1993; Canessa et al., 1994).

The voltage-gated Na^+, K^+, and Ca^{2+} channels control nerve impulse conduction and frequency, and they are common targets for anesthetics. Some Ca^{2+} channels, reviewed in later chapters, are the link between electrical and chemical signal transduction. As such, they have especially wide relevance to drug design in many systems. They are especially important in the immune response, in heartbeat regulation, in transmitter release, and in cardiac muscle contraction. A subclass of Ca^{2+} channels comprise the target for the Ca^{2+} blockers such as nifedipine.

Closely related to the voltage-gated family are the **cyclic nucleotide-gated channels** important in visual and olfactory signal transduction. The amino acid sequence from the cloning of the retinal rod channel (Kaupp et al., 1989) and the CNG-channel of olfactory neurons (Dhallan et al., 1990) predicts a structure similar to that of the voltage-gated family, with six transmembrane domains, a charged S4 region, and a P region recently shown to line the pore (Goulding et al., 1993; Root and MacKinnon, 1993). The P-region of voltage-gated channels has two adjacent residues that do not appear in the homologous position of CNG channels. When voltage-gated K^+ channels are mutated to eliminate these two residues, K^+ selectivity is abolished, and the channel is blocked by divalent cations; these are pore characteristics of K^+

channels (Heginbotham et al., 1992). These results demonstrate the close evolutionary relationship between CNG channels and voltage-gated channels. In CNG channels, a long cytoplasmic C-terminal region contains the cyclic nucleotide binding site. Hill coefficients for ligand binding suggest that the full channel is an oligomer, and the resemblance to K^+ channels suggests a tetramer (Kaupp, 1991). Additional subunits of both the retinal and olfactory channels have recently been cloned; there is good evidence that the endogenous channel is actually a heteroligomer of both types of subunit (Chen et al., 1993; K. Zinn, personal communication; L. Buck, personal communication).

A new family of cloned K^+ channels, long-anticipated from physiology on animal cells, are the **inward rectifiers**. Sequence analysis of known clones predicts cytoplasmic N- and C- terminii, with two transmembrane domains (M1 and M2) separated by a P region homologous to that found for voltage-gated K^+ channels. The first inward rectifiers were cloned by expression, ROMK1 from rat kidney (Ho et al., 1993), and IRK-1 from mouse macrophage (Kubo et al., 1993). Intriguingly, chimeras between IRK-1 and ROMK1 suggest that it is not the P region, but the region C-terminal to M2 that governs Mg^{2+} block; both regions affect channel conductance (Taglialatela et al., 1994). This implies that the C-terminal region may in fact cross the membrane one or more times. The latest addition to the inward rectifier family is the atrial G-protein activated K^+ channel, termed either KGA (Dascal et al., 1993) or GIRK-1 (Kubo et al., 1993). Some or all of the inward rectification intrinsic to this family is

due to block by cytoplasmic Mg^{2+} (Vandenberg, 1987; Matsuda et al., 1987; Stanfield et al., 1994; Taglialatela et al., 1994). Future structure-function work on these channels will elucidate the domains responsible for regulation and pharmacology. It remains to be seen whether KGA/ GIRK1 accounts for inwardly rectifying K^+ conductances coupled to additional 7-helix receptors such as μ- and δ- opioid, α2 adrenergic, somatostatin, serotonin 1A, 1B, and 1D, adenosine, $GABA_B$, galanin, and dopamine receptors (North, 1989); they may be sites for future antipsychotic or analgesic drugs.

Also important in synaptic transmission are the well-known ion channels of the **ligand-gated superfamily**. Members of this family encode a ligand-binding domain for neurotransmitters and an ion channel for post-synaptic excitation or inhibition in the same protein. The prototype for the family, and the first cloned ion channel (Noda et al., 1983), is the nicotinic acetylcholine receptor, found in mammalian muscle and *Torpedo* electroplax. The receptor has pentameric subunit stoichiometry, with five subunits arranged around a central pore (Unwin, 1989; Unwin, 1993). Each subunit has a long extracellular N-terminal region containing the ligand-binding site, and four predicted transmembrane domains. Homologous nicotinic acetylcholine receptors are found in the peripheral and central nervous sytems. Other members of the superfamily that also form non-selective cation channels are the NMDA- and non-NMDA type glutamate receptors, the $5\text{-}HT_3$ serotonin receptor, and probably some ATP receptors. The $GABA_A$ and glycine receptors form Cl^-

channels. Mammalian GABA receptors are the target for the anxiolytic benzodiazepines. For review of this superfamily, see Hille, 1992, chapters six and nine.

Chloride channels

Cloned Cl^- channels are still few in number, and thus represent a new frontier of ion channel research. As such, they are worth considering in more detail. Even the few Cl^- channels cloned so far play exceptionally diverse roles *in vivo*--muscle contraction, epithelial secretion, and volume regulation, as well as inhibitory neuronal transmission. These and future channels may be targets of drugs regulating immune responses, electrolyte balance, and the central nervous system. Intriguingly, Cl^- channels overlap several families of channels. The longest known cloned Cl^- channels are the $GABA_A$ (Schofield et al., 1987) and glycine (Grenningloh et al., 1987; Grenningloh et al., 1990) receptor channels. These are expressed predominantly in neuronal tissue.

Another well-studied Cl^- channel is the cystic fibrosis transmembrane conductance regulator (CFTR), whose mutation causes cystic fibrosis (Riordan et al., 1989; Rommens et al., 1989). CFTR is a member of the ATP-binding cassette protein superfamily (for review see Higgins, 1992). Sequence analysis predicts two homologous domains, each consisting of six transmembrane domains and a nucleotide binding fold, linked by a regulatory (R) domain (for review see Riordan, 1993). CFTR is activated dually by protein kinase A

phosphorylation and hydrolysis of ATP (Anderson et al., 1991). Initial reports indicated that a close relative of CFTR, the multidrug resistance transporter, was also a Cl^- channel (Valverde et al., 1992; Gill et al., 1992). This remains controversial (Ehring et al., 1994).

More recently cloned Cl^- channels form a distinct family unrelated to other channels. The voltage-gated Cl^- channel from *Torpedo*, termed ClC-0, was cloned in 1990 by functional expression (Jentsch et al., 1990); hydropathy analysis predicts 12 (possibly 13) transmembrane domains. Based on homology to ClC-0, the skeletal muscle Cl^- channel ClC-1 was cloned (Steinmeyer et al., 1991), followed by ClC-2 (Thiemann et al., 1992), ClC-K1 (Uchida et al., 1993) and ClC-3 (Kawasaki et al., 1994). More are doubtless on the way. All members of the family have 12 putative transmembrane domains, with a long intracellular cytoplasmic domain (termed D13) that includes a hydrophobic stretch.

The members of the ClC family have intriguing functional properties and patterns of expression. ClC-0 forms a double-barreled Cl^- channel when expressed in *Xenopus* oocytes (Bauer et al., 1991), consistent with the original description of the reconstituted *Torpedo* protein (Hanke and Miller, 1983). ClC-1 is developmentally regulated and specifically expressed in skeletal muscle (Steinmeyer et al., 1991), while ClC-2 is expressed in pancreas, lung, and liver tissue, as well as in brain and muscle (Thiemann et al., 1992). Mutations in ClC-1 can cause recessive and dominant myotonia congenita (Koch et al., 1992).

Interestingly, analysis of these mutations suggests that like K^+ channels, ClC-1 is a homotetramer (Steinmeyer et al., 1994). Unlike other members of the family, ClC-2 is volume-regulated (Grunder et al., 1992). ClC-3 is expressed in rat brain, and its activity in oocytes is inhibited by activation of protein kinase C (Kawasaki et al., 1994), implying an important role in signal transduction. ClC-K1 expresses predominantly in kidney (Uchida et al., 1993); it may regulate urinary electrolyte concentration. ClC-0, 1, and 2 share ≈ 50% sequence identity among themselves, ≈ 40% identity with ClC-K1, and ≈ 25% identity with ClC-3. Further investigation of the novel gating, permeation, and modulation mechanisms of this family will make fertile ground for structure-function work.

Historically, the vast number of Cl^- conductances have taken a back seat to cationic conductances. With so many exciting new clones, an explosion in Cl^- channel molecular biology cannot be far off. A most eagerly awaited clone is the epithelial outward rectifier Cl^- channel whose regulation is defective in cystic fibrosis (Gabriel et al., 1993; Egan et al., 1992) and which may be the main mechanism of Cl^- secretion in airway epithelia (Stutts et al., 1992).

An emerging class of molecules related to ion channels, with great potential relevance to drug design, are the **neurotransmitter transporters**; for comprehensive review, see Lester et al., 1994. Energy for neurotransmitter transport is often obtained from cotransport of inorganic ions. Plasma membrane transporters serve to remove neurotransmitters from the synaptic

cleft after their release; vesicular transporters concentrate neurotransmitters into presynaptic vesicles prior to release. These two subfamilies each have 12 putative transmembrane domains, though they share no significant sequence homology. Cloned transporters include those for GABA (Guastella et al., 1990), norepinephrine (Pacholczyk et al., 1991), dopamine (Kilty et al., 1991; Shimada et al., 1991), serotonin (Hoffman et al., 1991), and glycine (Guastella et al., 1992). The recently cloned glutamate transporters (Pines et al., 1992) form a separate subfamily with fewer transmembrane domains. Of clinical relevance, drug abuse and clinical depression have been linked to defects in neurotransmitter transport. Cocaine blocks dopamine, serotonin, and norepinephrine transporters (Ritz et al., 1987; Kuhar et al., 1991), and newer antidepressants such as fluoxetine specifically inhibit serotonin uptake (Fuller and Wong, 1990). Structure-function work will identify the activation, modulation, and blocking mechanisms for these transporters.

Common functional domains

Especially when combined with electrophysiology, mutagenesis is the most sensitive tool available for domain analysis. Domains within proteins involved in activation, inactivation, ion selectivity, ligand binding, and subunit assembly have all been localized. Of special relevance to drug discovery, as developed in the previous chapter, is the identification of ion channel blocker or toxin binding sites. Mapping of such sites serves as a tool for channel

analysis, as developed below, and structure-function techniques may allow detailed reverse pharmacology on any cloned channel of medical interest.

In addition to detailed characterization of individual channels, structure-function work has given new conceptual insights about ion channels in general. A large advance in thought is that separate domains of ion channels are indeed responsible for distinct functions in some cases, as originally postulated by Hodgkin and Huxley for activation and inactivation gating (Hodgkin and Huxley, 1952). For example, the fast inactivation gate of the *Shaker* K^+ channel can be removed without perturbing single-channel conductance or activation (Hoshi et al., 1990). As another example, introduction of three residues from the M2 sequence of a $GABA_A$ receptor into the M2 pore-lining region of the homomeric α7 acetylcholine receptor results in a channel gated by acetylcholine, but selective for Cl^- (Galzi et al., 1992). Although some studies, particularly on activation gating, have given more complex results, physiologists routinely speak of separable selectivity domains or gating regions.

Detailed structure-function studies on a wide array of channels give a picture of mechanisms common within families. The positively charged S4 regions of voltage-gated channels are common to K^+ channels and to each of the four linked domains of Na^+ and Ca^{2+} channels. Replacement of the individual charged residues within S4 leads to reductions in gating charge for both K^+ (Papazian et al., 1991; Logothetis et al., 1992) and Na^+ (Stuhmer et al.,

1989) channels, although the individual contributions of each of the charges are non-equivalent. Other mutations of hydrophobic residues within S4, but not within any other putative transmembrane domains, shift the voltage-dependence of gating (Auld et al., 1990; Lopez et al., 1991). Even CNG channels retain a small voltage sensitivity, presumably due to a poorly conserved S4 region that comprises fewer R/K residues than found in the true voltage-gated channels.

Inactivation gating is also common among the members of the voltage-gated channel family. In Na^+ channels, disruption of the positively charged linker between domains III and IV removes fast inactivation (Stuhmer et al., 1989). Similar charged cytoplasmic domains have been found in K^+ channels. Deletions in the first 22 residues of the *Shaker* K^+ channel disrupt fast inactivation (Hoshi et al., 1990), and reapplication of a synthetic peptide corresponding to the first 20 residues to noninactivating mutants restores inactivation (Zagotta et al., 1990). This peptide is also effective on non-inactivating K^+ channels (Zagotta et al., 1990; Isacoff et al., 1991) and calcium-activated K^+ channels (Foster et al., 1992). Intriguingly, the peptide segment connecting domains III and IV of an Na^+ channel, when attached to the N-terminus of a non-inactivating K^+ channel, inactivates the K^+ channel (Patton et al., 1993). In addition, the K^+ channel inactivation peptide also blocks CNG channels by binding to the P region (Kramer et al., 1994). These results indicate commonality of structure and function between Na^+, K^+, and CNG

channels for activation and inactivation gating. For a thorough review of K^+ channel structure-function work, see Jan and Jan, 1992a.

Similarly, among all members of the ligand-gated superfamily, the M2 region appears to serve as the pore-forming structure. Examples below are illustrative of the wide variety of permeation properties governed by M2; for a comprehensive review, see Lester, 1992. The M2 motif was found for the ACh receptor via studies of mutations that altered permeation, and block by the open-channel blocker QX-222 (Imoto et al., 1988; Leonard et al., 1988; Charnet et al., 1990). A site in M2 of non-NMDA glutamate receptors governs Ca^{2+} permeability (Hume et al., 1991; Verdoorn et al., 1991), and a binding site for Mg^{2+} and MK-801 has been localized to M2 for NMDA-type glutamate receptors (Burnashev et al., 1992; Sakurada et al., 1993). Mutation of residues in M2 of the glycine receptor abolish picrotoxinin block (Pribilla et al., 1992). Similarly, cysteine substitutions of amino acids lining the M2 segment of the $GABA_A$ receptor (Xu and Akabas, 1993) and the ACh receptor (Akabas et al., 1992) confer sulfhydryl sensitivity upon the channels.

Structure-function work has also provided evidence for assembly mechanisms common to the ligand-gated superfamily. Extracellular domains involved in subunit assembly have been found for the glycine receptor (Kuhse et al., 1993) and for the ACh receptor (Yu and Hall, 1991; Verrall and Hall, 1992). Individual residues have been localized for the ACh receptor (Gu et al., 1991).

Mutations for effective structure-function analysis, however, need not always be *in vitro* mutations planned by the investigator. An exciting new approach was taken by Teem et al. to identify mutations that reverse the cystic fibrosis-causing phenotype of the CFTRΔF508 mutant (Teem et al., 1993). A portion of the first nucleotide-binding fold of yeast STE-6 **a**-factor mating peptide transporter, a member of the ABC superfamily (McGrath and Varshavsky, 1989), was replaced with the corresponding portion of the (nonfunctional) CFTRΔF508 Cl^- channel. This construct results in loss of **a**-factor transport, and loss of mating phenotype. Two revertant mutations were identified by gain of mating efficieny and sequenced. The revertant mutations were introduced into the corresponding position in CFTRΔF508. When transfected into mammalian cells, functional Cl^- channels are generated, showing that these mutations suppress the defect in Cl^- permeability caused by the ΔF508 mutation.

Structure-function analysis has localized drug binding sites on many channels. Such localization has helped identify pore domains for ligand-gated channels and for K^+ channels, as noted above, and might eventually lead to ligands that are specific for individual K^+ channel subtypes. Other future clinically relevant blockers might include subtype-specific blockers of glutamate receptors or transporters, neuronal acetylcholine receptors, or Ca^{2+} channels, to block neuronal excitotoxicity (Choi and Rothman, 1990; Choi, 1992). Perhaps inhibitors of cocaine binding to neurotransmitter transporters will yield

therapies for drug abuse. Understanding the mechanisms that couple opioid receptors to channels may lead to new analgesics or addiction therapies. Outside of the CNS, specific Ca^{2+} or K^+ channel blockers could suppress components of immune response. Any such blockers, however, will have to be specific and non-global for best response. In the present day view of rational drug design, one requires precise atomic coordinates of the drug binding site. It is not yet clear whether heterologous expression and site-directed mutagenesis will provide structure-function information in sufficient detail to suggest specific new drugs that affect only specific channel subtypes.

Limitations of mutagenesis and expression

As with any class of experiments, the limitations and pitfalls of mutagenesis and expression must be kept in mind. First and foremost, structure-function analysis can begin only with a cloned cDNA sequence and a functional expression system. Differences among expression systems can account for major differences in findings and interpretation. For example, the major mutation in CFTR, the cystic fibrosis Cl^- channel, is a deletion of a single phenylalanine residue in the first nucleotide binding fold. In mammalian cells, CFTRΔF508 is improperly processed; little (Dalemans et al., 1991) or none (Cheng et al., 1990) reaches the cell membrane. However, in other culture systems, such as Sf9 cells (Li et al., 1993) or *Xenopus* oocytes (Drumm et al., 1991), the mutant protein reaches the membrane and retains Cl^- channel

function. Uncertainty about the effect of the ΔF508 mutation, by far the most prevalent disease-causing mutation, was cleared up by the discovery that the intracellular processing of CFTRΔF508 is sensitive to the temperature of cell culture (Denning et al., 1992).

A particularly detailed analysis of functional differences among heterologously expressed ion channels due to the expression system is found for sodium channels. When expressed in neonatal rat ventricular myocytes, the rat brain IIA sodium channel α-subunit inactivates more quickly than when expressed in Chinese hamster ovary cells, though TTX sensitivity is unaffected. The same subunit expresses only poorly in undifferentiated BC3H-1 muscle cells, and not at all in Ltk^- cells, even though *Drosophila Shaker* H4 K^+ channels express in all four cell types (Yang et al., 1992). These results may indicate that cell-specific post-translational modifications, such as glycosylation or attachment of fatty acids, can cause functional differences; or they may point to the involvement of additional subunits in channel assembly (Isom et al., 1992).

Results from heterologous expression are also easily contaminated by endogenous channels, and the separation of the desired channels from contaminating channels can be non-trivial. For example, the commonly used *Xenopus* oocyte has a strong endogenous calcium-activated Cl^- current (Dascal, 1987) and a large amount of nonselective stretch-activated cation channels (Yang and Sachs, 1990). These endogenous channels complicate experiments dealing with pathways involving Ca^{2+} at the whole-cell level or experiments

dealing with cation channels at the single-channel level (Vernino et al., 1992).

There is also the possibility of cryptic channels that only appear upon heterologous expression of another protein. Such cryptic channels may result unexpectedly from expression cloning assays. One such activator of an endogenous oocyte channel is the protein I_{Cln}. I_{Cln} was cloned by expression in *Xenopus* oocytes and was originally thought to be a Cl^- channel itself (Paulmichl et al., 1992). Later work, however, showed that I_{Cln} localizes to the cytosolic fraction, not the membrane fraction (Krapivinsky et al., 1994), and that the Cl^- current due to its expression is likely due to a hypotonicity-activated current endogenous to the oocytes (Ackerman et al., 1994).

Another example of unexpected results from expression in oocytes is the small protein termed either IsK or MinK. IsK, cloned by functional expression in *Xenopus* oocytes (Takumi et al., 1988), produces a slowly activating voltage-sensitive K^+ conductance when expressed either in oocytes or in mammalian cells (Freeman and Kass, 1993). The endogenous conductance most similar to IsK is in ventricular muscle (Varnum et al., 1993; Freeman and Kass, 1993). Its gating (Takumi et al., 1991) and selectivity (Goldstein et al., 1991) are altered by point mutations, good evidence that IsK itself is the K^+ channel. In other work, however, purified IsK displays no observable channel activity when incorporated into bilayers (Lesage et al., 1993), possibly because IsK has an unusually low single-channel conductance. Furthermore, recent work shows that IsK has the capacity to produce both K^+ and Cl^- currents with different

pharmacology when expressed in oocytes, depending on the cRNA concentration of IsK injected (Attali et al., 1993). Mutagenesis reveals that different domains of IsK are responsible for induction of the K^+ and the Cl^- current. Most intriguing, mutants producing only Cl^- channel activity act as dose-dependent antagonists of mutants producing only K^+ channel activity, as though the heterologously expressed IsK (now also termed IsK,Cl by Attali et al., 1993) is binding to a pool of endogenous subunits, present in limiting amounts, that can participate in assembly of either K^+ or Cl^- channels.

When a mutant protein is finally expressed in a heterologous system, there always remains the ambiguity of whether changes in phenotype are due to the actual residue(s) mutated, or rather to allosteric interactions propagated through the protein to a domain different from the one mutated. In the absence of crystal structures, such objections to structure-function can never be totally dispelled. However, multiple mutations can be assayed to show an internally consistent story. For example, deletion of the N-terminal domain of the *Shaker* channel removes the inactivation gate (Hoshi et al., 1990). In addition, reapplication of the corresponding peptide restores inactivation in a dose-dependent manner, and point mutations in the reapplied peptide render the peptide ineffective (Zagotta et al., 1990). Moreover, the *Shaker* ball peptide acts as an open-channel blocker (Demo and Yellen, 1991), and residues have been found at the putative mouth of the channel corresponding to the receptor for the ball (Isacoff et al., 1991). In the absence of high-resolution structural

data, confidence in the specifity of results of structure-function work often resides either in additive effects of multiple mutations or in multiple effects of a single mutation.

There are also intrinsic limitations to the present techniques of in vitro mutagenesis and heterologous expression. There are but 20 naturally occurring amino acids, and incorporation of an unnatural amino acid into a system suitable for analysis is very laborious. Moreover, the peptide backbone cannot be mutated, only the side chains. Fortunately, major roles for the peptide backbone seem unlikely, since differences in selectivity and activation among ion channels evolved through modifications in side-chains, and not in the backbone (but see Heginbotham et al., 1994). Mutations can seldom address coupling mechanisms--how ligand binding is coupled to channel opening, or what conformational changes open a voltage-activated channel. Most irritating, many in vitro mutations do not express, for unknown reasons, even when wild-type constructs do.

Future directions

With so many channels already taken apart, residue by residue, where will structure-function go next? First, whole families of channels have yet to be cloned, as well as some intriguing individual channels within families. Channels gated by mechanotransduction, for example, represent an entire family of channels important for cellular volume regulation and for hearing

sensory transduction. Stretch channels are ubiquitous (Sachs, 1991), and their biophysical properties are well-described, but the molecular bases for their activation are unknown. The hair cell mechanotransduction channel, for example, appears to be gated by direct physical pull on an activation gate (Hudspeth and Gillespie, 1994). What are the residues involved in this novel gating mechanism, and what residues make up the activation gate? Stretch channels in oocytes are known to be nonspecific cation channels (Yang and Sachs, 1990), while many volume-regulated channels are Cl^--selective (McCarty and O'Neil, 1992). What insights will the primary sequence, when deduced, give about the nature of ion selectivity? Stretch channels are still awaiting a clean system for expression cloning; their very abundance has hindered their study. Note, however, that the recently cloned amiloride-sensitive sodium channel shares homology with *C. elegans* gene products involved in mechanotransduction (Canessa et al., 1994). This implies that it may be a stretch channel.

In addition to the stretch channels, channels activated by Ca^{2+} need further exploration. Ca^{2+}-activated K^+ channels are especially intriguing because some of them have high conductances, well over 100 pS. This conductance has made possible detailed studies of the pore (Eisenman et al., 1986). Families of clones, from the *Drosophila slo* locus (Atkinson et al., 1991; Adelman et al., 1992), and mammalian homologs (Butler et al., 1993), have been reported, but no Ca^{2+}-activated Cl^- channel is cloned. Volume-activated Cl^-

conductances are important for immunological response (Lewis et al., 1993) and for regulatory volume decrease in a variety of cell types (McCarty and O'Neil, 1992). Cloning of the channels involved may resolve a number of issues, including whether volume-activated channels are activated directly by membrane stretch or by some other mechanism, such as dilution of a cytoplasmic regulatory component. Another uncloned Cl^- channel is the histamine-gated Cl^- channel, a presumed member of the ligand-gated superfamily (Hardie, 1989).

Molecular biology has uncovered a bewildering array of sequence variations among channels, but the in vivo functions of different subtypes remain largely unknown. Acetylcholine receptors, glutamate receptors, and K^+ channels are all large families that may still contain uncloned members. Heterologous expression has found significant functional differences among channel subtypes, such as between the R/Q subtypes of AMPA glutamate receptors (Hume et al., 1991; Verdoorn et al., 1991; Sommer et al., 1991). How are these channel subtypes spatially organized? How are these channel subtypes the bases for cellular function? To answer these more cellular questions, structure-function analysis will move towards changing the individual components of signaling pathways, rather than changing the residues of individual channels. Tools include not only mutagenesis, but also gene knockout and antisense technology. Such work has already begun. Transfection of Na^+ and K^+ channels can reconstruct the properties of an entire

neuron (Hsu et al., 1993), albeit a rather simple one. Analysis of the cystic fibrosis knockout mouse has confirmed defective regulation of an outward rectifier Cl^- channel separate from the cystic fibrosis gene product (Gabriel et al., 1993).

In the future, primary physiology and biochemistry will uncover more transduction pathways. Knockout of the individual components, or more subtle manipulation of the individual components through mutagenesis and expression, will reveal the function of each piece. Perhaps knockout of dopamine receptors will lead to a Parkinson's-like phenotype. With the cloning of the G-protein-activated potassium channel KGA, or GIRK1 (Dascal et al., 1993; Kubo et al., 1993) the components of the famous cardiac *vagusstoff* signaling pathway have all been cloned. What will mutation or antisense knockout of the receptors and channels involved reveal about heartbeat regulation?

Structure-function work on cloned ion channels will take a quantum leap forward with the advent of high-resolution structural data. Although the time scale for crystallization of a full ion channel is not predictable, we can hope for timely high-resolution structures of individual domains, especially soluble domains. Then past domain analyses will be tested, and future mutations will be guided and improved exponentially by knowledge of the actual structures involved. Until now, channel biologists have been working with a black box; with crystal structures, work will be at the level of the

mutagenesis done on hemoglobin. The excitement generated by the dissection of individual channels will continue and increase, as structure-function analysis is applied to increasingly complex systems.

Figure 1. Predicted transmembrane topologies of ion channel families. Shaded background represents the plasma membrane; dark rectangles are putative transmembrane α-helices. N and C indicate the terminii of the amino acid sequence. **A**, single subunit of a voltage-gated K^+ channel. *P* indicates the pore region; jagged structure signifies putative β-strand. **B**, voltage-gated Na^+ or K^+ channel topology. **C**, cyclic nucleotide-gated channel. **D**, inward rectifier K^+ channel. **E**, ligand-gated channel. Left, side view of a single α-subunit. Ligand-binding domain is extracellular; M2 pore-lining domain is shown as a rounded rectangle. Right, view of the full receptor, made up of five subunits, along an axis perpendicular to the plane of the membrane. Each circle represents a transmembrane domain; M2 domain is shaded. Small shaded circles represent ligand-binding domains. **F**, cystic fibrosis transmembrane conductance regulator Cl^- channel (CFTR). NBF1 and NBF2, nucleotide binding folds 1 and 2. R, R-domain. **G**, ClC Cl^- channel. D13, cytoplasmic hydrophobic domain.

Ackerman MJ, Wickman KD, Clapham DE (1994): Hypotonicity activates a native chloride current in *Xenopus* oocytes. J Gen Physiol 103:153-179.

Adelman JP, Shen KZ, Kavanaugh MP, Warren RA, Wu YN, Lagrutta A, Bond CT, North RA (1992): Calcium-activated potassium channels expressed from cloned complementary DNAs. Neuron 9:209-216.

Akabas MH, Stauffer DA, Xu M, Karlin A (1992): Acetylcholine receptor channel structure probed in cysteine-substitution mutants. Science 258:307-310.

Anderson JA, Huprikar SS, Kochian LV, Lucas WJ, Gaber RF (1992): Functional expression of a probable *Arabidopsis thaliana* potassium channel in *Saccharomyces cerevisiae*. Proc Natl Acad Sci USA 89:3736-3740.

Anderson MP, Berger HA, Rich DP, Gregory RJ, Smith AE, Welsh MJ (1991): Nucleoside triphosphates are required to open the CFTR chloride channel. Cell 67:775-784.

Atkinson NS, Robertson GA, Ganetzky B (1991): A component of calcium-activated potassium channels encoded by the *Drosophila* slo locus. Science 253:551-554.

Attali B, Guillemare E, Lesage F, Honore E, Romey G, Lazdunski M, Barhanin J (1993): The protein IsK is a dual activator of K^+ and Cl^- channels. Nature 365:850-852.

Auld VJ, Goldin AL, Krafte DS, Marshall J, Dunn JM, Catterall WA, Lester HA, Davidson N, Dunn RJ (1990): A neutral amino acid change in segment IIS4 dramatically alters the gating properties of the voltage-dependent sodium channel. Proc Natl Acad Sci USA 87:323-327.

Bauer CK, Steinmeyer K, Schwarz JR, Jentsch TJ (1991): Completely functional double-barreled chloride channel expressed from a single *Torpedo* cDNA. Proc Natl Acad Sci USA 88: 11052-11056.

Burnashev N, Schoepfer R, Monyer H, Ruppersberg JP, Gunther W, Seeburg PH, Sakmann B (1992): Control by asparagine residues of calcium permeability and magnesium blockade in the NMDA receptor. Science 257:1415-1419.

Butler A, Tsunoda A, McCobb DP, Wei A, Salkoff L (1993): MSLO, a complex mouse gene encoding maxi calcium-activated potassium channels. Science 261:221-224.

Canessa CM, Shild L, Buell G, Thorens B, Gautschi I, Horisberger J-D, Rossier

BC (1994): Amiloride-sensitive epithelial Na^+ channel is made of three homologous subunits. Nature 367, 463-467.

Charnet P, Labarca C, Leonard RJ, Vogelaar NJ, Czyzyk L, Gouin A, Davidson N, Lester HA (1990): An open-channel blocker interacts with adjacent turns of α-helices in the nicotinic acetylcholine receptor. Neuron 2:87-95.

Chen T-Y, Peng VW, Dhallan RS, Ahamed B, Reed RR, Yau KW (1993): A new subunit of the cyclic nucleotide-gated cation channel in retinal rods. Nature 362:764-767.

Cheng SH, Gregory RJ, Marshall J, Paul S, Souza DW, White GA, Riordan JR, Smith AE (1990): Defective intracellular transport and processing of CFTR is the molecular basis of most cystic fibrosis. Cell 63:827-834.

Choi DW (1992): Amyotrophic lateral sclerosis and glutamate - too much of a good thing? New Eng J Med 326:1493-1494.

Choi DW, Rothman SM (1990): The role of glutamate neurotoxicity in hypoxic-ischemic neuronal death. Ann R Neur 13:171-182.

Dalemans W, Barbry P, Champigny G, Jallet S, Dott K, Dreyer D, Crystal RG,

Pavirani A, Lecocq J-P, Lazdunski M (1991): Altered chloride ion channel kinetics associated with (Δ)F508 cystic fibrosis mutation. Nature 354:526-528.

Dascal N (1987): Use of the *Xenopus* oocyte system to study ion channels. CRC Crit Rev Biochem 22:317-387.

Dascal N, Schreibmayer W, Lim NF, Wang W, Chavkin C, DiMagno L, Labarca C, Kieffer BL, Gaveriaux-Ruff C, Trollinger D, Lester HA, Davidson N (1993): Atrial G protein-activated K^+ channel: Expression cloning and molecular properties. Proc Natl Acad Sci USA 90:10235-10239.

Demo SD, Yellen G (1991): The inactivation gate of the Shaker K^+ channel behaves like an open-channel blocker. Neuron 7:743-753.

Denning GM, Anderson MP, Amara JF, Marshall J, Smith AE, Welsh MJ (1992): Processing of mutant cystic fibrosis transmembrane conductance regulator is temperature-sensitive. Nature 358:761-764.

Dhallan RS, Yau KW, Schrader KA (1990): Primary structure and functional expression of a cyclic nucleotide-activated channel from olfactory neurons. Nature 347:184-187.

Drumm ML, Wilkinson DJ, Smit LS, Worrell RT, Strong TV, Frizzell RA, Dawson DC, Collins FS (1991): Chloride conductance expressed by ΔF508 and other mutant CFTRs in *Xenopus* oocytes. Science 254:1797-1799.

Egan M, Flotte T, Afione S, Solow R, Zeitlin P, Carter BJ, Guggino WJ (1992): Defective regulation of outwardly rectifying Cl^- channels by protein kinase A corrected by insertion of CFTR. Nature 358:581-584.

Ehring GR, Osipchuk YV, Cahalan MD (1994): Volume-activated chloride channels in drug-senstive and -resistant cell lines. Biophys J 66:A142.

Eisenman G, Latorre R, Miller C (1986): Multi-ion conduction and selectivity in the high-conductance Ca^{2+}-activated K^+ channel from skeletal muscle. Biophys J 50:1025-1034.

Foster CD, Chung SK, Zagotta WN, Aldrich RW, Levitan IB (1992): A peptide derived from the Shaker-B K^+ channel produces short and long blocks of reconstituted $Ca2^+$-dependent K^+ channels. Neuron 9:229-236.

Freeman LC, Kass RS (1993): Expression of a minimal K-channel protein in mammalian cells and immunolocalization in guinea pig heart. Circ Res 73:968-973.

Fuller RW, Wong DT (1990): Serotonin uptake and serotonin uptake inhibition. Ann NY Acad Sci 600:68-80.

Gabriel SE, Clarke LL, Boucher RC, Stutts MJ (1993): CFTR and outward rectifying chloride channels are distinct proteins with a regulatory relationship. Nature 363:263-266.

Galzi J-L, Devillers-Thiery A, Hussy N, Bertrand S, Changeux J-P (1992): Mutations in the channel domain of a neuronal nicotinic receptor convert ion selectivity from cationic to anionic. Nature 359:500-505.

Gill DR, Hyde SC, Higgins CF, Valverde MA, Mintenig GM, Sepulveda FV (1992): Separation of drug transport and chloride channel functions of the human multidrug resistance P glycoprotein. Cell 71:23.

Goldstein SAN, Miller C (1991): Site-specific mutations in a minimal voltage-dependent K^+ channel alter ion selectivity and open-channel block. Neuron 7, 403-408.

Goulding EH, Tibbs GR, Liu D, Siegelbaum SA (1993): Role of H5 domain in determining pore diameter and ion permeation through cyclic nucleotide-gated

channels. Nature 364:61-64.

Grenningloh G, Pribilla I, Prior P, Malthap G, Beyreuther K, Taleb O, Betz H (1990): Cloning and expression of the 58 kd β subunit of the inhibitory glycine receptor. Neuron 4:963-970.

Grenningloh G, Rienitz A, Schmitt B, Methfessel C, Zensen M, Beyreuther K, Gundelfinger E, Betz H (1987): The strychnine-binding subunit of the glycine receptor shows homology with nicotinic acetylcholine receptors. Nature 328:215-220.

Grunder S, Thiemann A, Pusch M, Jentsch TJ (1992): Regions involved in the opening of C1C-2 chloride channel by voltage and cell volume. Nature 360:759-762.

Gu Y, Camacho P, Gardner P, Hall ZW (1991): Identification of two amino acid residues in the ε subunit that promote mammalian muscle acetylcholine receptor assembly in COS cells. Neuron 6:879-887.

Guastella J, Brecha N, Welgmann C, Lester HA, Davidson N (1992): Cloning, expression, and localization of a rat brain high-affinity glycine transporter. Proc Natl Acad Sci USA 89:7189-7193.

Guastella JG, Nelson N, Nelson H, Czyzyk L, Keynan S, Midel MC, Davidson N, Lester H, Kanner B (1990): Cloning and expression of a rat brain GABA transporter. Science 249:1303-1306.

Hanke W, Miller C (1983): Single chloride channels from *Torpedo* electroplax. J Gen Physiol 82:25-42

Hardie RC (1989): A histamine-activated chloride channel involved in neurotransmission at a photoreceptor synapse. Nature 339:704-706.

Hartmann HA, Kirsch GE, Drewe JA, Taglialatela M, Joho R, Brown AM (1991): Exchange of conduction pathways between two related K^+ channels. Science 251:942-944.

Heginbotham L, Abramson T, MacKinnon R (1992): A functional connection between the pores of distantly related ion channels as revealed by mutant K^+ channels. Science 258:1152-1155.

Heginbotham L, Lu Z, Abramson T, MacKinnon R (1994): Mutations in the K^+ channel signature sequence. Biophys J 66, 1061-1067.

Heinemann S, Terlau H, Stuhmer W, Imoto K, Numa S (1992): Calcium channel characteristics conferred on the sodium channel by single mutations. Nature 356:441-443.

Higgins CF (1992): ABC transporters--from microorganisms to man. Ann R Cell Biol 8:67-113

Hille B (1992): Ionic channels of excitable membranes. Sunderland, MA: Sinauer.

Ho K, Nichols C, Lederer G, Lytton J, Vassilev PM, Kanazirska MV, Hebert SC (1993): Cloning and expression of an inwardly rectifying ATP-regulated potassium channel. Nature 362:31-38.

Hodgkin AL, Huxley AF (1952): A quantitative description of membrane current and its application to conduction and excitation in nerve. J Physiol (London) 117:500-544.

Hoffman BJ, Mezey E, Brownstein MJ (1991): Cloning of a serotonin transporter affected by antidepressants. Science 254:579-580.

Hoshi T, Zagotta WN, Aldrich RW (1990): Biophysical and molecular

mechanisms of Shaker potassium channel inactivation. Science 250:533-538.

Hsu H, Huang E, Yang X-C, Karschin A, Labarca C, Figl A, Ho B, Davidson N, Lester HA (1993): Slow and incomplete inactivations of voltage-gated channels dominate encoding in synthetic neurons. Biophys J 65:1196-1206.

Hudspeth AJ, Gillespie PG (1994): Pulling springs to tune transduction: Adaptation by hair cells. Neuron 12:1-9.

Hume RI, Dingledine R, Heinemann SF (1991): Identification of a site in glutamate receptor subunits that controls calcium permeability. Science 253:1028-1031.

Imoto K, Busch C, Sakmann B, Mishina M, Konno T, Nakai J, Bujo H, Mori Y, Fukuda K, Numa S (1988): Rings of negatively charged amino acids determine the acetylcholine receptor channel conductance. Nature 335:645-648.

Isacoff EY, Jan YN, Jan LY (1991): Putative receptor for the cytoplasmic inactivation gate in the Shaker K^+ channel. Nature 353:86-90.

Isom LL, Dejongh KS, Patton DE, Reber BFX, Offord J, Charbonneau H, Walsh K, Goldin AL, Catterall WA (1992): Primary structure and functional expression

of the beta-1 subunit of the rat brain sodium channel. Science 256:839-842.

Jan LY, Jan YN (1992a): Structural elements involved in specific K^+ channel functions. Ann Rev Physiol 54:535-555.

Jan LY, Jan YN (1992b): Tracing the roots of ion channels. Cell 69:715-718.

Jentsch TJ, Steinmeyer K, Schwartz G (1990): Primary structure of *Torpedo marmorata* chloride channel isolated by expression cloning in *Xenopus* oocytes. Nature 348:510-514.

Kaupp UB (1991): The cyclic nucleotide-gated channels of vertebrate photoreceptors and olfactory epithelium. Trends Neurosci 14:150-157.

Kaupp UB, Niidome T, Tanabe T, Terada S, Binigk W, Stuhmer W, Cook NJ, Kangawa K, Matsuo EAH (1989): Primary structure and functional expression from complementary-DNA of the rod photoreceptor cyclic GMP-gated channel. Nature 342:762-766.

Kawasaki M, Uchida S, Monkawa T, Miyawaki A, Mikoshiba K, Marumo F, Sasaki S (1994): Cloning and expression of a protein kinase C-regulated chloride channel abundantly expressed in rat brain neuronal cells. Neuron

12:597-604.

Kilty JE, Lorang D, Amara S (1991): Cloning and expression of a cocaine-sensitive rat dopamine transporter. Science 254:578-579.

Koch MC, Steinmeyer K, Lorenz C, Richer K, Wolf F, Otto M, Zoll B, Lehmann-Horn F, Grzeschik K-H, Jentsch TJ (1992): The skeletal muscle chloride channel in dominant and recessive human myotonia. Science 257:797-800.

Kramer RH, Goulding E, Siegelbaum SA (1994): Potassium channel inactivation peptide blocks cyclic nucleotide-gated channels by binding to the conserved pore domain. Neuron 12:655-662.

Krapivinsky GB, Ackerman MJ, Gordon EA, Krapivinsky LD, Clapham DE (1994): Molecular characterization of a swelling-induced chloride conductance regulatory protein, pI_{Cln}. Cell 76:439-448.

Kubo Y, Baldwin TJ, Jan YN, Jan LY (1993): Primary structure and functional expression of a mouse inward rectifier potassium channel. Nature 362:127-133.

Kubo Y, Reuveny E, Slesinger PA, Jan YN, Jan LY (1993): Primary structure

and functional expression of a rat G protein-coupled muscarinic potassium channel. Nature 364:802-806.

Kuhar MJ, Ritz MC, Boja JW (1991): The dopamine hypothesis of the reinforcing properties of cocaine. Trends Neurosci 144:299-302.

Kuhse J, Laube B, Magalei D, Betz H (1993): Assembly of the inhibitory glycine receptor: identification of amino acid sequence motifs governing subunit stochiometry. Neuron 11:1049-1056.

Leonard RJ, Labarca C, Charnet P, Davidson N, Lester HA (1988): Evidence that the M2 membrane-spanning region lines the ion channel pore of the nicotinic receptor. Science 242:1578-1581.

Lesage F, Attali B, Lakey J, Honore E, Romey G, Faurobert E, Lazdunski M, Barhanin J (1993): Are Xenopus oocytes unique in displaying functional IsK channel heterologous expression? Receptors and Channels 1:143-152.

Lester HA (1992): The permeation pathway of neurotransmitter-gated ion channels. Ann Rev Biophys Biomol Struc 21:267-292.

Lester HA, Mager S, Quick MW, Corey JW (1994): Permeation properties of

neurotransmitter transporters. Annu Rev Pharmacol Toxicol 34:219-249.

Lewis RS, Ross PE, Cahalan MD (1993): Chloride channels activated by osmotic stress in T lymphocytes. J Gen Physiol 101:801-826.

Li C-H, Ramjeesingh M, Reyes E, Jensen T, Chang X-B, Rommens JM, Bear CE (1993): The cystic fibrosis mutation (Δ-F508) does not influence the chloride channel activity of CFTR. Nature Genetics 3:311-316.

Lingueglia E, Voilley N, Waldmann R, Lazdunski M, Barbry P (1993): Expression cloning of an epithelial amiloride-sensitive Na+ channel. FEBS Lett. 318:95-99.

Logothetis DE, Movahedi S, Satler C, Lindpainter K, Nadal-Ginard B (1992): Incremental reductions of positive charge within the S4 region of a voltage-gated K channel result in corresponding decreases in gating charge. Neuron 8:531-540.

Lopez GA, Jan YN, Jan LY (1991): Hydrophobic substitution mutations in the S4 sequence alter voltage-dependent gating in Shaker K channels. Neuron 7:327-335.

MacKinnon R (1991): Determination of the subunit stoichiometry of a voltage-activated potassium channel. Nature 350:232-235.

MacKinnon R, Miller C (1989): Mutant potassium channels with altered binding of charybdotoxin, a pore-blocking peptide inhibitor. Science 245:1382-1385.

Matsuda H, Saigusa A, Irisawa H (1987): Ohmic conductance through the inwardly rectifying K^+ channel and blocking by internal Mg^{2+}. Nature 325:156-159.

McCarty NA, O'Neil RG (1992): Calcium signaling in cell volume regulation. Physiol Rev 72:1037-1061.

McGrath JP, Varshavsky A (1989): The yeast STE6 gene encodes a homolog of the mammalian multidrug resistance P-glycoprotein. Nature 340:400-404.

Noda M, Takahashi H, Tanabe T, Toyosato M, Kikyotani S, Furutani Y, Hirose T, Takashima H, Inayama S, Miyata T, Numa S (1983): Structural homology of *Torpedo californica* acetylcholine receptor subunits. Nature 302:528-532.

North RA (1989): Drug receptors and the inhibition of nerve cells. Br J Pharmacol 98:13-28.

Pacholczyk T, Blakely RD, Amara SG (1991): Expression cloning of a cocaine-sensitive and antidepressant-sensitive human noradrenaline transporter. Nature 350:350-354.

Papazian DM, Timpe LC, Jan YN, Jan LY (1991): Alteration of voltage-dependence of Shaker potassium channel by mutations in the S4-sequence. Nature 349:305-310.

Patton DE, West JW, Catterall WA, Goldin AL (1993): A peptide segment critical for sodium channel inactivation functions as an inactivation gate in a potassium channel. Neuron 11:967-974.

Paulmichl M, Li Y, Wickman K, Ackerman M, Peralta E, Clapham D (1992): New mammalian chloride channel identified by expression cloning. Nature 356:238-241.

Pines G, Danbolt NC, Bjorias M, Zhang Y, Bendahan A, Elde L, Koepsell H, Storm-Mathisen J, Seeburg PE, Kanner BI (1992): Cloning and expression of a rat brain L-glutamate transporter. Nature 360:464-467.

Pribilla I, Takagi T, Langosch D, Bormann J, Betz H (1992): The atypical M2 subunit of the β subunit confers picrotoxinin resistance to inhibitory glycine

receptor channels. EMBO J 11:4305-4311.

Riordan JR (1993): The cystic fibrosis transmembrane conductance regulator. Annu Rev Physiol 55:609-630.

Riordan JR, Rommens JM, Kerem B, Alon N, Rozmahel R, Grzelczak Z, Zielenski J, Lok S, Plasvic N, Chou J-L, Drumm ML, Iannuzzi MC, Collins FS, Tsui L-C (1989): Identification of the cystic fibrosis gene: Cloning and characterization of complementary DNA. Science 245:1066-1072.

Ritz MC, Lamb RJ, Goldberg SR, Kuhar MJ (1987): Cocaine receptors on dopamine transporters are related to self-administration of cocaine. Science 237:1219-1223.

Rommens JM, Iannuzzi MC, Kerem B, Drumm ML, Melmer G, Dean M, Rozmahel R, Cole JL, Kennedy D, Hidaka N, Zsiga M, Buchwald M, Riordan JR, Tsui L-C, Collins FS (1989): Identification of the cystic fibrosis gene: Chromosome walking and jumping. Science 245:1059-1065.

Root MJ, MacKinnon R. (1993): Identification of an external divalent cation-binding site in the pore of a cGMP-activated channel. Neuron 11:459-466.

Sachs F (1991): Stretch-sensitive ion channels: an update. In Corey DP, Roper SD (eds): Sensory Transduction. New York: Rockefeller University Press.

Sakurada K, Masu M, Nakanishi S (1993): Alteration of Ca^{2+} permeability and sensitivity to Mg^{2+} and channel blockers by a single amino acid substitution in the N-methyl D-aspartate receptor. J Biol Chem 268:410-415.

Schofield PR, Darlison M, Fujita N, Burt D, Stephenson FA, Rodriguez H, Rhee L, Ramachandran J, Reale V, Glencorse T, Seeburg P, Barnard E (1987): Sequence and functional expression of the GABA-A receptor shows a ligand-gated receptor super-family. Nature 328:221-327.

Shimada S, Kitayama S, Lin CL, Patel A, Nanthakumar E, Kuhar M, Uhl G (1991): Cloning and expression of a cocaine-sensitive dopamine transporter complementary-DNA. Science 254:576-578.

Sommer B, Kohler M, Sprengler R, Seeburg PH (1991): RNA editing in brain controls a determinant of ion flow in glutamate-gated channels. Cell 67:11-19.

Stanfield PR, Davies NW, Shelton PA, Khan IA, Brammar WJ, Standen NB, Conley EC (1994): The intrinsic gating of inward rectifier K channels expressed

from the murine IRK1 gene depends on voltage, K^+ and Mg^{2+}. J. Physiol 475:1-7.

Steinmeyer K, Lorenz C, Pusch M, Koch MC, Jentsch TJ (1994): Multimeric structure of ClC-1 chloride channel revealed by mutations in dominant myotonia congenita (Thomsen). EMBO J 13:737-743.

Steinmeyer K, Ortland C, Jentsch TJ (1991): Primary structure and functional expression of a developmentally regulated skeletal muscle chloride channel. Nature 354:301-304.

Stuhmer W, Conti F, Suzuki H, Wang X, Noda M, Yahagi N, Kubo H, Numa S (1989): Structural parts involved in activation and inactivation of the sodium channel. Nature 339:597-603.

Stutts MJ, Chinet TC, Mason SJ, Fullton JM, Clarke LL, Boucher RC (1992): Regulation of Cl^- channels in normal and cystic fibrosis airway epithelial cells by extracellular ATP. Proc Natl Acad Sci USA 89:1621-1625.

Taglialatela M, Wible BA, Caporaso R, Brown AM (1994): Specification of pore properties by the carboxyl terminus of inwardly rectifying K^+ channels. Science 264:844-847.

Takumi T, Moriyoshi K, Aramori I, Ishii T, Oiki S (1991): Alteration of channel activities and gating by mutations of slow IsK potassium channel. J Biol Chem 266:2192-2198.

Takumi T, Ohkubo H, Nakanishi S (1988): Cloning of a membrane protein that induces a slow voltage-gated potassium channel. Science 242:1042-1045.

Teem JL, Berger HA, Ostedgaard LS, Rich DP, Tsui L-C, Welsh MJ (1993): Identification of revertants for the cystic fibrosis ΔF508 mutation using STE6-CFTR chimeras in yeast. Cell 73:335-346.

Thiemann A, Grunder S, Pusch M, Jentsch TJ (1992): A chloride channel widely expressed in epithelial and non-epithelial cells. Nature 356:57-60.

Tufty RM, Kretsinger RH (1975): Troponin and parvalbumin calcium binding regions predicted in myosin light chain and T4 lysosome. Science 187:167-169.

Uchida S, Sasaki S, Furukawa T, Hiraoka M, Imai T, Hirata Y, Marumo F (1993): Molecular cloning of a chloride channel that is regulated by dehydration and expressed predominantly in kidney medulla. J Biol Chem 268:3821-3824.

Unwin N (1993): Neurotransmitter action: opening of ligand-gated ion channels. Neuron 10:13-41.

Unwin N (1989): The structure of ion channels in membranes of excitable cells. Neuron 3:665-676.

Valverde MA, Diaz M, Sepulveda FV, Gill DR, Hyde SC, Higgins CF (1992): Volume-regulated chloride channels associated with the human multidrug-resistance P-glycoprotein. Nature 355:830-833.

Vandenberg CA (1987): Inward rectification of a potassium channel in cardiac ventricular cells depends on internal magnesium ions. Proc Natl Acad Sci USA 84:2560-2564.

Varnum M, Busch AE, Bond CT, Maylie J, Adelman JP (1993): The Min K-channel underlies the cardiac potassium current I(KS) and mediates species-specific responses to protein kinase C. Proc Natl Acad Sci USA 90:11528-11534.

Verdoorn TA, Burnashev N, Monyer H, Seeburg PH, Sakmann B (1991): Structural determinants of ion flow through recombinant glutamate receptor channels. Science 252:1715-1718.

Vernino S, Amador M, Luetje CW, Patrick J, Dani JA (1992): Calcium modulation and high calcium permeability of neuronal nicotinic acetylcholine receptors. Neuron 8:127-134.

Verrall S, Hall ZW (1992): The N-terminal domains of acetylcholine receptor subunits contain recognition signals for the initial steps of receptor assembly. Cell 88:23-31.

Walker JE, Saraste M, Runswick MJ, Gay NJ (1982): Distantly related sequences in the α- and β-subunits of ATP synthase, myosin, kinases, and other ATP-requiring enzymes and a common nucleotide binding fold. EMBO J 1:945-951.

Xu M, Akabas MH (1993): Amino acids lining the channel of the γ-aminobutyric acid type A receptor identified by cysteine substitution. J Biol Chem 268:21505-21508.

Yang X-C, Labarca C, Nargeot J, Ho B, Davidson N, Lester HA (1992): Cell-specific posttranslational events affect functional expression at the plasma membrane but not tetrodotoxin sensitivity of the rat brain IIA sodium channel α subunit expressed in mammalian cells. J Neurosci 12:268-277.

Yang X-C, Sachs F (1990): Characterization of stretch-activated ion channels in *Xenopus* oocytes. J Physiol 431:103-122.

Yellen G, Jurma ME, Abramson T, MacKinnon R (1991): Mutations affecting internal TEA blockade identify the probable pore-forming region of a K^+ channel. Science 251:939-941.

Yool AJ, Schwartz TL (1991): Alteration of ionic selectivity of a K channel by mutation of the H5 region. Nature 349:700-704.

Yu X-M, Hall ZW (1991): Extracellular domains mediating ε subunit interactions of muscle acetylcholine receptor. Nature 352:64-67.

Zagotta WN, Hoshi T, Aldrich RW (1990): Restoration of inactivation in mutants of Shaker potassium channels by a peptide derived from SHB. Science 250: 568-571.

Figure 1. Predicted transmembrane topologies of ion channel families. Shaded background represents the plasma membrane; dark rectangles are putative transmembrane α-helices. N and C indicate the terminii of the amino acid sequence. **A**, single subunit of a voltage-gated K^+ channel. *P* indicates the pore region; jagged structure signifies putative β-strand. **B**, voltage-gated Na^+ or K^+ channel topology. **C**, cyclic-nucleotide gated channel. **D**, inward rectifier K^+ channel. **E**, ligand-gated channel. Left, side view of a single α-subunit. Ligand-binding domain is extracellular; M2 pore-lining domain is shown as a rounded rectangle. Right, top view of the full receptor, made up of five subunits. Each circle represents a transmembrane domain; M2 domain is shaded. Small shaded circles represent ligand-binding domains. **F**, cystic fibrosis transmembrane conductance regulator chloride channel (CFTR). NBF1 and NBF2, nucleotide binding folds 1 and 2. R, R-domain. **G**, ClC chloride channel. D13, cytoplasmic hydrophobic domain.

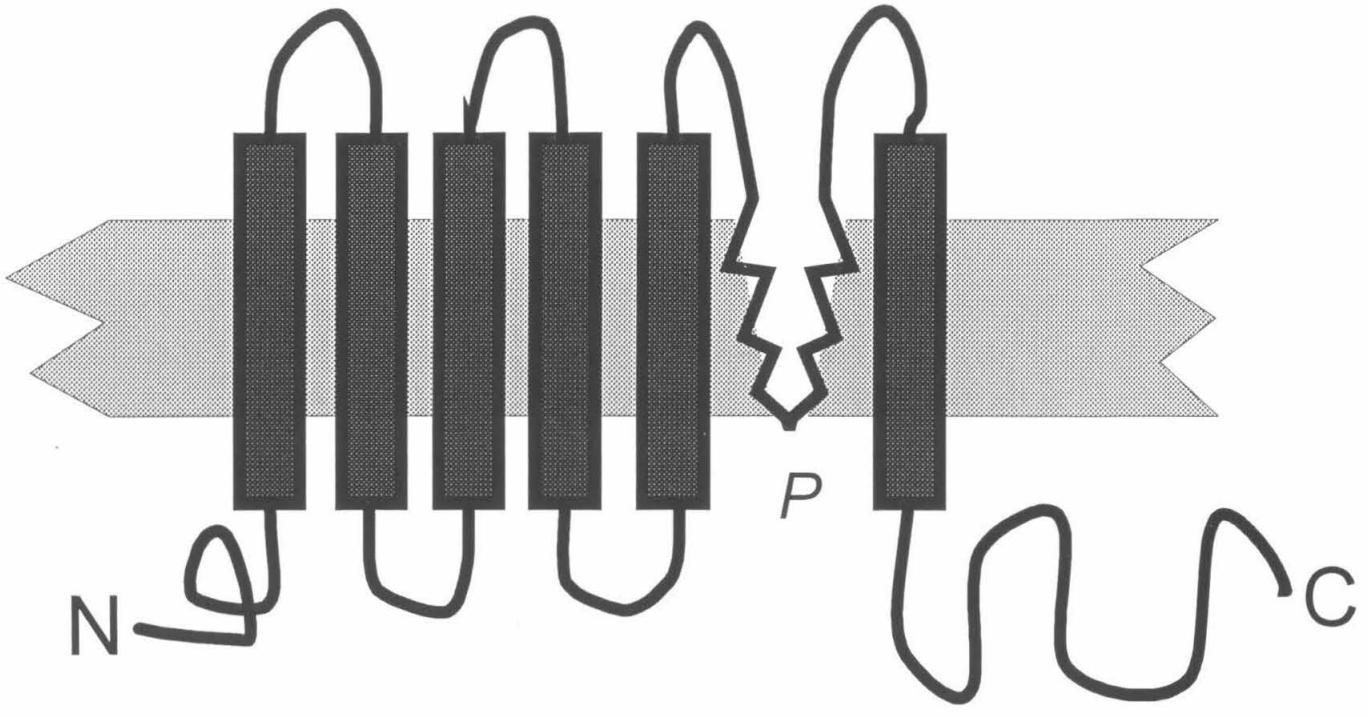

Voltage-gated K channel subunit

Figure 1A

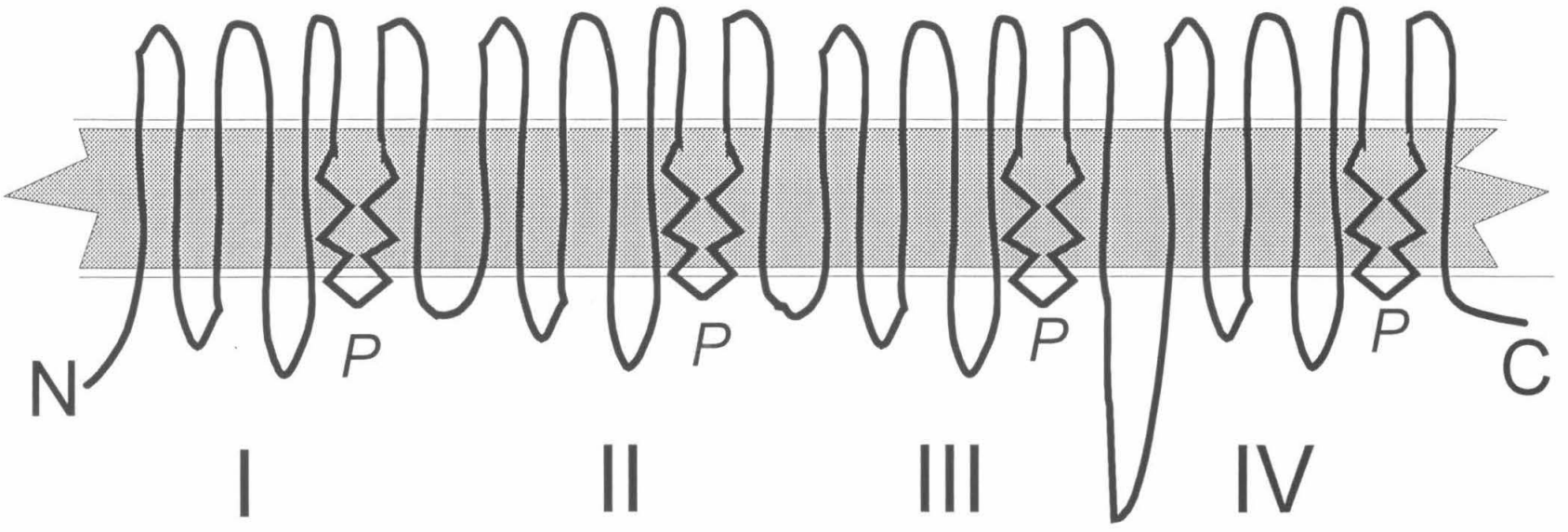

fourfold internal repeat

Voltage-gated Na and Ca channels

Figure 1B

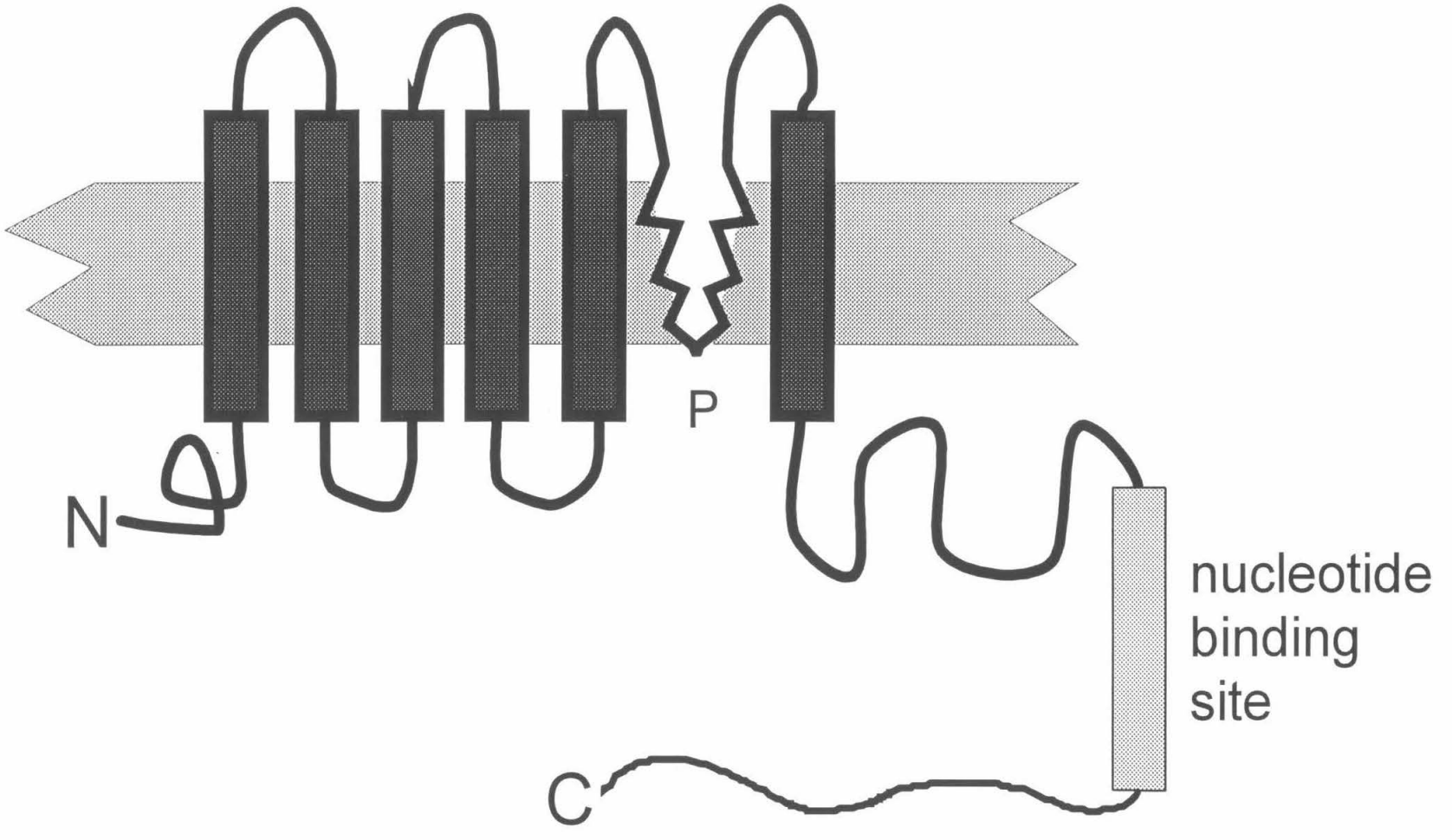

Cyclic nucleotide-gated channel

Figure 1C

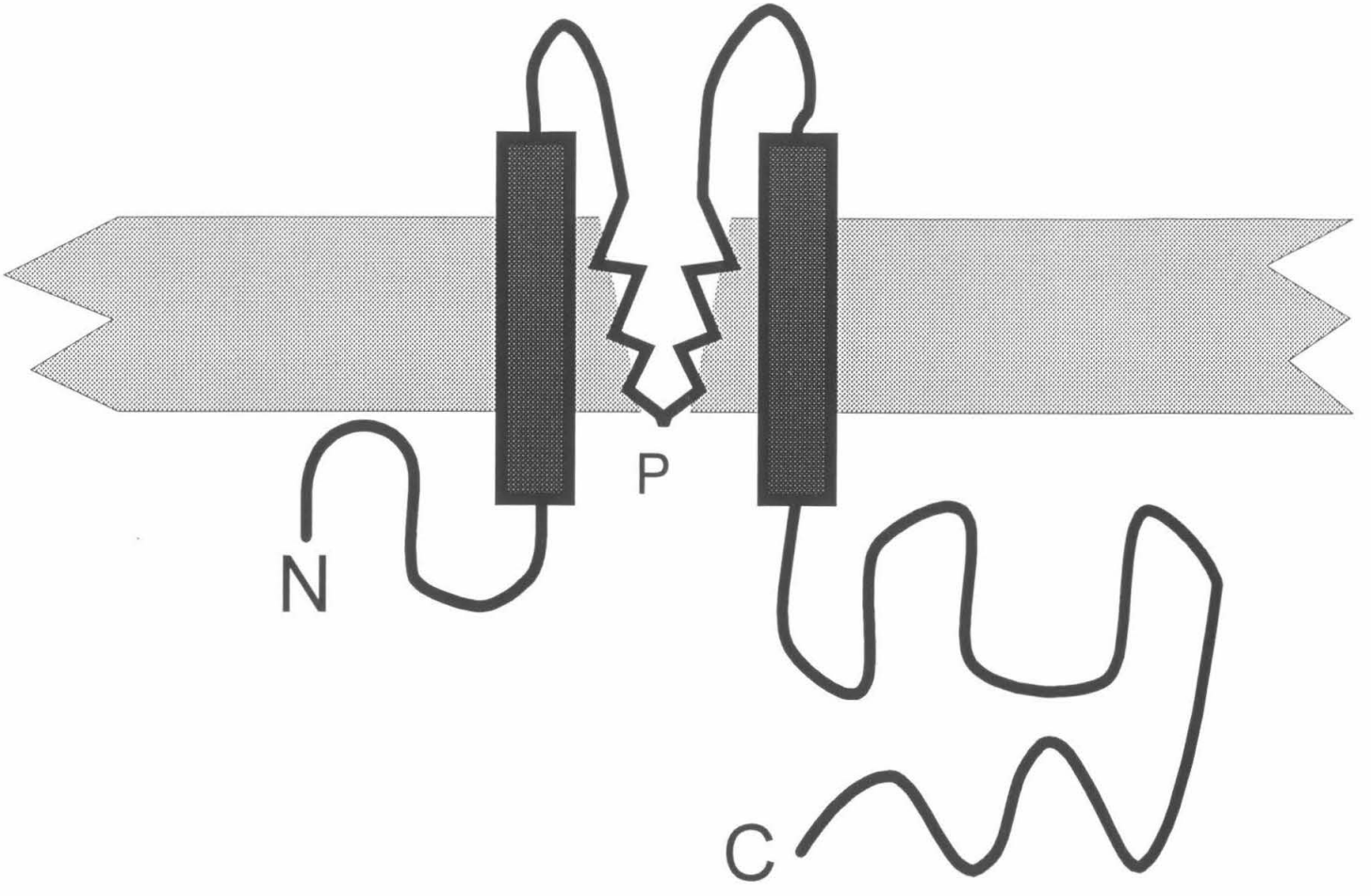

Inward rectifier K channel

Figure 1D

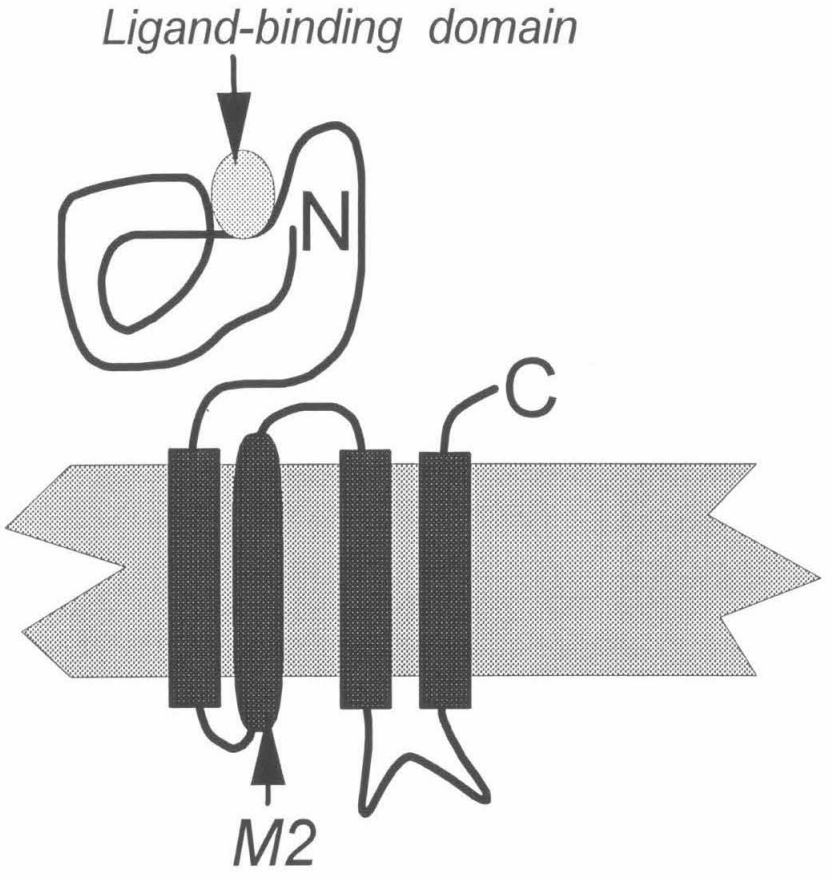

Single subunit

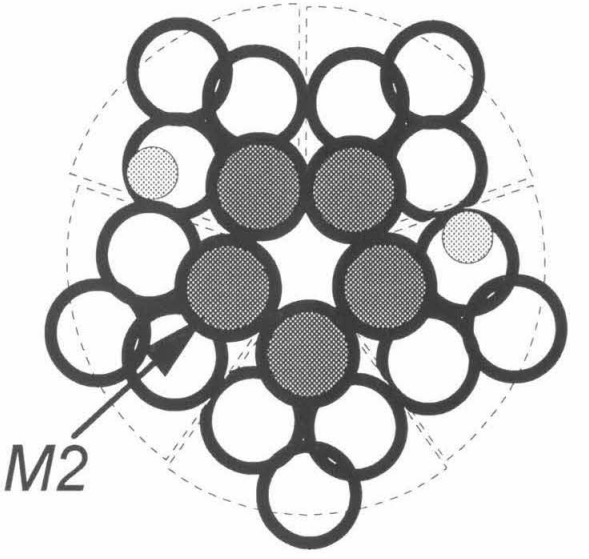

Full receptor has
5 pseudo-symmetric
subunits

Ligand-gated channel

Figure 1E

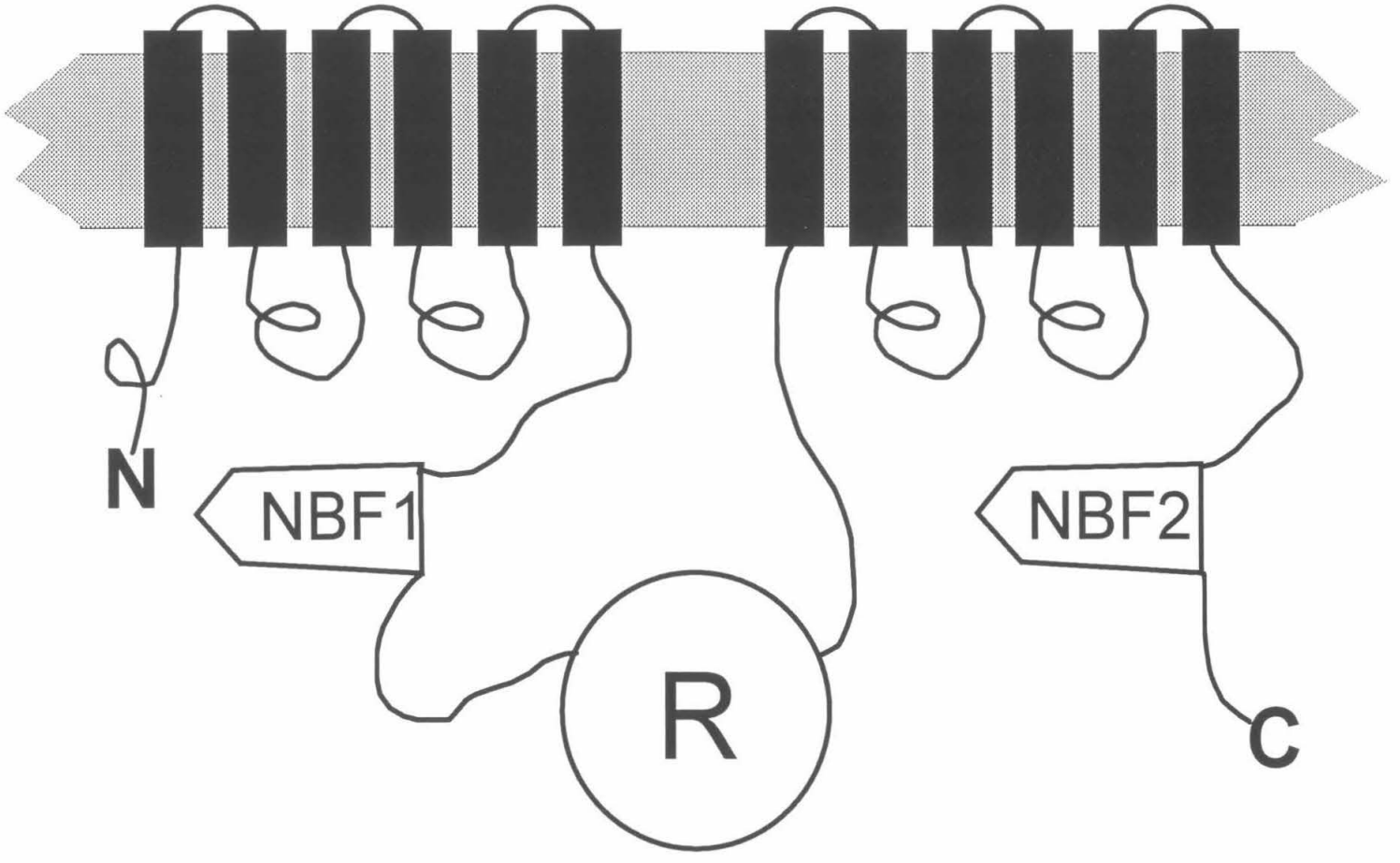

Cystic fibrosis chloride channel (CFTR)

Figure 1F

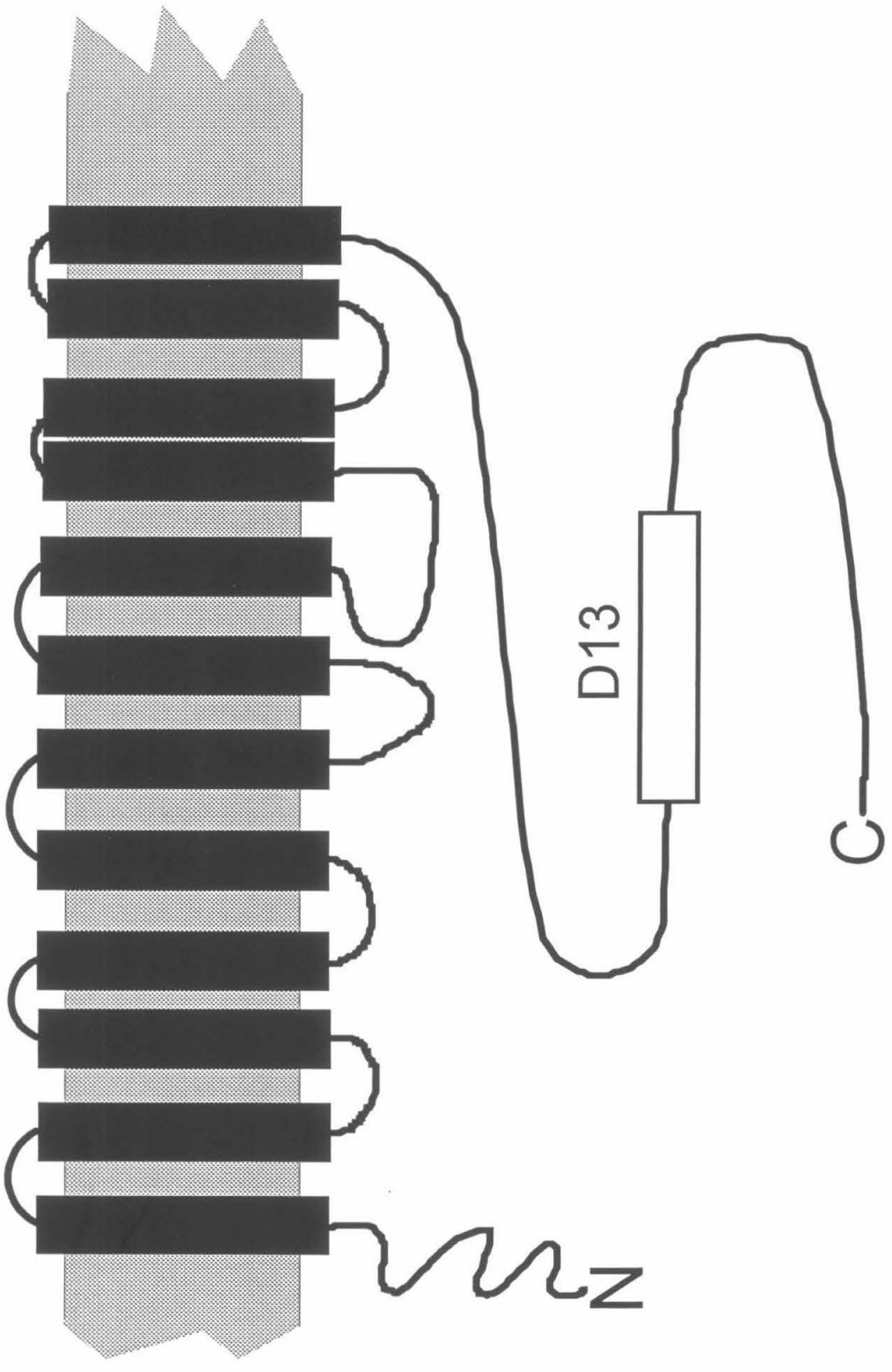

ClC chloride channel

Figure 1G

Voltage-Dependent Block of the CFTR Cl^- Channel By Two Closely Related Arylaminobenzoates

N.A. McCarty, S. McDonough, B.N. Cohen,

J.R. Riordan[1], N. Davidson, and H.A. Lester

Division of Biology 156-29, California Institute of Technology,
Pasadena, California 91125
and
[1]The Hospital for Sick Children, Toronto, Ontario, and
Dept. of Biochemistry and Clinical Biochemistry,
University of Toronto
Toronto, Ontario, Canada M5G 1X8

ABSTRACT

The gene defective in cystic fibrosis encodes a Cl^- channel, the cystic fibrosis transmembrane conductance regulator (CFTR). CFTR is blocked by diphenylamine-2-carboxylate (DPC), when applied extracellularly at mM concentrations. We studied the block of CFTR expressed in *Xenopus* oocytes by DPC or by a closely related molecule, flufenamic acid (FFA). Block of whole-cell CFTR currents by bath-applied DPC or by FFA, both at 200 μM, requires several min to reach full effect. Blockade is voltage dependent, suggesting open-channel block: currents at positive potentials are not affected but currents at negative potentials are reduced. The binding site for both drugs senses ~40% of the electric field across the membrane, measured from the inside. In single-channel recordings from excised patches without blockers, the conductance was 8.0 ± 0.4 pS in symmetric 150 mM Cl^-. A subconductance state, measuring approximately 60% of the main conductance, was often observed. Bursts to the full open state lasting up to tens of seconds were uninterrupted at depolarizing membrane voltages. At hyperpolarizing voltages, bursts were interrupted by brief closures. Either DPC or FFA (50 μM) applied to the cytoplasmic face or to the extracellular face of the channel led to an increase in flicker at V_m = -100 mV and not at V_m = +100 mV, in agreement with whole-cell experiments. DPC induced a higher frequency of flickers from

the cytoplasmic side than the extracellular side. FFA produced longer closures than DPC; the FFA closed time was roughly equal (~1.2 ms) at -100 mV with application from either side. In cell-attached patch recordings with DPC or FFA applied to the bath, there was flickery block at V_m = -100 mV, confirming that the drugs permeate through the membrane to reach the binding site. The data are consistent with the presence of a single binding site for both drugs, reached from either end of the channel. Open-channel block by DPC or FFA may offer tools for use with site-directed mutagenesis to describe the permeation pathway.

INTRODUCTION

The gene that is defective in cystic fibrosis encodes the cystic fibrosis transmembrane conductance regulator (CFTR); secondary structure predictions suggested that the protein may serve as an ion channel (Riordan, Rommens, Kerem, Alon, Rozmahel, Grzelczak, Zielenski, Lok, Plavsic, Chou, Drumm, Iannuzzi, Collins, and Tsui, 1989). Heterologous expression of the CFTR gene in epithelial and non-epithelial cells indicates that this gene encodes a Cl^- channel activated by the cAMP-protein kinase A pathway (Gregory, Cheng, Rich, Marshall, Paul, Hehir, Ostedgaard, Klinger, Welsh, and Smith, 1990; Rich, Anderson, Gregory, Cheng, Paul, Jefferson, McCann, Klinger, Smith, and Welsh, 1990; Anderson, Rich, Gregory, Smith, and Welsh, 1991; Kartner, Hanrahan, Jensen, Naismith, Sun, Ackerley, Reyes, Tsui, Rommens, Bear, and Riordan, 1991). The characteristics of the channel--low conductance, linear current-voltage relation, and selectivity for Cl^- over I^---match those of the Cl^- permeability pathway now believed to be defective in cystic fibrosis (Welsh, 1990; Cliff, Schoumacher, and Frizzell, 1992).

This study concerns the permeation properties of the CFTR channel, as probed by small blocking molecules. By investigating the interaction of an open channel blocker with the pore of the protein, we hope to improve our

understanding of CFTR function.

Several classes of molecules have been developed as inhibitors of various kinds of Cl^- channels. The disulfonic stilbenes, first developed as inhibitors of the red blood cell anion exchanger, block the outward rectifier Cl^- channel of epithelial cells (Singh, Afink, Venglarik, Wang, and Bridges, 1991; Tilmann, Kunzelmann, Fröbe, Cabantchik, Lang, Englert, and Greger, 1991). The phenoxyacetic acid derivative, indanyloxyacetic acid 94, was developed as a probe for isolation of an epithelial Cl^- channel (Landry, Reitman, Cragoe, and Al-Awqati, 1987). Anthracene-9-carboxylate is a useful inhibitor of the voltage-gated Cl^- channel of skeletal muscle, but is ineffective on the Cl^- channels of canine trachea and shark rectal gland, two chloride-secreting tissues (*see* Cabantchik and Greger, 1992). The arylaminobenzoates were developed by Greger and co-workers, who showed that diphenylamine-2-carboxylate (DPC) inhibited the basolateral Cl^- channel of renal thick ascending limb cells (DiStefano, Wittner, Schlatter, Lang, Englert, and Greger, 1985). DPC and its congeners are effective inhibitors of several epithelial Cl^- channels (Wangemann, Wittner, DiStefano, Englert, Lang, Schlatter, and Greger, 1986; Bijman, Englert, Lang, Greger, and Frömter, 1987; Tilmann, Kunzelmann, Fröbe, Cabantchik, Lang, Englert, and Greger, 1991).

The disulfonic stilbene, DIDS, is not an effective blocker of CFTR when applied to the bath (Kartner et al., 1991; Cunningham, Worrell, Benos, and

Frizzell, 1992). In contrast, DPC has been used in several CFTR heterologous expression studies, in which it inhibited whole-cell currents at fairly high concentrations (Rich et al., 1990). However, the single-channel and molecular bases of blockade of CFTR have not yet been described. In this report, we describe results from our studies of CFTR using two closely-related arylaminobenzoates (DPC and flufenamic acid, Fig. 1) as probes to investigate permeation properties of the channel. We find that both DPC and flufenamic acid (FFA) block the CFTR channel in a voltage-dependent manner, by introducing brief closures in the open channel bursts. Analyses of the voltage dependence and kinetics of drug-channel interactions allow us to suggest possible mechanisms for blockade of the pore by DPC and FFA. These results will serve as a basis for future studies involving site-directed mutagenesis of proposed pore-lining segments of the CFTR protein.

Portions of these data have been published previously in abstract form (McCarty, Cohen, Quick, Riordan, Davidson, and Lester, 1992; McDonough, McCarty, Riordan, Davidson, and Lester, 1993).

METHODS AND MATERIALS

Preparation of oocytes and cRNA

Stage V - VI oocytes from female *Xenopus* were prepared as described (Quick, Naeve, Davidson, and Lester, 1992), and incubated at 18°C in incubation medium (see below). For the first day after isolation, incubation medium also contained 5% horse serum (Quick et al., 1992). In some cases, horse serum was continued for several days. In all cases, however, serum was removed at least 8 h prior to recording. cRNA was prepared from a construct carrying the full coding region of CFTR in a pSP64(poly A) vector (Bear, Duguay, Naismith, Kartner, Hanrahan, and Riordan, 1991). Oocytes were injected with 1 - 2 ng or 12 - 25 ng cRNA for whole-cell or single-channel recordings, respectively, in a volume of ~50 nL. Recordings were made 48 - 96 h after injection. In experiments using heterologous expression of the human beta-2 adrenergic receptor (β_2-AR), 0.1 to 5 ng of this cRNA were injected along with CFTR. Injection of higher concentrations of β_2-AR cRNA in CFTR-injected oocytes led to spontaneous oscillations of holding current. This was likely due to spontaneous activation of the beta receptor, leading to high concentrations of cAMP, and could be prevented by incubation in propranolol (50 μM) for 8 h prior to recording.

Electrophysiology

Standard two-electrode voltage clamp techniques were used to study whole-cell currents. Electrodes were pulled in four stages from borosilicate glass (Sutter Instr. Co., Novato, CA), and filled with 3 M KCl. Pipette resistances measured 0.5 to 2.5 MΩ in bath solution. Membrane voltages were typically held at either -30 mV or -45 mV and stepped to a series of test potentials by an Axoclamp 2A amplifier (Axon Instuments, Foster City, CA). Currents filtered at 500 Hz were stored on videotape after digitization or were acquired directly on-line using the Clampex program of pCLAMP (Axon).

DPC and FFA also block the endogenous Ca^{2+}-activated Cl^- conductance, but with time course and voltage dependence different from CFTR blockade. Blockade of the endogenous conductance was complete within 1-2 min of exposure, suggesting an action from the outer surface of the membrane. The effects of DPC and FFA were not dependent upon voltage: inward and outward currents were inhibited equally (data not shown). These results are consistent with the initial description of blockade of the oocyte channel by FFA and niflumic acid (White and Aylwin, 1990). It should be noted, however, that Wu and Hamill (1992) recently reported a slight voltage-dependence of the blockade of the endogenous channel in oocytes by 5-nitro-2-(3-

phenylpropylamino) benzoic acid (NPPB), a blocker related to DPC and FFA. In our experiments, cAMP-activated currents were at least five times greater than the background currents; therefore, blockade of the endogenous channel produced negligible distortion in the overall effect of DPC and FFA.

For single-channel recordings, oocytes were shaken in stripping solution (see below) for 15 min. The vitelline membrane was then removed manually using fine forceps. Recordings were performed in both cell-attached and excised, inside-out modes, using electrodes pulled in four stages from borosilicate glass (Sutter). Pipette resistances ranged from 10 to 40 MΩ. Seal resistances ranged from 20 to ~200 GΩ. Patch currents were measured with an Axopatch 1D amplifier (Axon). Data were filtered at 2 - 2.5 kHz and stored on videotape. For subsequent analysis, records were filtered at 1 kHz with an 8-pole Bessel filter (Frequency Devices model 902, Haverhill, MA) and digitized at 100 μs per point during acquisition by the Fetchex program of pClamp (Axon). In the single-channel traces shown, inward currents (anions passing from the cytoplasm to the external solution) are shown as negative (downward) deflections from baseline. Voltages in single-channel experiments are indicated as transmembrane voltage (internal minus external). In cell-attached recordings, we assume that the resting cell membrane potential is zero.

Analysis

Whole-cell current records were analyzed using the Clampfit program of pClamp (Axon). For construction of I/V curves and for calculation of voltage dependence of block, data were taken from the latter half of a 75 ms step to each potential and averaged. The current at each potential before cAMP stimulation and after washout was subtracted to determine cAMP-dependent current. For single-channel measurements, digitized Fetchex records were analyzed to produce idealized records and histogram files by the IPROC program (Axon) (Sachs, Neil, and Barkakati, 1982; Sachs, 1983). IPROC uses a cubic splining function to interpolate between data points. Transition analysis employed an open/closed border midway between the open and closed levels. The histogram files generated by IPROC were analyzed by NFITS (Island Products, Galveston, TX), a nonlinear least squares curve-fitting procedure.

For calculation of open probability within a burst (P_O), closings longer than 5 ms defined the end of a burst, since longer bursts often exceeded the IPROC burst memory. Bursts with baseline shift or more than one channel were not used for P_O calculations. System dead time was calculated and experimentally confirmed to be ~0.3 ms for a corner frequency (F_C) = 1 kHz. In closed-time histograms, curve-fitting began with the first bin past the dead time, the bin from 0.3 to 0.4 ms. Time constants were then taken from the extrapolated curves. Unless noted otherwise, values given are mean ± S.E.M.

Solutions

The bath solution for whole-cell studies was ND96 without added Ca^{2+} salts, containing (mM): 96 NaCl; 2 KCl; 1 $MgCl_2$; 5 HEPES; pH 7.5. Incubation medium was ND96 with added $CaCl_2$ (1.5 mM), Na-pyruvate (2.5 mM) and gentamycin (50 μg/ml), pH 7.5. The hypertonic stripping solution contained (mM): 200 monopotassium aspartate; 20 KCl; 1 $MgCl_2$; 10 EGTA; 10 HEPES-KOH; pH 7.2. For patch-clamp experiments, the pipette contained (mM): 150 N-methyl-D-glucamine·Cl; 0.5 $MgCl_2$; 10 TES; pH adjusted to 7.4 with Tris. The intracellular solution for inside-out patches contained (mM): 150 NMDG·Cl; 1.1 $MgCl_2$; 2 Tris·EGTA; 1 MgATP (from equine muscle, <1 ppm vanadium); 10 TES; pH 7.4; and in some cases, 2 MgATP; and 10 NaF. Bath solutions were delivered by gravity feed at a rate of ~3 ml/min. Intracellular cAMP levels were increased by application of either 1 μM isoproterenol or the cAMP-elevating cocktail of (μM): 1-10 forskolin; 10-200 dibutyryl-cAMP; and 10-200 3-isobutyl-1-methylxanthine. Cytoplasmic (4.3 mM) and extracellular (7.3 mM) ethanol, cytoplasmic 10 mM NaF, and raising cytoplasmic ATP concentration from 1 to 2 mM had no effects on channel kinetics; these data were combined to form the unblocked channel data. Four mM ethanol was also without effect on whole-cell CFTR currents.

When patches containing activated CFTR channels were excised into ATP solution, channel activity frequently ran down over the course of seconds.

We considered it likely that this was due to a membrane-bound phosphatase that reversed the phosphorylation of CFTR by protein kinase A, or perhaps due to intrinsic phosphatase activity of CFTR. We found that addition of 10 mM NaF to the intracellular solution slowed, although did not prevent, this run-down.

DPC and FFA were dissolved in 100% ethanol at stock concentrations of 1.25 M and 0.15 M, respectively.

Source of reagents

Unless otherwise noted, all reagents were obtained from Sigma Chemical Co. (St. Louis, MO). TES and DPC (N-phenylanthranilic acid) were from Aldrich Chemical Co. (Milwaukee, WI); FFA was from Sigma. Tris was from Boehringer Mannheim Biochemicals (Indianapolis, IN) and serum was from Irvine Scientific (Santa Ana, CA).

RESULTS

Whole-cell recordings

Cyclic AMP-dependent Cl^- currents were strongly activated in oocytes injected with CFTR and stimulated by either (1) application of cAMP-stimulating cocktail in cells injected with CFTR alone or (2) exposure to isoproterenol in cells coinjected with the human β_2-AR and CFTR. In cells expressing β_2-AR alone or CFTR alone, exposure to 10 μM isoproterenol did not lead to activation of currents significantly greater than prestimulation control (data not shown). Similarly, exposure of noninjected cells to the cAMP cocktail was without effect.

We took steps to avoid significant contamination of our whole-cell records by the endogenous Ca^{2+}-activated Cl^- [$Cl_{(Ca)}$] channels (see Methods). We used nominally Ca-free solutions and recorded only from oocytes whose resting conductances were low (holding current at V_m = -45 mV ≤ 250 nA). CFTR currents were easily distinguished from currents through the endogenous $Cl_{(Ca)}$ channel, because (1) the latter typically showed some decay of outward current through time while CFTR currents were consistently time-independent; and (2) the endogenous currents show pronounced outward rectification, but CFTR currents are characterized by a nearly linear I/V relation. The slightly sublinear conductance of CFTR currents (see below)

observed in our experiments at strongly hyperpolarizing voltages probably arises from the lower value of cytoplasmic Cl^- concentration relative to that in the bath. Parenthetically, we found that prolonged clamping of oocytes at holding potentials more negative than -30 mV led to further decreases of conductance at highly negative potentials. Presumably this effect arose from re-equilibration of intracellular [Cl^-] at the new holding potential.

Effects of DPC on whole-cell currents

DPC blockade of CFTR was slow and voltage dependent. Exposure of cAMP-activated oocytes to DPC led to reduction in inward holding current in two phases. The initial, fast phase was probably due to partial blockade of the $Cl_{(Ca)}$ channel in addition to partial block of CFTR from the outside. The magnitude of this phase varied depending upon the size of the background $Cl_{(Ca)}$ current. The subsequent phase required 7 - 10 min and involved a further decline in holding current. The extent of blockade of cAMP-stimulated holding current (at V_m = -30 mV) after this period was 37 ± 4 % (n=6) for 200 μM DPC and 80 ± 5 % (n=8) for 1 mM DPC. At equilibrium, DPC blockade of CFTR was clearly voltage dependent: there was pronounced outward rectification in the I/V relation (Fig. 2). Inward currents were greatly reduced, while outward currents were mostly unaffected. DPC and some congeners block non-selective cation channels (Gögelein, Dahlem, Englert, and Lang, 1990)

and inhibit prostaglandin biosynthesis (Flower, 1974), thus affecting intracellular metabolism. These secondary actions do not affect CFTR and are not apparent in the oocyte system at the drug concentrations used, because outward CFTR currents do not change over time. The persistence of outward current levels also serves as an internal control to ensure that the activation level of CFTR had not decreased over the 7 - 10 min required for equilibrium

blockade. The effects of DPC were fully reversible with a 10 min wash (data not shown).

The voltage-dependence of block was calculated using average current values from the latter half of the 75 ms voltage steps to potentials ranging from -100 to +80 mV. Thus, the effect of voltage upon the apparent dissociation constant was calculated as follows:

$$K_D(V) = [\text{drug}] \bullet \frac{I}{I_o - I}$$

where I_o is the current level at voltage V in cAMP-activated oocytes in the absence of blocker and I is the current level after several min of treatment with drug (Fig. 3). The calculated K_D at 0 mV averaged 912 ± 60 μM and K_D at -100 mV averaged 237 ± 34 μM for cells acutely exposed to 200 μM DPC (n = 7). For experiments with 1 mM DPC (for instance, Fig. 3), the data gave the following values: K_D(0 mV) = 1116 ± 51 μM and K_D(-100 mV) = 346 ± 41 μM (n = 3). The electrical distance sensed by the blocker molecule, θ, is proportional to the slope of the curve of K_D versus voltage. Assuming valence = -1 and a single binding site for DPC, we calculated an average θ = 41 ± 7.0 %, as measured from the inside.

Effects of FFA on whole-cell currents

Oocytes expressing CFTR currents displayed a biphasic response to

bath-applied 200 μM FFA. There was an initial fast block followed by a sizeable increase in inward current after ~15 sec, contrary to the expected blockade (n=4, data not shown). We circumvented this secondary effect by injecting oocytes with 500 pmol EGTA (50 nL of a 10 mM stock, pH 8.4) 4 to 8 h prior to recording. Assuming a volume of 1 μL per oocyte, the final EGTA concentration was 0.5 mM. FFA applied to EGTA-injected oocytes did not cause increased current. With EGTA-injected oocytes, block of CFTR currents was similar to DPC block: there was an initial decline over 1-2 min, followed by a slower decline requiring several min to reach completion.

Release of calcium from intracellular stores, as shown to occur in some cell types (McDougall, Markham, Cameron, and Sweetman, 1988; Poronnik, Ward, and Cook, 1992) upon exposure to FFA and some congeners but not DPC, could have caused the secondary increase in conductance via activation of the $Cl_{(Ca)}$ current. However, the effect of FFA on noninjected oocytes, or on CFTR-injected but unstimulated oocytes, was a simple fast block of the endogenous current (n = 8). We believe that the EGTA-injection result indicates that the secondary effect of FFA might be due to potentiation of CFTR activation, either by (1) an additional intracellular signaling pathway or (2) modification of membrane recycling at the oocyte surface.

Like DPC, FFA blocked inward currents without large effects upon outward currents (Fig. 4). Block of CFTR holding current (at -30 mV) by 200

μM FFA averaged 38 ± 7% (n = 6), as compared to 37 ± 4% for 200 μM DPC. The voltage-dependence of blockade was also similar to that of DPC. Calculated K_D (0 mV) was 1222 ± 88 μM, and K_D (-100 mV) was 289 ± 34 μM (n = 6). Voltage dependence of FFA block showed that $\theta = 41 \pm 3$ %, similar to the value for DPC.

Single-channel recordings

Given the long time course of block and the pronounced voltage dependence for DPC and FFA, we considered it likely that these drugs block the CFTR channel by an interaction with the pore from the cytoplasmic side of the channel. This notion was further investigated in patch-clamp experiments where drug concentrations and site of delivery could be more closely controlled.

Single-channel CFTR currents were measured in oocytes activated by cocktail or heterologous expression of β_2-AR or both (Fig. 5). CFTR channels are characterized by openings lasting up to several tens of seconds, a hallmark which renders this channel easily distinguished from contaminating channels (Bear et al., 1991). In symmetrical 150 mM Cl^-, the single-channel conductance was linear for voltages ±100 mV and ranged from 6.4 to 9.3 pS, averaging 8.0 ± 0.4 pS (n=6). This channel was never seen in noninjected or mock-injected

oocytes (n = 33). A subconductance state of approximately 60% the size of the main conductance was frequently observed at both V_m = -100 and V_m = +100 mV (see for instance asterisk in Fig. 7e, below). The subconductance state often lasted for several seconds, though the time spent in the subconductance state was less than ~5% of total time. At positive V_m, openings to the full conductance level were relatively uninterrupted. At negative V_m, bursts were highly interrupted by brief closures on a ms time scale. As shown in Fig. 5, the brief closures in unblocked channels are more prevalent in cell-attached mode, perhaps reflecting blockade by a cytoplasmic molecule which is lost upon excision (see Tabcharani, Chang, Riordan, and Hanrahan, 1991). In cell-attached mode, currents reversed close to the resting potential (data not shown). The currents shown in Fig. 5 at V_m = ±100 mV in the cell-attached mode, therefore, show slight outward rectification, as expected from the fact that internal Cl^- concentration is several times lower than the pipette concentration of 150 mM.

Effect of cytoplasmic DPC and FFA on single-channel currents

As expected from the whole-cell data, 200 μM DPC applied directly to the cytoplasmic side of an excised patch led to reversible blockade of the single-channel openings at V_m = -100 mV, causing an increase in flicker (Fig. 6;

see especially the expanded traces at right). Detailed analysis of block was carried out with 50 μM DPC or 50 μM FFA; these concentrations produced more clearly resolved open and closed intervals (Fig. 7, Table I). DPC and FFA blockade showed the voltage dependence expected from whole-cell data described earlier; currents recorded at positive V_m were normal, but those at negative V_m were clearly blocked (Fig. 7).

Fig. 8 displays open and closed time histograms for control solutions and for cytoplasmic application of 50 μM DPC or FFA to patches containing activated CFTR channels, in representative experiments; Table I summarizes these effects for several patches. The major point of these single-channel analyses is that blockade by either DPC or FFA is revealed as a decrease in mean open times and an increase in brief closed times. Despite the similar effects of DPC and FFA on whole-cell currents, the details of the kinetic action of these two drugs differed. There was a more pronounced increase in flicker with FFA as compared to DPC, resulting in a clear additional closed time constant. Hence, the mean closed time within a burst (τ_c) for CFTR channels was increased much more by FFA than by DPC. The average closed time for unblocked channels was 0.27 ms. For cytoplasmic DPC, the closed times were increased, but were still fit with a single exponential (τ_c). There was no reliable improvement in histogram fits with two exponential terms, presumably because the DPC-induced closures were several fold more frequent than the

endogenous closings and yet differed from them by less than threefold in average duration. In contrast, closed times with cytoplasmic FFA were much longer, resulting in a fit with two exponentials: one corresponding to unblocked channels (τ_{c1}) and a longer constant from FFA block (τ_{c2}). The mean open time within a burst was greatly reduced by cytoplasmic DPC and FFA. However, mean open times showed no striking differences between drugs (Table I). Therefore, DPC and FFA produced roughly equal frequency of flickers, when applied from the cytoplasmic side.

Effect of extracellular DPC and FFA on single-channel currents

Because we interpreted the fast component of whole-cell block by DPC and FFA to be due to block from outside of the cell, we also studied single channels in excised, inside-out patches with DPC or FFA in the pipette (*i.e.*, bathing the external face of the channel). At 50 μM, neither drug reduced the open-channel conductance when applied from the outside. Both drugs caused a substantial increase in flicker at V_m = -100 mV (Fig. 9). Extracellular FFA blocked the channel more markedly than DPC (Fig. 9). The bursts with FFA in the pipette solution were more frequently interrupted by closures, some as long as several ms. Closures of this duration were not apparent with DPC.

Dwell time analysis of extracellular DPC and FFA on single-channel currents are illustrated for representative patches in Fig. 10 and summarized in

Table I. From the pipette, FFA clearly induced longer closed times than did DPC. As was the case for cytoplasmically-applied drugs, closed time distributions with DPC are fit with one exponential while closed time distributions with FFA are fit with two exponentials. The open time distributions show that both DPC and FFA reduced the mean open time from 8.23 ms in the absence of blockers to 2.5 to 3 ms in the presence of blockers, with no significant difference between DPC and FFA.

Permeation of bath-applied DPC and FFA through the membrane

The slow phases of block by DPC and FFA in whole-cell mode implied that both blockers were membrane permeant. Cell-attached channels were more flickery than excised channels (Fig. 5), vitiating quantitative analysis of additional block by DPC or FFA. Nonetheless, to confirm that DPC can permeate through the plasma membrane to block CFTR from the inside, we activated channels in the cell-attached mode; the oocyte was then exposed to 200 μM DPC in the bath solution. After several min, channel openings were clearly interrupted at V_m = -100 (Fig. 11), but not at V_m = +100 mV (data not shown). FFA applied to the bath (50 μM) also blocked in the cell-attached mode (Fig. 11). Because the drug did not have access to the external side of the channels in the patch in this configuration, these results show that drug molecules can cross the

membrane from the bath and access their binding site from the cytoplasmic side of the channel.

DISCUSSION

The gene that is defective in cystic fibrosis encodes a Cl^- channel which is regulated by the cAMP/protein kinase A pathway. That the protein itself is a Cl^- channel is indicated by the findings that: 1) individuals carrying mutant CFTR gene alleles often show decreased Cl^- transport in affected tissues (Quinton, 1983; Boat, Welsh, and Beaudet, 1989); 2) expression of the CFTR gene in cells from a variety of non-epithelial and CF epithelial sources results in the appearance of a cAMP-activatable Cl^- conductance of specific character (Anderson et al., 1991b; Bear et al., 1991; Kartner et al., 1991; Cunningham et al., 1992); 3) site-directed mutations in the CFTR cDNA result in discrete changes in Cl^- channel function (*e.g.*, Anderson, Gregory, Thompson, Souza, Paul, Mulligan, Smith, and Welsh, 1991; Cheng, Rich, Marshall, Gregory, Welsh, and Smith, 1991; Rich, Gregory, Anderson, Manavalan, Smith, and Welsh, 1991); and 4) purified CFTR protein provides functional Cl^- channels upon incorporation into planar lipid bilayers (Bear, Li, Kartner, Bridges, Jensen, Ramjeesingh, and Riordan, 1992).

The present study characterizes the blocking action of two arylaminobenzoates: diphenylamine-2-carboxylate (DPC) and its derivative, flufenamic acid (FFA). Both DPC and FFA block CFTR in a voltage-dependent manner, by mechanisms to be discussed below. Thus, DPC and FFA will be

useful as probes to characterize the pore of the CFTR channel.

In pioneering studies on heterologous expression of the CFTR gene, 3 mM DPC caused blockade of Cl^- currents in CF airway epithelial cells, CHO cells, and HeLa cells transfected with CFTR (Rich et al., 1990; Anderson et al, 1991b). Blockade was not immediate, and voltage dependence was not investigated. 5-nitro-2-(3-phenyl-propylamino) benzoic acid (NPPB), also blocks the CFTR-like channel found in pancreatic duct cell apical membranes (Gray, Pollard, Harris, Coleman, Greenwell, and Argent, 1990), T84 cell membranes (Tabcharani, Low, Elie, and Hanrahan, 1990), and *Xenopus* oocytes injected with mRNA from shark rectal gland (Sullivan, Swamy, and Field, 1991). In contrast, both DPC and NPPB were only marginally effective at blocking CFTR expressed in oocytes in one study (Cunningham et al., 1992). However, this contradictory finding may be due to fact that Cunningham et al. (1992) determined cAMP-dependent currents by stepping the voltage to 80 mV depolarized from the resting potential. Hence, only outward currents were measured, and our results show that DPC is not an effective blocker of outward currents. We have found no reports on blockade of CFTR by FFA.

In contrast to block of CFTR by arylaminobenzoates, disulfonic stilbenes appear to be ineffective. CFTR currents are insensitive to block by 4,4′-diisothiocyanatostilbene-2,2′-disulfonic acid (DIDS) upon expression in oocytes (Cunningham et al., 1992) and Sf9 cells (Kartner et al., 1991). The small-

conductance CFTR-like channels in pancreatic duct cell apical membranes (Gray et al., 1990) and T84 cell membranes (Tabcharani et al., 1990) were also insensitive to block by DIDS. However, disulfonic stilbenes are effective blockers of the intermediate conductance outward-rectifier anion channel of epithelia (Singh et al., 1991; Tilmann et al., 1991) and the Ca^{2+}-activated Cl^- channel in several cell types. In oocytes, 50 μM DIDS blocked the background conductance in a voltage-independent manner (Cunningham et al., 1992).

Voltage-dependent block of macroscopic currents

Whole-cell currents in CFTR-injected oocytes activated by cAMP were inhibited by both DPC and FFA. Blockade by both drugs was strongly voltage dependent: the K_D decreased as transmembrane potential became more negative at a rate of *e*-fold per ~60 mV. This voltage dependence contrasts with the much weaker, voltage-independent blockade of the endogenous Ca^{2+} - activated Cl^- channels by DPC. CFTR block by DPC and FFA required several min to reach maximal effect. Blockade occurred in two phases: a fast phase due to partial block from the external side of the channel, followed by a slower phase, presumably due to block from the cytoplasmic side after drug permeation through the plasma membrane. The voltage dependence of blockade, as determined by the variation in K_D with voltage, indicates that DPC and FFA molecules sense a similar fraction (0.4 - 0.5) of the electrical field

across the membrane and hence may share a common binding site.

Voltage-dependent block of single-channel currents

Single-channel data indicate that both DPC and FFA block CFTR by increasing the frequency of brief non-conducting periods: the current traces become more flickery without a reduction in the apparent single-channel conductance. Thus, DPC and FFA may be classified as "intermediate" drugs, in the terminology of Hille (1992), regarding the kinetics of drug/receptor interaction. Interestingly, the subconductance state showed much less flicker than the main state upon application of drugs to either side (data not shown). This effect has not been studied systematically.

As indicated in Table I, the block of DPC and FFA is revealed both by (a) an increase in average closed times and (b) a decrease in average open times in the presence of blockers. In Table I, the average closed times for all four drug configurations were significantly different from closed times for unblocked channels ($p < 0.05$, unpaired t-test). The same is true for average open times, with the exception of open times with external DPC, the least potent blocking condition ($p = 0.051$). Single-channel measurements confirm the whole-cell data: the flickery block occurs only at negative membrane potentials. Block of single channels by DPC was reversible, as was the case for whole-cell measurements. Increasing order of potency of block at a given

concentration and voltage is as follows: DPC applied externally, DPC internally, FFA internally, and FFA externally.

Open-channel block

Two general classes of block involve either (1) direct block of conduction due to binding within the pore itself or (2) allosteric inhibition due to binding outside the pore. That FFA and DPC blockade is voltage dependent, with an apparent binding site 40 - 50% of the electrical distance from the cytoplasmic face, suggests that the blockade actually occurs within the channel. In addition, the blocked single-channel traces resemble classic open-channel block; brief blocked times would represent the residence time of the blocker on its site. We have no formal proof of this mechanism, however; future experiments will test this suggestion by examining antagonism of the blockade by permeant ions.

Assuming for the moment that open-channel block is the mechanism, a simple kinetic model may be discussed. A drug molecule, T, binds to a single class of receptor sites, R, as follows:

$$T + R \underset{k_{-1}}{\overset{k_1}{\rightleftharpoons}} TR \qquad\qquad K_D = \frac{k_{-1}}{k_1} \quad ,$$

where k_1 is the second-order bimolecular rate constant for binding, k_{-1} is the

first-order unimolecular rate constant for dissociation, and K_D is the equilibrium dissociation constant for the drug-receptor complex. Because $[T]k_1 = 1/\tau_o$ and $k_{-1} = 1/\tau_c$, we can estimate the apparent dissociation constant from the single-channel data at a given drug concentration and at a given membrane voltage, $K_D(V)$ as

$$K_D(V) = \frac{1/\tau_c}{1/\tau_o}\,[T] \quad .$$

Applying values for τ_o and τ_{c1} or τ_{c2} at V_m = -100 mV from Table I, we calculate values for $K_D(-100)$ under the following conditions: for DPC_{ext}, 345 μM; for DPC_{cyto}, 175 μM; for FFA_{cyto}, 105 μM; and for FFA_{ext}, 85 μM, where the subscripts ext and cyto refer to drugs in the extracellular and cytoplasmic solutions, respectively. This quantitative order of potency agrees with the perceived order of potency listed above and with the similarity in values for K_D (-100 mV) measured from block of whole-cell currents, which averaged 237 ± 34 μM and 289 ± 33 μM for DPC and FFA, respectively. The single-channel data suggest that FFA binds 2 - 3 times more tightly than DPC; the whole-cell data suggest roughly equal equilibrium dissociation constants. We believe that the single-channel data give the more accurate picture because the drug concentrations are more directly controlled in excised-patch experiments.

The similarity in τ_o values for DPC and FFA in all four configurations suggests that $k_1 \approx 6 \times 10^7\ s^{-1}$, close to the value of $2 \times 10^7\ s^{-1}$ determined for open-channel blockers of the acetylcholine receptor channel (Charnet, Labarca,

Leonard, Vogelaar, Czyzyk, Gouin, Davidson, and Lester, 1990). The most striking difference in kinetic effects between DPC and FFA in the four configurations is seen in the closed time constants. FFA apparently remains bound to its site several times longer than does DPC.

Access through the conduction pathway?

How do the blockers reach their binding sites? The most important constraint for modeling this process is that the blockers appear to reach their binding site from either side of the membrane; furthermore, kinetics of FFA, which yields equal voltage dependence and residence time with application from either side, suggest that the binding site is the same from either side. Possible routes of access are (1) through the conducting pathway, or (2) through the membrane itself. There are precedents for both routes (Hille, 1992).

Permeant blocker; asymmetric energy barriers.

One possible view of block in the CFTR channel invokes permeant blockers and asymmetric energy barriers, similar to more detailed models that explain block of Na^+ channels by protons (Woodhull, 1973) and block of retinal cyclic nucleotide-gated cation channels by divalent cations (Zimmerman and Baylor, 1992). In its simplest form, this model would incorporate two barriers

(with energy peaks E_{outer} and E_{inner}) flanking one well located at a distance ~0.4 - 0.5 from the inside edge. The well depth for DPC is shallower than for FFA, accounting for the longer residence time of FFA (longer closed time constant, τ_c). At zero transmembrane potential, the external energy barrier E_{outer} is less than E_{inner}. At V_m = -100 mV, the inner and outer energy barriers experienced by a blocker molecule are of equal height, so that the drugs can reach the binding site equally well from either side, accounting for the similar forward binding rates, k_1. Regardless of the side of drug application, upon unbinding at negative V_m the (negatively charged) drug molecules are more likely to exit down the electrical gradient, over the external barrier. At positive membrane voltages, the internal barrier is lowered to the point where externally applied drug rapidly exits to the internal solution down the electrical gradient, resulting in little or no blockade. Internally applied drugs cannot overcome the larger internal barrier against the electrical gradient. The whole-cell data do show a small degree of block by both DPC and FFA at depolarizing voltages (see Fig. 3 and 4), which could represent very short-lived residence of the blocker on the binding site; this brief block would not be resolved in our single-channel measurements.

The asymmetric barrier model explains the counterintuitive result that externally applied DPC and FFA are each capable of entering the channel and reaching their binding site against the applied membrane field. Similarly, Ca^{2+}

blocks the retinal cyclic nucleotide-gated channel although the apparent electrical gradient does not favor its entry into the channel (Zimmerman and Baylor, 1992).

Block due to lock-in

If the pore contains multiple anion binding sites, chloride occupancy of binding sites could impede dissociation of FFA or DPC from the pore. Such a "lock-in" phenomenon has been studied for the calcium-activated potassium channel of rat skeletal muscle, most recently by Neyton and Miller (1988a,b). However, CFTR channels are characterized by a low conductance and a low degree of size selectivity, implying that there may not be multiple anion binding sites within the pore.

Regardless of the exact mechanism for blocker binding, these models suggest that DPC and FFA are permeant blockers: they can exit in the opposite direction from their entrance. Their action is thus more complex than that of quaternary ammonium compounds at nicotinic acetylcholine receptors or voltage-gated Na^+ channels.

Access through the lipid phase?

Possibly the drugs do not reach their binding sites through the conduction pathway from the external surface, but rather through the

membrane phase. The membrane route might involve the uncharged form of the drugs. The charged form of the drugs would be the blocking form so that the observed voltage dependence would still be expected. This mechanism would be tested with measurements of pH dependence.

DPC vs. FFA

We consider it likely that the major interaction between the drug molecules and the walls of the pore involves the negative charge of the carboxylate moiety. However, kinetic differences between FFA and DPC indicate that substitution of a trifluoromethyl group influences binding energy, either through a direct interaction of the CF_3 group with the channel or through an altered charge distribution on FFA as compared to DPC.

FFA blocked whole-cell currents somewhat faster than DPC; similarly, externally applied FFA blocks single channels more effectively than externally applied DPC. The difference in K_D values between whole-cell and single-channel measurements is most likely due to the presence of blockers on both sides of the membrane in the whole-cell experiments, counteracting the difference in sidedness observed in single-channel experiments. We do not know the exact intracellular concentration of drugs even after prolonged incubation, although block of CFTR in cell-attached patch mode by bath-applied DPC and FFA indicates that both drugs are capable of crossing the

membrane. The mechanism of voltage-dependent block by FFA and DPC needs to be addressed more fully in future experiments employing a wider range of pH, permeant ion concentrations, and membrane potentials. It is also of interest to determine whether site-directed mutations of the CFTR gene can be identified that alter the blocking process. Voltage dependent blockade of CFTR channels by FFA and DPC constitutes a promising tool for structure-function studies of CFTR.

Acknowledgments

The authors wish to thank Dr. Xian-cheng Yang for advice on single-channel analysis, Profs. Anita Zimmerman and Dennis Dougherty for helpful discussions, Dr. Michael Quick for assistance, and Dr. B.K. Kobilka and colleagues (Dept. of Cellular and Molecular Physiology, Stanford University Medical Center) for supplying us with the β_2-AR cDNA. This project was supported by grants from the Cystic Fibrosis Foundation (#Z139) and from the NIH (#GM-29836). N.A.M. was supported by an NIH NRSA fellowship (#DK08559), and S.M. was supported by an NIH training grant (#GM-07737).

REFERENCES

Anderson, M.P., R.J. Gregory, S. Thompson, D.W. Souza, S. Paul, R.C. Mulligan, A.E. Smith, and M.J. Welsh. 1991. Demonstration that CFTR is a chloride channel by alteration of its anion selectivity. *Science* 253:202-205.

Anderson, M.P., D.P. Rich, R.J. Gregory, A.E. Smith, and M.J. Welsh. 1991. Generation of cAMP-stimulated chloride currents by expression of CFTR. *Science* 251:679-682.

Bear, C.E., F. Duguay, A.L. Naismith, N. Kartner, J.W. Hanrahan, and J.R. Riordan. 1991. Cl^- channel activity in *Xenopus* oocytes expressing the cystic fibrosis gene. *Journal of Biological Chemistry* 266:19142-19145.

Bear, C.E., C. Li, N. Kartner, R.J. Bridges, T.J. Jensen, M. Ramjeesingh, and J.R. Riordan. 1992. Purification and functional reconstitution of the cystic fibrosis transmembrane conductance regulator (CFTR). *Cell* 68:809-818.

Bijman, J., H.C. Englert, H.J. Lang, R. Greger, and E. Frömter. 1987. Characterization of human sweat duct chloride conductance by chloride channel blockers. *Pflügers Archiv* 408:511-514.

Boat, T.F., M.J. Welsh, and A.L. Beaudet. 1989. Cystic fibrosis. *In*: The Metabolic Basis of Inherited Disease. Scriver, C.R., A.L. Beaudet, W.S. Sly, and D. Valle, editors, 6th ed. McGraw-Hill, New York. pp. 2649-2680.

Cabantchik, Z.I. and R. Greger. 1992. Chemical probes for anion transporters of mammalian cell membranes. *American Journal of Physiology* 262:C803-C827.

Charnet, P., C. Labarca, R.J. Leonard, N.J. Vogelaar, L. Czyzyk, A. Gouin, N. Davidson, and H.A. Lester. 1990. An open-channel blocker interacts with adjacent turns of α-helices in the nicotinic acetylcholine receptor. *Neuron* 2:87-95.

Cheng, S.H., D.P. Rich, J. Marshall, R.J. Gregory, M.W. Welsh, and A.E. Smith. 1991. Phosphorylation of the R domain by cAMP-dependent protein kinase regulates the CFTR chloride channel. *Cell* 66:1027-1036.

Cliff, W.H., R.A. Schoumacher, and R.A. Frizzell. 1992. cAMP-activated Cl channels in CFTR-transfected cystic fibrosis pancreatic epithelial cells. *American Journal of Physiology* 262:C1154-C1160.

Cunningham, S.A., R.T. Worrell, D.J. Benos, and R.A. Frizzell. 1992.

cAMP-stimulated ion currents in *Xenopus* oocytes expressing CFTR cRNA. *American Journal of Physiology* 262:C783-C788.

DiStefano, A., M. Wittner, E. Schlatter, H.J. Lang, H. Englert, and R. Greger. 1985. Diphenylamine-2-carboxylate, a blocker of the Cl^--conductive pathway in Cl^--transporting epithelia. *Pflügers Archiv* 405 (Suppl. 1):S95-S100.

Flower, R.J. 1974. Drugs which inhibit prostaglandin biosynthesis. *Pharmacological Reviews* 26:33-67.

Frizzell, R.A. 1987. Cystic fibrosis: a disease of ion channels? *Trends in Neurosciences* 10:190-193.

Gögelein, H., D. Dahlem, H.C. Englert, and H.J. Lang. 1990. Flufenamic acid, mefenamic acid and niflumic acid inhibit single nonselective cation channels in the rat exocrine pancreas. *FEBS Letters* 268:79-82.

Gray, M.A., C.E. Pollard, A. Harris, L. Coleman, J.R. Greenwell, and B.E. Argent. 1990. Anion selectivity and block of the small-conductance chloride channel on pancreatic duct cells. *American Journal of Physiology* 259:C752-C761.

Greger, R. 1990. Chloride channel blockers. *Methods in Enzymology* 191:793-810.

Gregory, R.J., S.H. Cheng, D.P. Rich, J. Marshall, S. Paul, K. Hehir, L. Ostedgaard, K.W. Klinger, M.J. Welsh, and A.E. Smith. 1990. Expression and characterization of the cystic fibrosis transmembrane conductance regulator. *Nature London* 347:382-386.

Hille, B. 1992. Ionic Channels of Excitable Membranes. 2nd ed., Sinauer Associates, Inc., Sunderland, Massachusetts, pp. 607.

Kartner, N., J.W. Hanrahan, T.J. Jensen, A.L. Naismith, S. Sun, C.A. Ackerley, E.F. Reyes, L.-C. Tsui, J.M. Rommens, C.E. Bear, and J.R. Riordan. 1991. Expression of the cystic fibrosis gene in non-epithelial invertebrate cells produces a regulated anion conductance. *Cell* 64:681-691.

Landry, D.W., M. Reitman, E.J. Cragoe, Jr., and Q. Al-Awqati. 1987. Epithelial chloride channel. Development of inhibitory ligands. *Journal of General Physiology* 90:779-798.

McCarty, N.A., B.N. Cohen, M.W. Quick, J.R. Riordan, N. Davidson, and H.A. Lester. 1992. Diphenylamine-2-carboxylate (DPC) blocks the CFTR Cl^- channel

from the cytoplasmic side. *Biophysical Journal* 61:A10.

McDonough, S., N.A. McCarty, J.R. Riordan, N. Davidson, and H.A. Lester. Block of CFTR by diphenylamine-2-carboxylate (DPC) and flufenamic acid (FFA). *Biophysical Journal* 64:A99

McDougall, P., A. Markham, I. Cameron, and A.J. Sweetman. 1988. Action of the nonsteroidal anti-inflammatory agent, flufenamic acid, on calcium movements in isolated mitochondria. *Biochemical Pharmacology* 37:1327-1330.

Neyton, J. and C. Miller. 1988a. Discrete Ba^{2+} block as a probe of ion occupancy and pore structure in the high-conductance Ca^{2+}-activated K^+ channel. *Journal of General Physiology* 92:569-586.

Neyton, J. and C. Miller. 1988b. Potassium blocks barium permeation through a calcium-activated potassium channel. *Journal of General Physiology* 92:549-567.

Poronnik, P., M.C. Ward, and D.I. Cook. 1992. Intracellular Ca^{2+} release by flufenamic acid and other blockers of the non-selective cation channel. *FEBS Letters* 296:245-248.

Quick, M.W., J. Naeve, N. Davidson, and H.A. Lester. 1992. Incubation with horse serum increases viability and decreases background neurotransmitter uptake in *Xenopus* oocytes. *BioTechniques* 13:358-362.

Quinton, P.M. 1983. Chloride impermeability in cystic fibrosis. *Nature London* 301:421-422.

Rich, D.P., M.P. Anderson, R.J. Gregory, S.H. Cheng, S. Paul, D.M. Jefferson, J.D. McCann, K.W. Klinger, A.E. Smith, and M.J. Welsh. 1990. Expression of cystic fibrosis transmembrane conductance regulator corrects defective chloride channel regulation in cystic fibrosis airway epithelial cells. *Nature London* 347:358-363.

Rich, D.P., R.J. Gregory, M.P. Anderson, P. Manavalan, A.E. Smith, and M.J. Welsh. 1991. Effect of deleting the R domain on CFTR-generated chloride channels. *Science* 253:205-207.

Riordan, J.R., J.M. Rommens, B.-S. Kerem, N. Alon, R. Rozmahel, Z. Grzelczak, J. Zielenski, S. Lok, N. Plavsic, J.-L. Chou, M.L. Drumm, M.C. Iannuzzi, F.S. Collins, and L.-C. Tsui. 1989. Identification of the cystic fibrosis gene: cloning and characterization of complementary DNA. *Science* 245:1066-1073.

Sachs, F. 1983. Automated analysis of single-channel records. *In*: Single-Channel Recording. Sakmann, B. and E. Neher, editors. Plenum Press, New York, pp. 265-285.

Sachs, F., J. Neil, and N. Barkakati. 1982. The automated analysis of data from single ionic channels. *Pflügers Archiv* 395:331-340.

Singh, A.K., G.B. Afink, C.J. Venglarik, R. Wang, and R.J. Bridges. 1991. Colonic Cl^- channel blockade by three classes of compounds. *American Journal of Physiology* 260:C51-C63.

Sullivan, S.K., K. Swamy, and M. Field. 1991. cAMP-activated Cl conductance is expressed in *Xenopus* oocytes by injection of shark rectal gland mRNA. *American Journal of Physiology* 260:C664-C669.

Tabcharani, J.A., X.-B. Chang, J.R. Riordan, and J.W. Hanrahan. 1991. Phosphorylation-regulated Cl^- channel in CHO cells stably expressing the cystic fibrosis gene. *Nature London* 352:628-631.

Tabcharani, J.A., W. Low, D. Elie, and J.W. Hanrahan. 1990. Low-conductance chloride channel activated by cAMP in the epithelial cell line T84. *FEBS Letters*

270:157-164.

Tilmann, M., K. Kunzelmann, U. Fröbe, I. Cabantchik, H.J. Lang, H.C. Englert, and R. Greger. 1991. Different types of blockers of the intermediate-conductance outwardly rectifying chloride channel in epithelia. *Pflügers Archiv* 418:556-563.

Wangemann, P., M. Wittner, A. DiStefano, H.C. Englert, H.J. Lang, E. Schlatter, and R. Greger. 1986. Cl^--channel blockers in the thick ascending limb of the loop of Henle. Structure activity relationship. *Pflügers Archiv* 407 (Suppl. 2):S128-S141.

Welsh, M.J. 1990. Abnormal regulation of ion channels in cystic fibrosis epithelia. *FASEB Journal* 4:2718-2725.

White, M.M. and M. Aylwin. 1990. Niflumic and flufenamic acids are potent reversible blockers of Ca^{2+}-activated Cl^- channels in *Xenopus* oocytes. *Molecular Pharmacology* 37:720-724.

Woodhull, A.M. 1973. Ionic blockage of sodium channels in nerve. *Journal of General Physiology* 61:687-708.

Wu, G. and O.P. Hamill. 1992. NPPB block of Ca^{++}-activated Cl^- currents in *Xenopus* oocytes. *Pflügers Archiv* 420:227-229.

Zimmerman, A.L. and D.A. Baylor. 1992. Cation interactions within the cyclic GMP-activated channel of retinal rods from the tiger salamander. *Journal of Physiology* 449:759-783.

Table I. Kinetic effects of 50 μM DPC and FFA in excised patches at V_m = -100 mV.

	Unblocked*	DPC Cytoplasmic	DPC Pipette	FFA Cytoplasmic	FFA Pipette
τ_o (ms) ±	8.23 ± 1.4	2.17 ± 0.43	3.16 ± 0.56	2.42 ± 0.41	2.37 ± 0.10
τ_{c1} (ms) ±	0.27 ± 0.01	0.62 ± 0.075	0.46 ± 0.05	0.28 ± 0.03	0.37 ± 0.08
τ_{c2} (ms) ±				1.11 ± 0.05	1.41 ± 0.12
P_O‡ ±	0.94 ± 0.01	0.69 ± 0.07	0.80 ± 0.03	0.75 ± 0.03	0.70 ± 0.02
n	6	4	3	4	3

Time analyzed (s)

739	161	160	388	1020

---

*Unblocked values combine data from all controls in the presence and absence of ethanol (7.3 mM in the pipette and 4.3 mM in the cytoplasm), 1 or 2 mM ATP, and 10 mM NaF, all of which had no effect.

‡Values for P_O are measured within a burst. The data presented exclude two records where it could not be determined: one each for FFA cytoplasmic and FFA pipette.

Figure 1. Molecular structures of the two blockers used in this study: diphenylamine-2-carboxylic acid (DPC) and flufenamic acid (FFA). FFA differs from DPC only with the addition of a trifluoromethyl group *meta* to the amine.

Figure 2. Blockade of whole-cell CFTR currents by 200 μM DPC. **A.** Membrane currents elicited by stepping from the holding potential of -45 mV to a series of test potentials from -100 mV to +80 mV, at 20 mV increments. Potential was held at the new value for 75 ms before returning to the holding potential. Capacitive currents have been subtracted. The dashed line in each trace indicates the zero-current level. *Top*: control currents measured before cAMP-activation. *Middle*: CFTR currents measured after application of cyclic AMP-stimulating cocktail. *Bottom*: activated CFTR currents measured 8 min after exposure to 200 μM DPC. All traces are from the same cell. Middle and bottom traces are not background-subtracted. **B.** Current-voltage (I/V) relation for cAMP-dependent CFTR currents (*open circles*) and blocked currents (*filled circles*) after subtraction of control currents. Data points are from the average currents measured during the latter half of the voltage steps in **A**. Note the blockade of inward currents induced by DPC.

Figure 3. Voltage dependence of blockade by 200 μM DPC (*filled circles*) or by 1 mM DPC on a different cell (*open circles*). **A.** Extent of blockade as a function of voltage. I is the current measured during exposure to drug, and I_o is the current measured in the absence of drug. **B.** Effect of membrane voltage on the affinity of DPC for the channel. K_D was calculated according to the text. The line shown is the regression line. Some data points at voltages near the reversal potential (0 and -20 mV) were omitted from the analysis.

Figure 4. Blockade of CFTR currents by bath application of 200 μM FFA. **A.** Current-voltage relations determined as in Figure 2. Shown are cAMP-dependent CFTR currents (*open circles*) and FFA-blocked currents (*filled circles*). **B, C.** I/I_o and K_D as functions of voltage, respectively.

Figure 5. Comparison of single-channel currents measured in cell-attached and excised, inside-out patches, at hyperpolarizing or depolarizing voltages. *Left*: Currents measured in cell-attached configuration, with membrane potential (V_m) equal to +100 mV (*top*) and -100 mV (*bottom*). *Right*: Currents measured in excised, inside-out patches, with V_m = +100 mV (*top*) and -100 mV (*bottom*). Traces are all from the same patch. Each trace shows 0.6 s of recording. The solid line indicates the closed level and the dashed line indicates the open level measured in excised mode.

Figure 6. Reversibility of blockade by DPC applied to the cytoplasmic surface in excised, inside-out patches. The patch was excised directly into intracellular solution containing 200 μM DPC. Membrane potential (V_m) = -100 mV. **A.** Currents measured in the presence of DPC in the cytoplasmic solution. **B.** Washout of the DPC returned CFTR currents to the unblocked condition. Expanded traces at right are taken from the region indicated by the short bar above the unexpanded trace. The horizontal line indicates the closed level in both expanded and unexpanded traces.

Figure 7. Effect of DPC and FFA at the cytoplasmic surface of excised, inside-out patches. **A-C.** V_m = +100 mV. **A.** No added blockers. **B.** Cytoplasmic solution contained 50 μM DPC. **C.** Cytoplasmic solution contained 50 μM FFA. **D-F.** V_m = -100 mV. **D.** Unblocked. **E.** Cytoplasmic solution contained 50 μM DPC. **F.** Cytoplasmic solution contained 50 μM FFA. Expanded traces at right are taken from the region indicated by the short bar above the unexpanded trace. Horizontal line indicates the closed level in both expanded and unexpanded traces. Asterisk in trace E denotes an example of a sojourn in the subconductance state.

Figure 8. Summary of the effects of cytoplasmic drugs on CFTR kinetics, in representative experiments. V_m = -100 mV. *Upper panel*: histograms of closed-time durations within a burst. Value of τ shown is the average closed time calculated from fitting the histogram with one (τ_1) or two (τ_1 and τ_2) exponential components. On each histogram, the maximum range of the ordinate is labeled. *Lower panel*: open-time duration histograms. Binwidth was 0.1 ms for closed-time histograms and 1 ms for open-time histograms. For cytoplasmically applied FFA, the ratio of areas under the curves for the short and long closed time constants indicates that the latter accounted for 49 ± 2% of the closed events (n = 4).

Figure 9. Effect of DPC and FFA at the external surface of excised, inside-out patches. **A-C.** V_m = +100 mV. **A.** No added blockers. **B.** Pipette solution contained 50 μM DPC. **C.** Pipette solution contained 50 μM FFA. **D-F.** V_m = -100 mV. **D.** No added blockers. **E.** Pipette solution contained 50 μM DPC. **F.** Pipette solution contained 50 μM FFA. Expanded traces at right are taken from the region indicated by the short bar above the unexpanded trace. Horizontal line indicates the closed level in both expanded and unexpanded traces.

Figure 10. Summary of the effects of external drugs on CFTR kinetics, in representative experiments. V_m = -100 mV. Axes and scales as in Figure 8. *Upper panel*: closed-time duration histograms. *Lower panel*: open-time duration histograms. For externally applied FFA, the ratio of areas under the curves for the short and long closed time constants indicates that the latter accounted for 45 ± 11% of the closed events (n = 3).

Figure 11. Blockade of CFTR currents by DPC and FFA in cell-attached mode. Patch currents measured before, **A**, and after, **B**, application of 200 μM DPC to the bathing medium. Expanded traces at the right are taken from the area indicated by the short bar above the unexpanded trace. The horizontal line indicates the closed level for channels at both time scales. **C** and **D** show currents measured before and after, respectively, application of 50 μM FFA to the bath. A and B are from the same patch, as are C and D. In each case, V_m = -100 mV. Traces shown in B and D were obtained 1-2 min after application of the drugs.

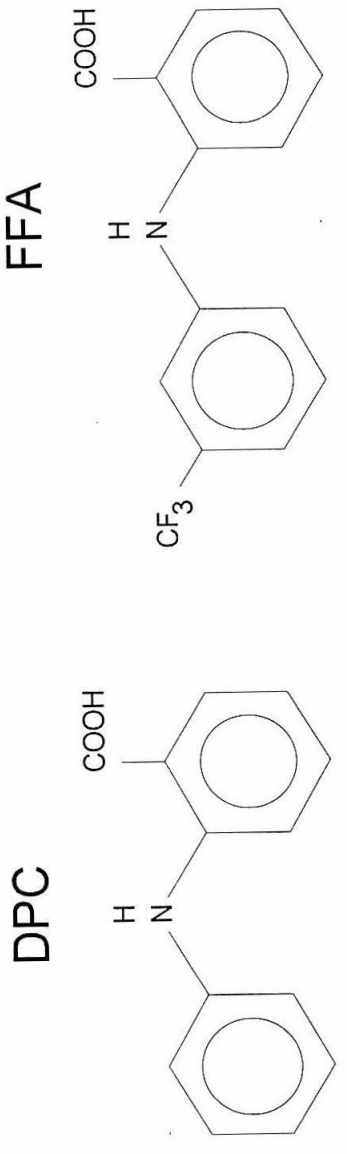

Figure 1

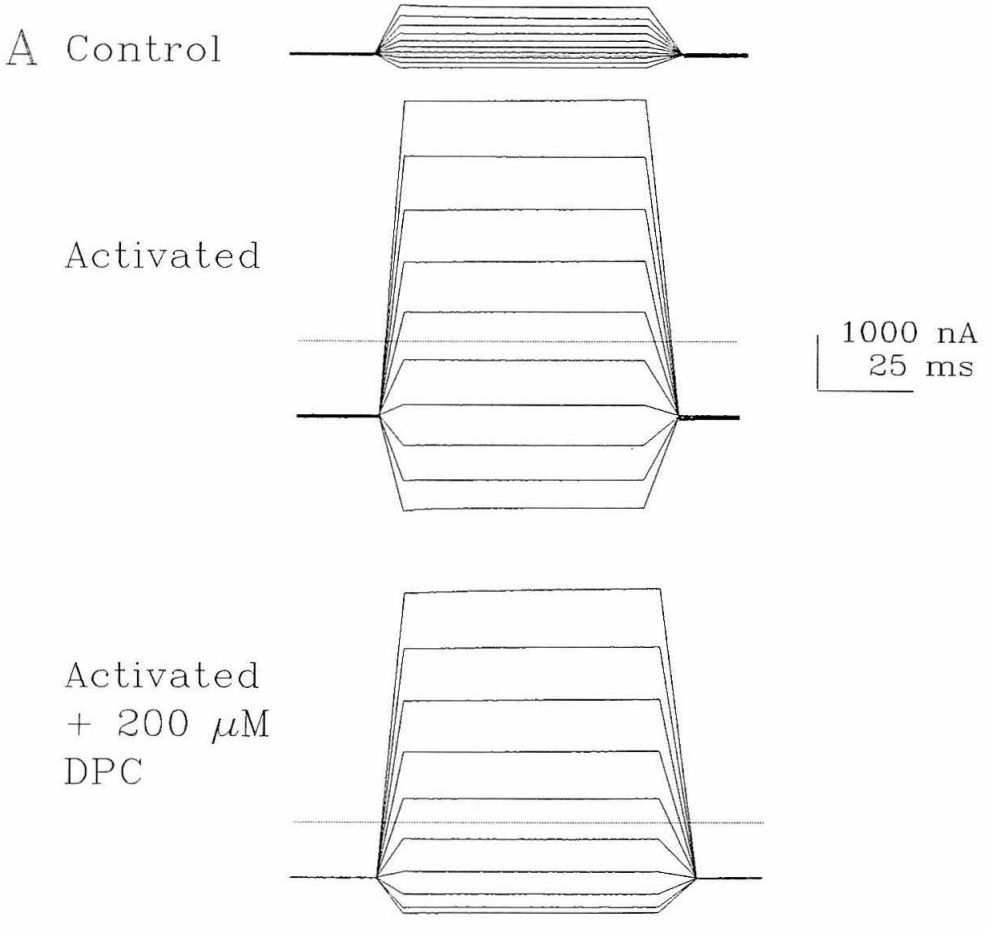
A Control
Activated
1000 nA
25 ms
Activated
+ 200 μM
DPC
B
I (μA)
4
2
−2
−4
−100
−50
0
50
100
V m (mV)

Figure 2

A

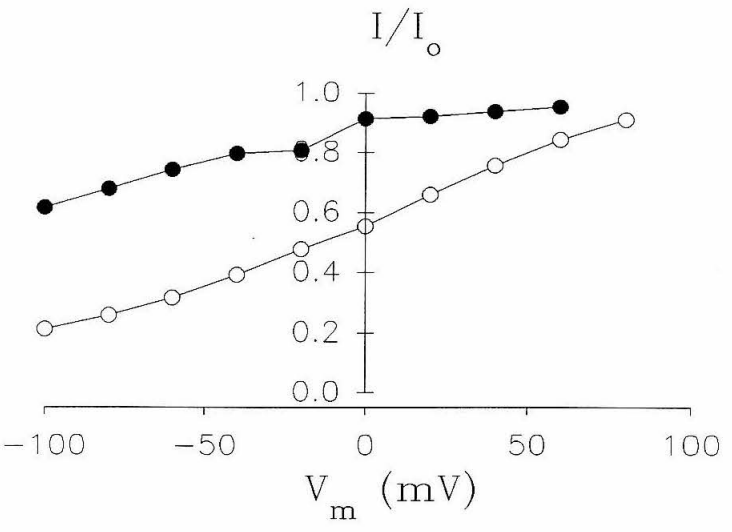
I/I$_o$
1.0
0.8
0.6
0.4
0.2
0.0
−100
−50
0
50
100
V$_m$ (mV)

B

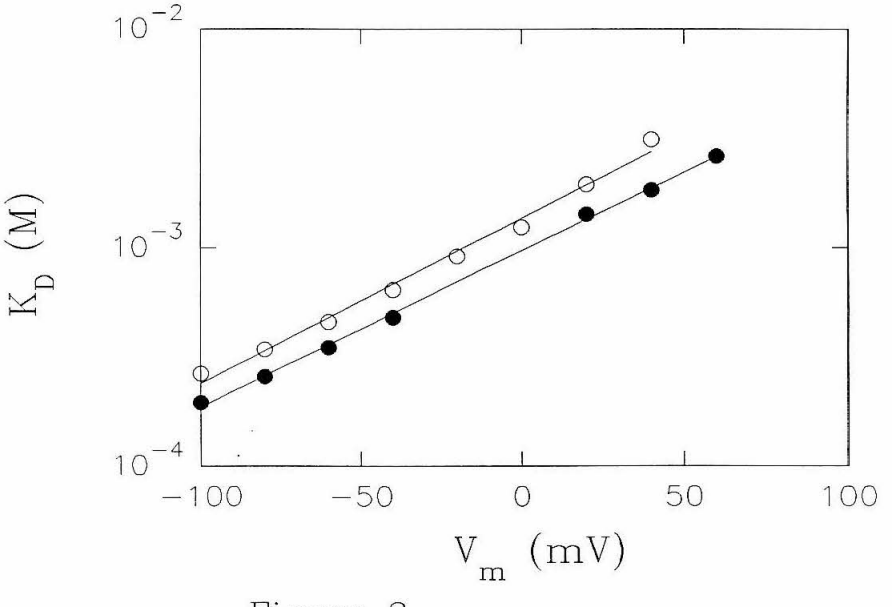
10^{-2}
10^{-3}
10^{-4}
K$_D$ (M)
−100
−50
0
50
100
V$_m$ (mV)

Figure 3

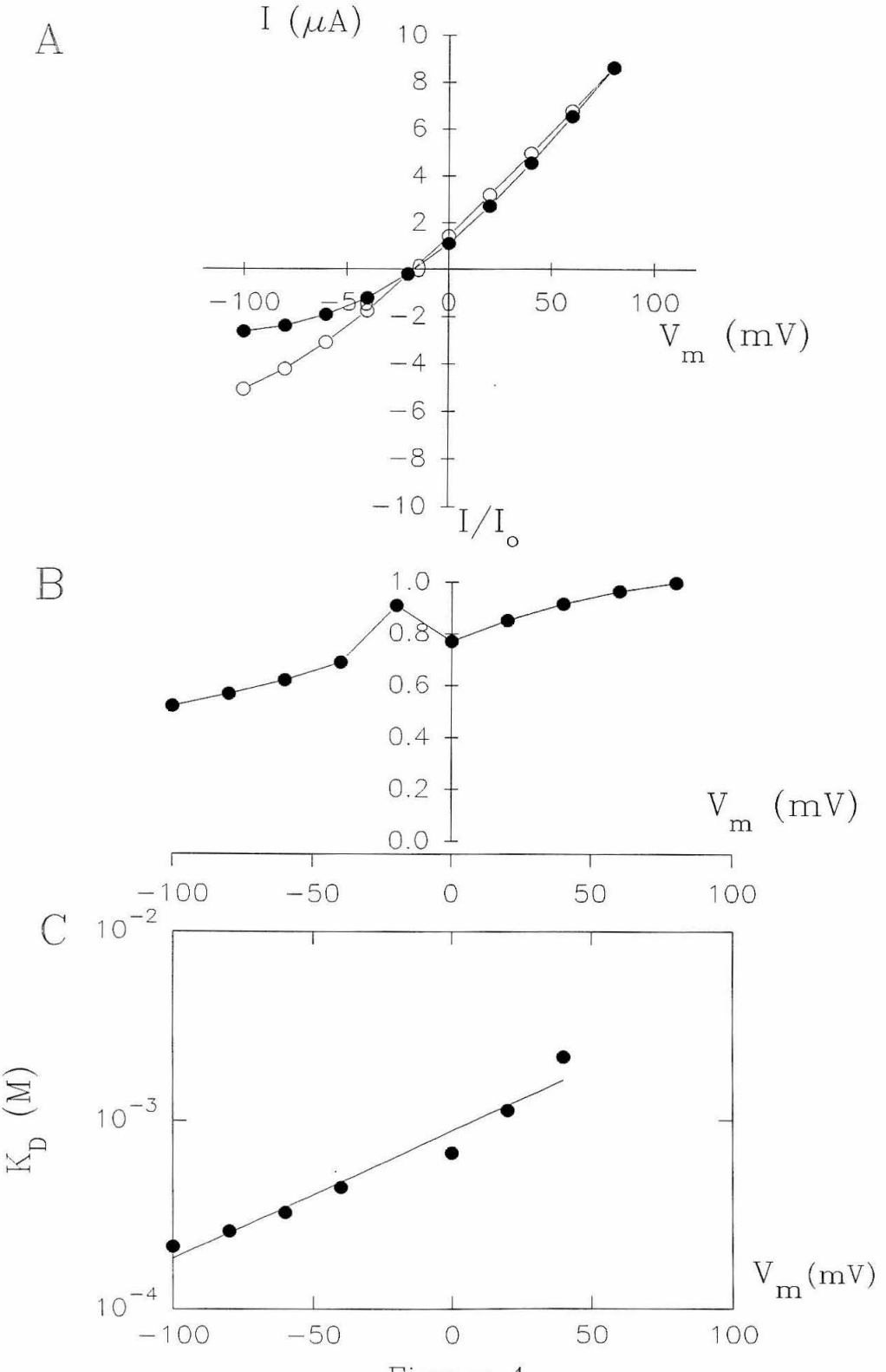
A
I (μA)
10
8
6
4
2
0
−2
−4
−6
−8
−10
−100
−50
0
50
100
V_m (mV)
I/I_o
B
1.0
0.8
0.6
0.4
0.2
0.0
V_m (mV)
−100
−50
0
50
100
C
10^-2
10^-3
10^-4
K_D (M)
V_m (mV)
−100
−50
0
50
100

Figure 4

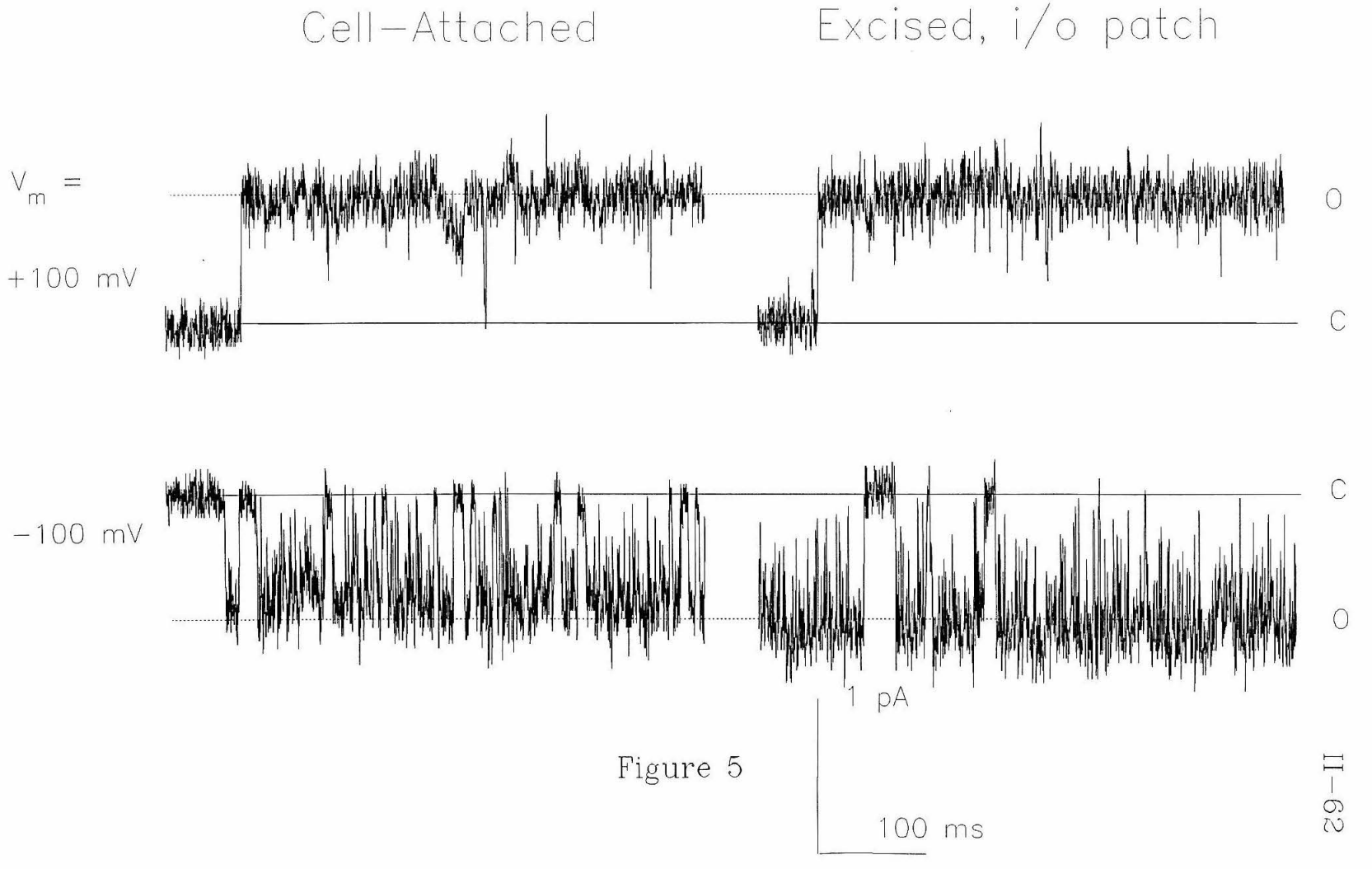
Cell–Attached
Excised, i/o patch
V_m =
+100 mV
−100 mV
O
C
C
O
1 pA
100 ms

Figure 5

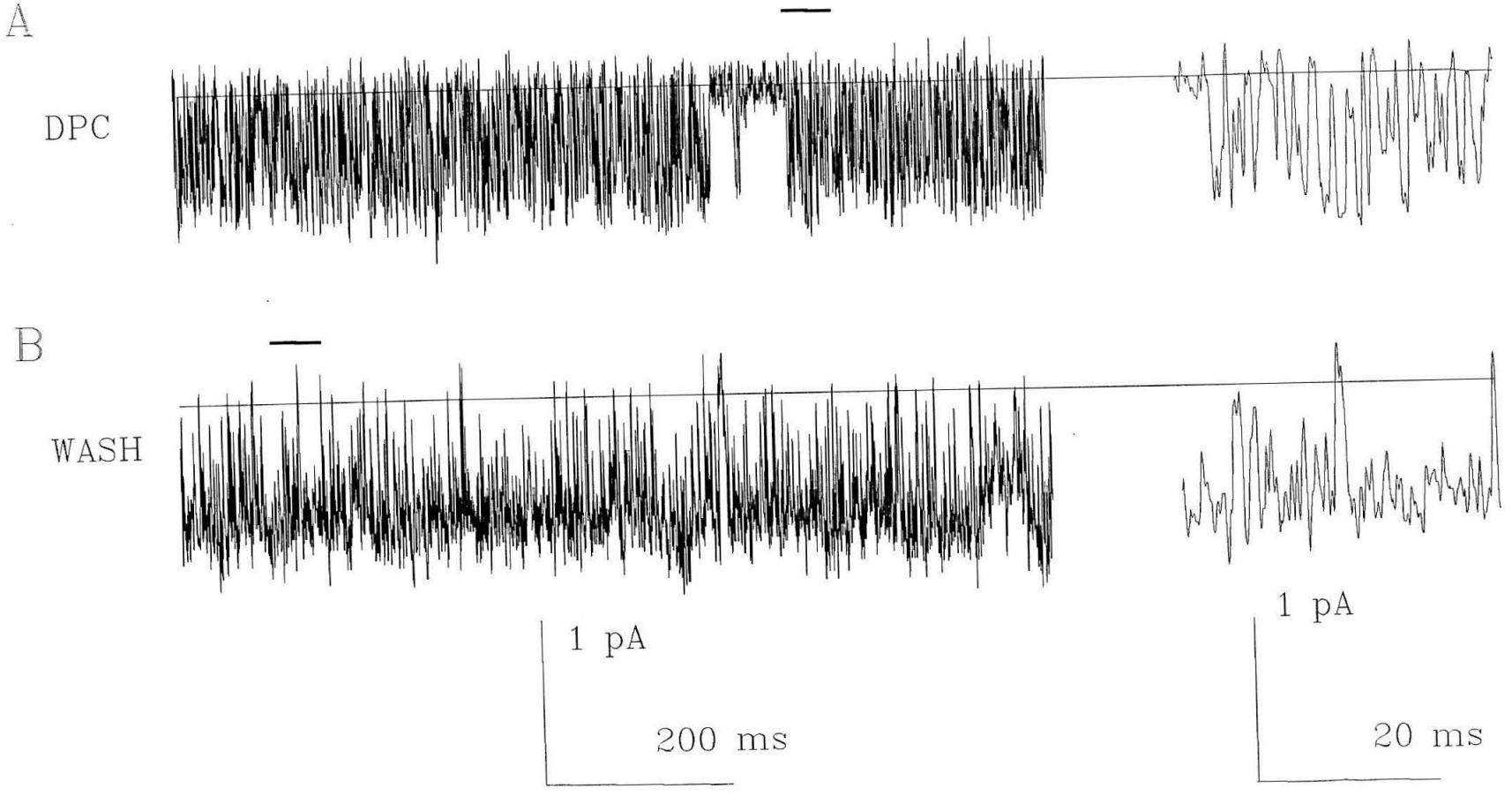

Figure 6

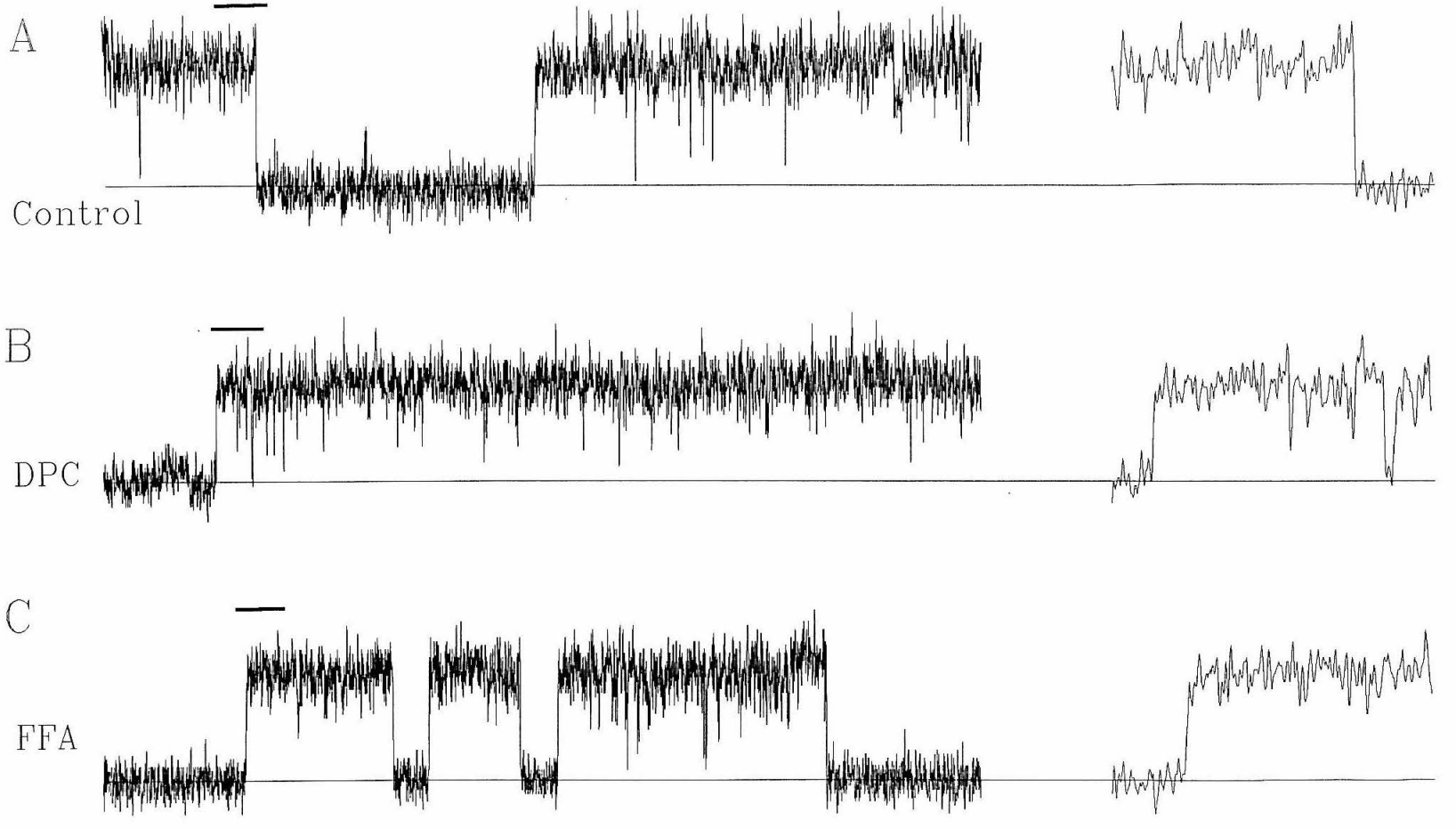

Figure 7 part I

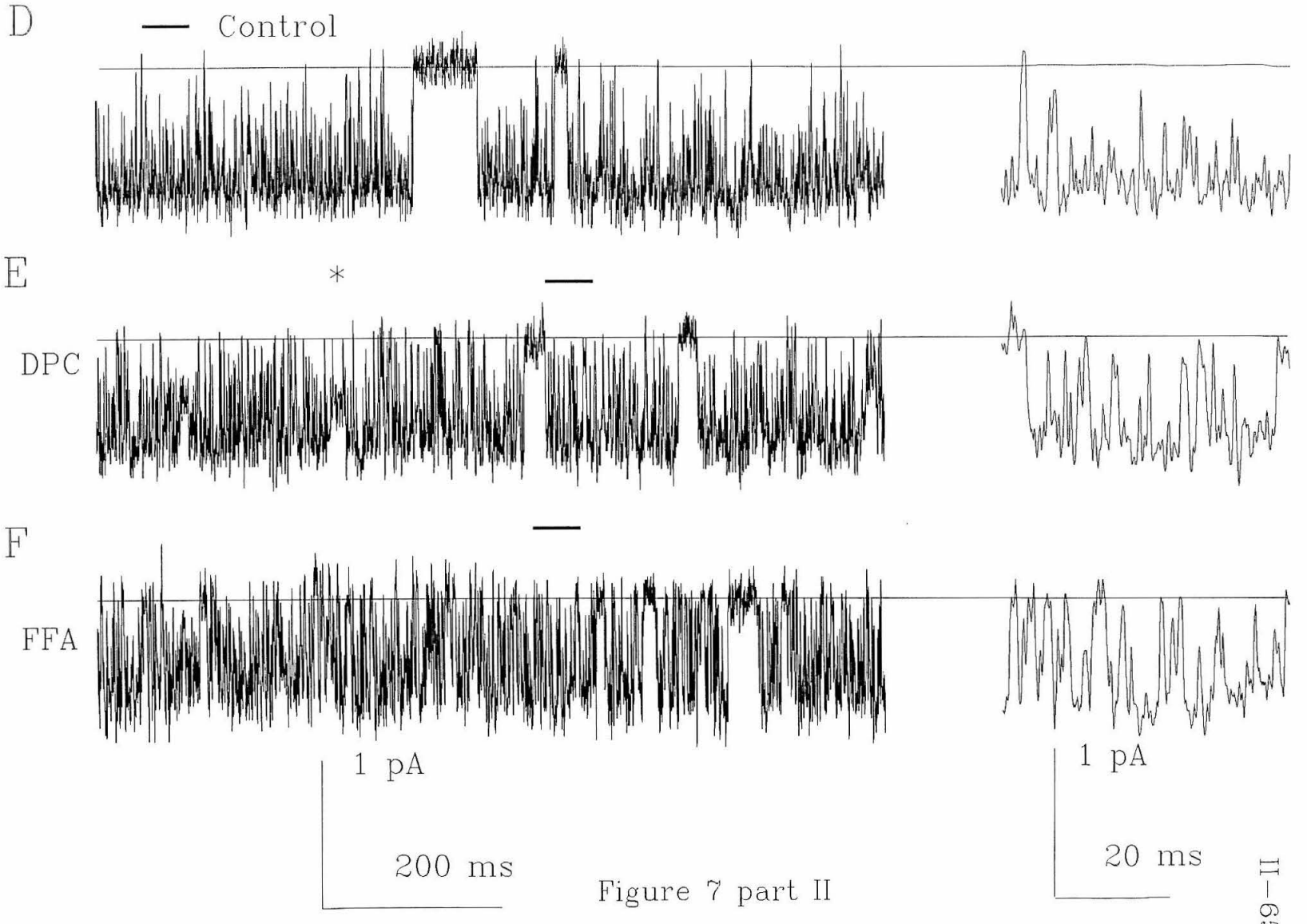

Figure 7 part II

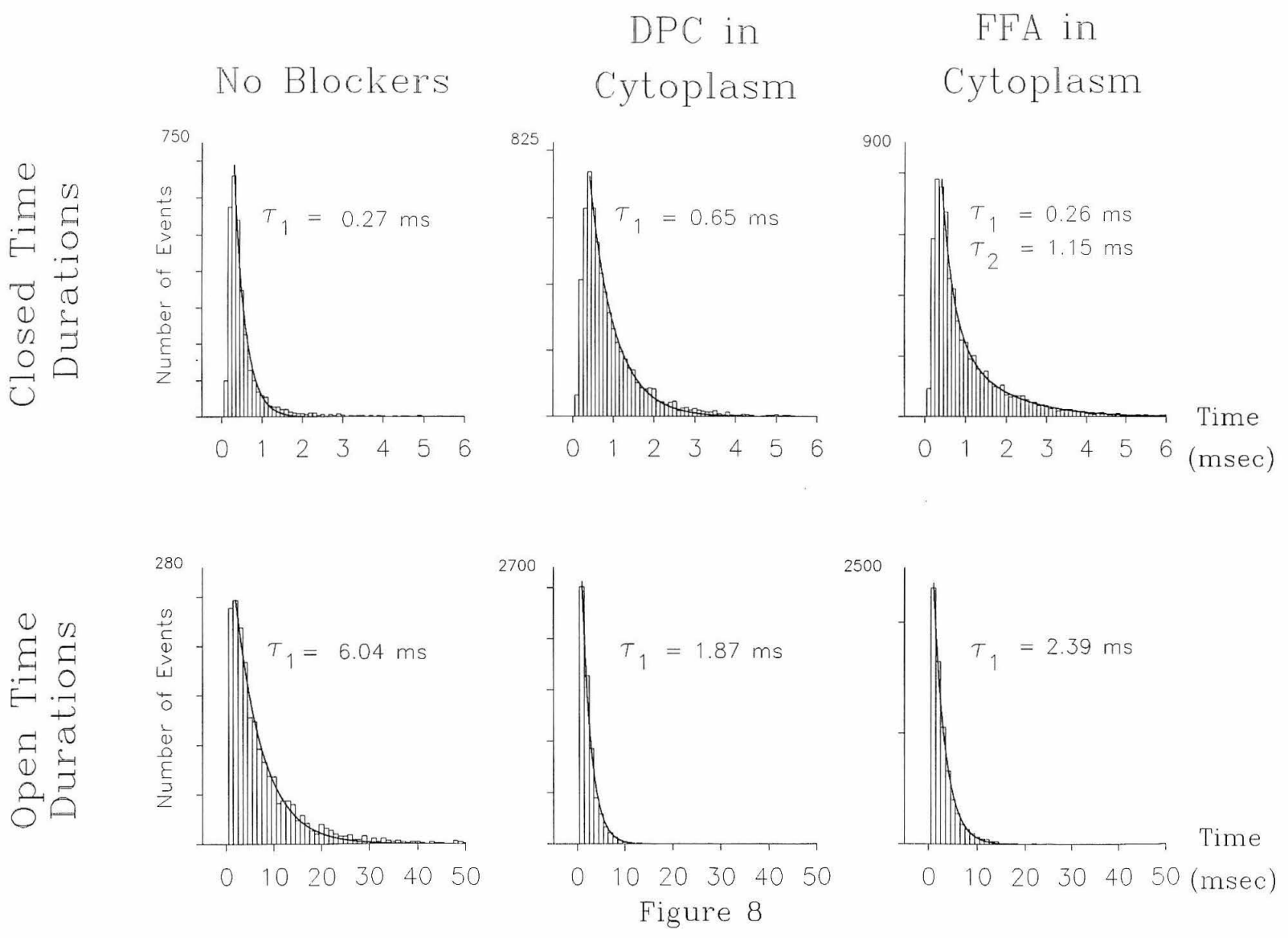
No Blockers
DPC in Cytoplasm
FFA in Cytoplasm
Closed Time Durations
Open Time Durations
Number of Events
750
825
900
280
2700
2500
τ_1 = 0.27 ms
τ_1 = 0.65 ms
τ_1 = 0.26 ms
τ_2 = 1.15 ms
τ_1 = 6.04 ms
τ_1 = 1.87 ms
τ_1 = 2.39 ms
0 1 2 3 4 5 6
0 10 20 30 40 50
Time (msec)

Figure 8

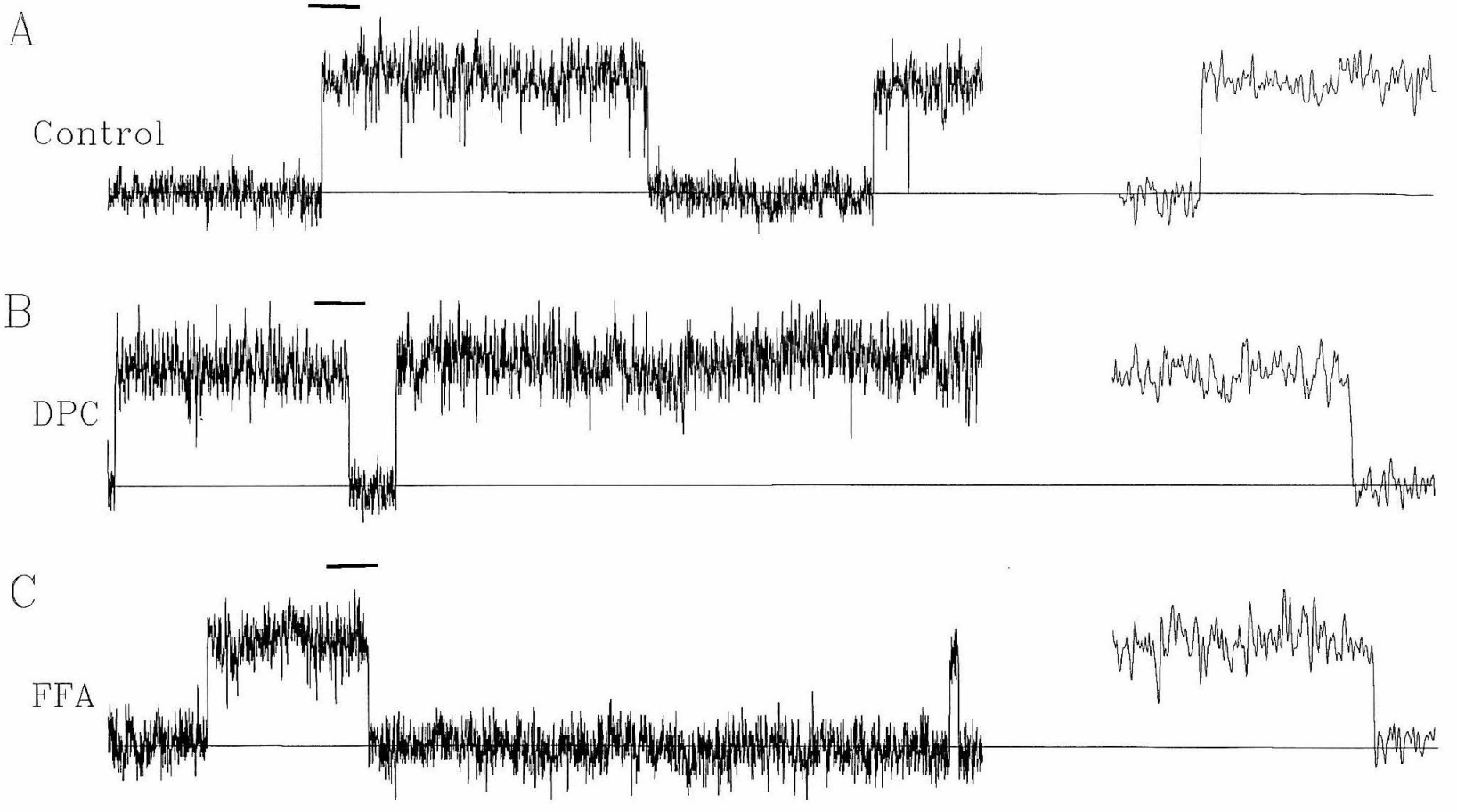

Figure 9 part I

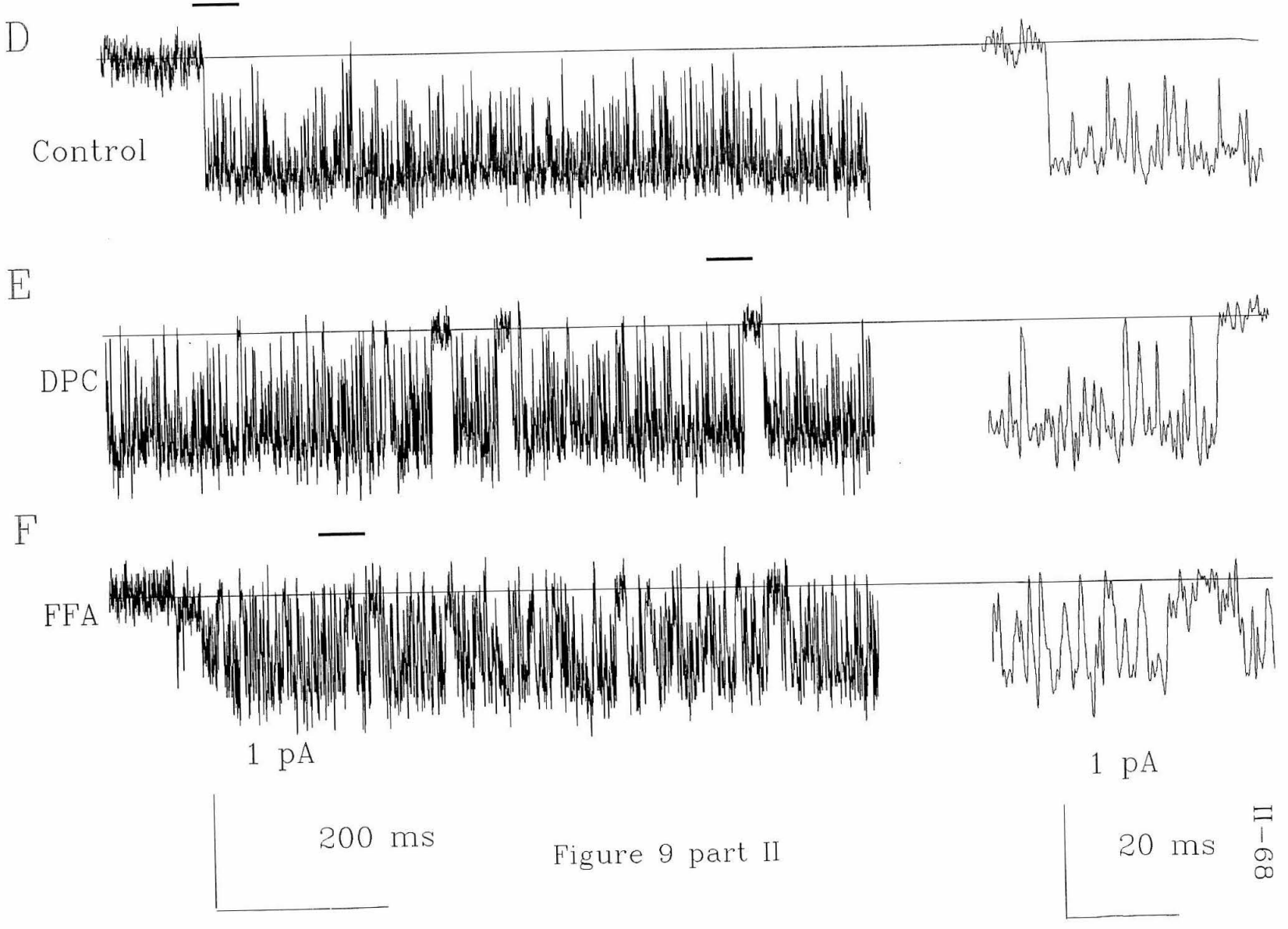

Figure 9 part II

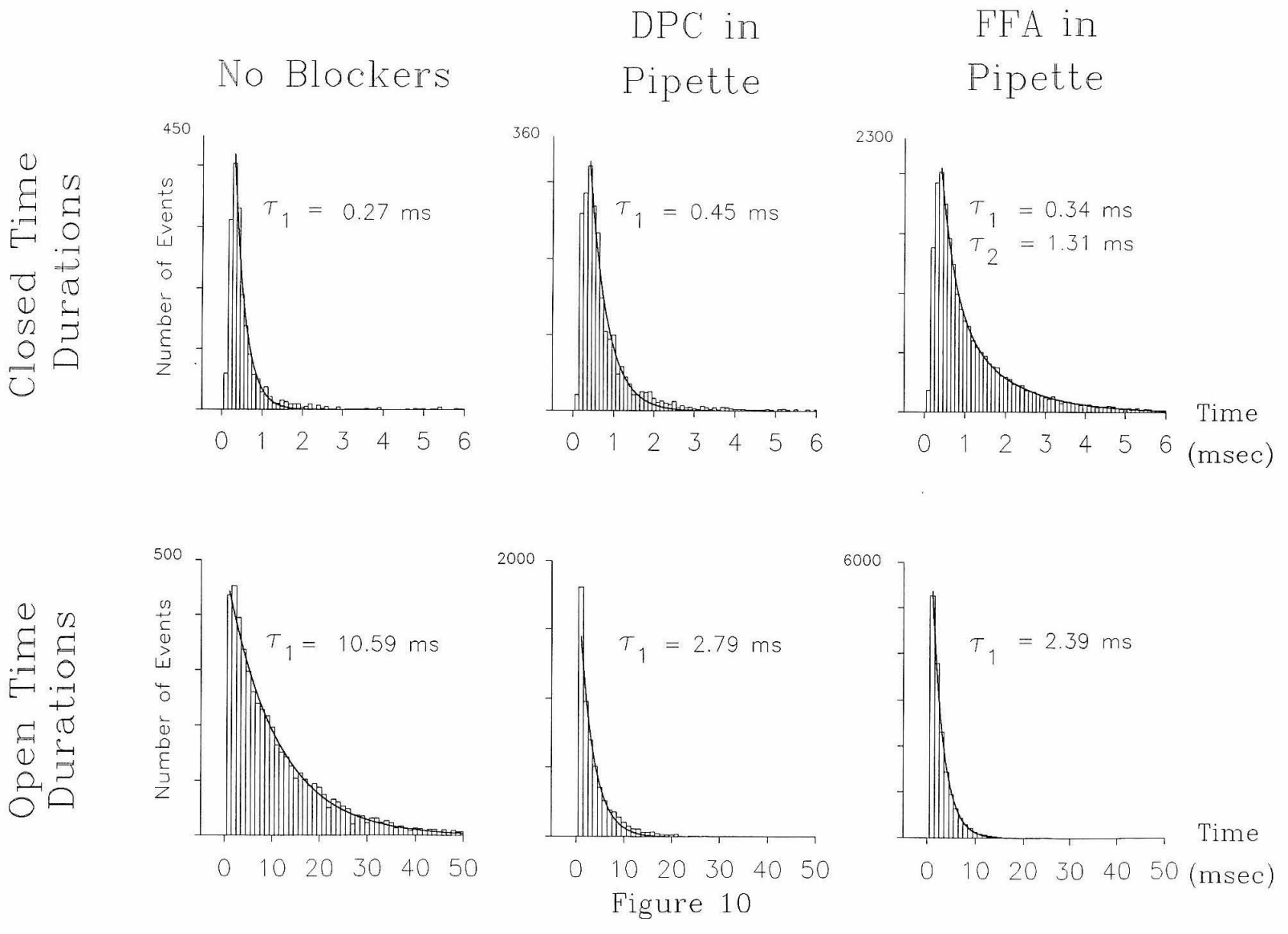
No Blockers
DPC in Pipette
FFA in Pipette
Closed Time Durations
Open Time Durations
Number of Events
450
360
2300
500
2000
6000
τ_1 = 0.27 ms
τ_1 = 0.45 ms
τ_1 = 0.34 ms
τ_2 = 1.31 ms
τ_1 = 10.59 ms
τ_1 = 2.79 ms
τ_1 = 2.39 ms
0 1 2 3 4 5 6
0 10 20 30 40 50
Time (msec)

Figure 10

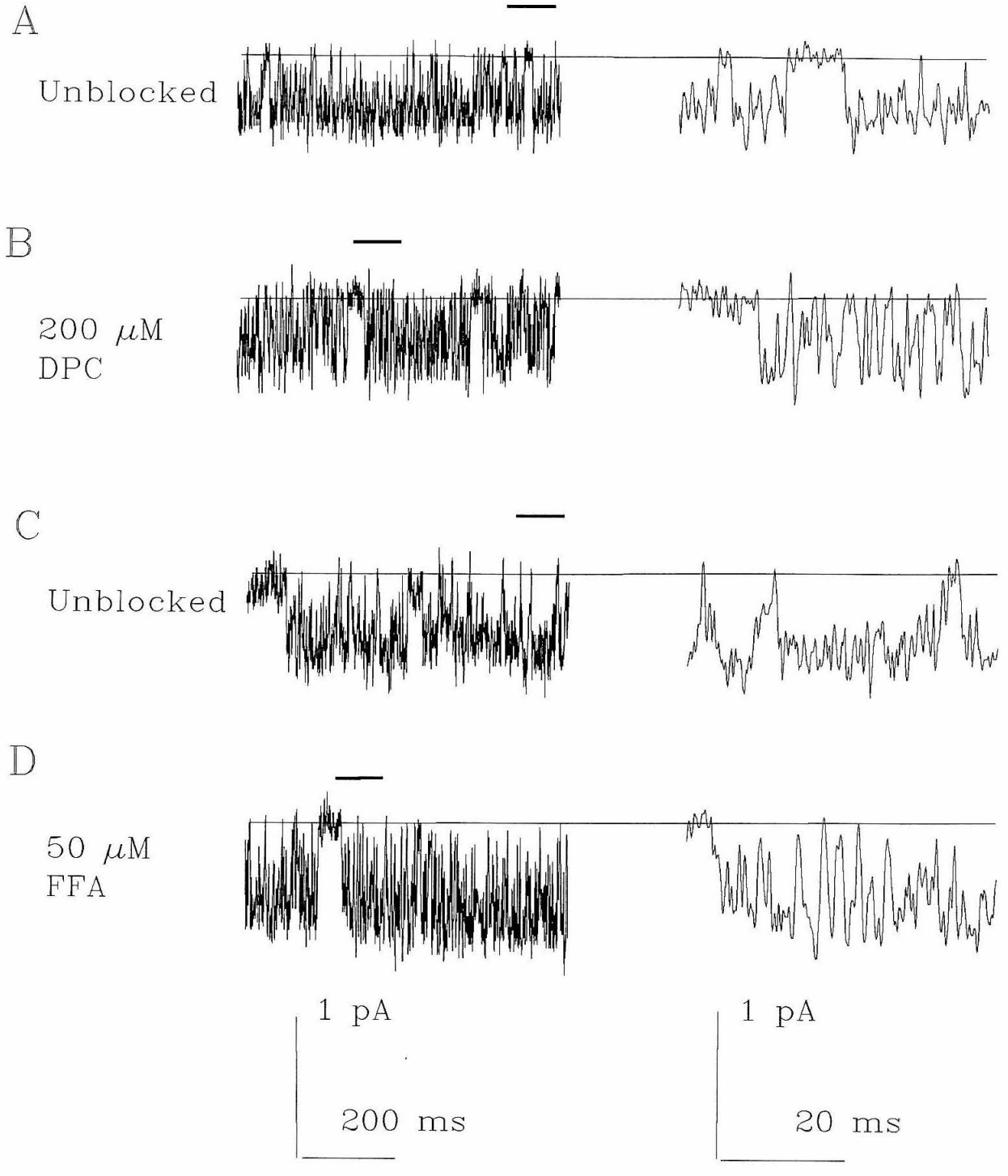
A
Unblocked
B
200 μM
DPC
C
Unblocked
D
50 μM
FFA
1 pA
200 ms
1 pA
20 ms

Figure 11

Novel Pore-Lining Residues in CFTR that Govern Permeation and Open Channel Block

Stefan McDonough, Norman Davidson, Henry A. Lester, and Nael A. McCarty

Division of Biology

California Institute of Technology

Pasadena, CA 91125

The cystic fibrosis transmembrane conductance regulator (CFTR) is both a member of the ATP-binding cassette (ABC) superfamily and a Cl^--selective ion channel. We investigated the permeation pathway of human CFTR with measurements on conduction and on open-channel blockade by diphenylamine-2-carboxylate (DPC). We used site-directed mutagenesis and oocyte expression to locate residues in transmembrane domains (TM) six and twelve that contact DPC, and that also control rectification and single-channel conductances. Thus TM-12 and the previously investigated TM-6 line the CFTR pore. In each TM domain, residues in contact with DPC are separated by two turns of an α-helix. The contributions of TM-6 and TM-12 to DPC block and Cl^- permeation, however, are not equivalent. The resulting structural model for the conduction pathway may guide future studies of permeation in other Cl^- channels and in other ABC transporters.

Introduction

The gene defective in cystic fibrosis encodes the cystic fibrosis transmembrane conductance regulator, or CFTR (Riordan et al., 1989). CFTR is expressed predominantly in epithelial tissue, such as the cells lining the pancreatic duct and sweat duct, airway epithelia, and intestinal brush-border epithelia (Riordan, 1993). When heterologously expressed in a variety of cells, CFTR forms a Cl^- channel activated by protein kinase A plus ATP (Rich et al., 1990; Anderson et al., 1991c; Kartner et al., 1991); in vivo, CFTR is essential for fluid secretion and absorption across epithelia, in at least some cases operating in tandem with an amiloride-sensitive sodium conductance (Jiang et al., 1993). Loss of function of CFTR leads to blockage of airway, pancreatic, and other ducts by abnormally thick mucus secretions. The predicted amino acid sequence reveals that CFTR is a member of the ATP-binding cassette (ABC) superfamily, with a common motif consisting of twelve putative membrane spanning domains and two nucleotide binding folds; CFTR also has a unique regulatory (R) domain (Riordan et al., 1989; Figure 1). The channel is opened by phosphorylation by protein kinase A (PKA) of consensus sites in the R-domain (Cheng et al., 1991) or cryptic sites (Chang et al., 1993), plus ATP binding (Quinton and Reddy, 1992) and hydrolysis (Anderson et al., 1991a; Baukrowitz et al., 1994) at the nucleotide binding folds. Unresolved issues include the mechanism by which phosphorylation plus ATP opens the channel, whether CFTR actively transports another substrate, how CFTR regulates an

additional, outwardly rectifying, epithelial Cl^- channel (Egan et al., 1992; Gabriel et al., 1993), and which domains of CFTR compose its pore region. We address the latter question here.

In an earlier study (McCarty et al., 1993), we showed that: (1) CFTR heterologously expressed in *Xenopus* oocytes is blocked by diphenylamine-2-carboxylic acid (DPC); (2) the block is voltage-dependent, with block occurring at hyperpolarizing, and not depolarizing, potentials; (3) Woodhull model analysis of the voltage dependence of blocker affinity indicates that the DPC binding site is ≈40% (θ = 0.41) of the electrical distance through the membrane field from the cytoplasmic side (Woodhull, 1973); (4) DPC can block the channel from either side of the membrane at hyperpolarizing voltages, and so may be permeant; and (5) DPC causes a rapid, flickery block of CFTR single channel openings. In the present study, we add data showing that (6) the flickery block displays a bimolecular forward rate and a unimolecular reverse rate; and (7) DPC binds more strongly at reduced Cl^- concentration. These data indicate that DPC binds within the permeation pathway of CFTR to produce brief interruptions in Cl^- current.

Because DPC binds within the Cl^- permeation pathway, residues in CFTR that alter DPC binding affinity when mutated may line the pore. Similar strategies were used to identify the M2 region of the nicotinic acetylcholine receptor (Leonard et al., 1988) and the H5 and S6 regions of potassium channels as lining the pore (MacKinnon and Miller, 1989; Yellen et al., 1991;

Lopez et al., 1994). We have measured both K_D, the binding affinity of DPC for the channel, and θ, the electrical distance of the DPC binding site within the pore. We combined site-directed mutagenesis with both whole-cell and single-channel recordings to identify residues in transmembrane domains (TM) six and twelve that govern Cl^- permeation and the affinity of the channel for DPC. DPC binding is weakened by some mutations in TM-6 and strengthened by some mutations in TM-12; in addition, some mutations actually move the major binding site from TM-6 to TM-12. The geometry of the residues mutated and the DPC molecule show that TM-6 and TM-12 are both α-helical. Other residues in TM-6 have been implicated in Cl^- permeation (Anderson et al., 1991b; Sheppard et al., 1993; Tabcharani et al., 1993), but no function has previously been found for the putative transmembrane domains in the C-terminal half of the CFTR sequence. Although TM-6 and TM-12 occupy homologous positions in the CFTR molecule, their contributions to DPC binding and Cl^- permeation are asymmetric. This structural asymmetry between the two domains is consistent with known permeation and substrate transport properties of other members of the ABC superfamily. These results may guide future structure-function studies on other Cl^- channels.

Results

DPC binds in the Cl^- permeation pathway

The voltage dependence of DPC block shows that it binds within the electric field of the membrane, presumably within the pore formed by CFTR (Figure 2 and Figure 3A). If DPC is an open-channel blocker of CFTR, interactions with Cl^- during the permeation process are expected. A change in DPC binding affinity under conditions of reduced extracellular Cl^- concentration, then, would indicate that DPC binding depends not only on voltage, but on the amount of Cl^- within the pore, as though DPC and Cl^- compete for a common binding site. Indeed, the K_D for DPC block of wild-type CFTR at V_m = -100 mV decreased, from K_D = 276 μM in 100 mM bath Cl^- to K_D = 181 μM in 10 mM bath Cl^- (compare Figure 3A and Figure 3B; Table 1). The reversal potential was -8 ± 1 mV with 100 mM Cl^- (n = 15), and +48 ± 2 mV with 10 mM Cl^- (n = 5), a shift near the value of +58 mV expected for a purely chloride-selective channel. Voltage-dependence of block was slightly weakened by lowered Cl^- (Table 1). Similar concentration effects occur for knockoff of tetraethylammonium (TEA), Ba^{2+}, and charybdotoxin from K^+ channel pores (Armstrong, 1971; Neyton and Miller, 1988; MacKinnon and Miller, 1988, respectively). The estimated CFTR pore diameter is 5.5 Å (Tabcharani, J. A. and Hanrahan, J. W., 1993, Biophysical Journal *64*, A17 *Abstract*). DPC measures approximately 3 Å at its narrowest and 9 Å along its longest axis in vacuum (*see* Figure 9a), and the unhydrated Cl^- ion diameter is 3.6 Å (Hille, 1992). These dimensions are consistent with DPC being itself permeant, yet also preventing simultaneous Cl^- permeation. We reason that

residues of CFTR directly involved in DPC binding lie within the pore region.

Serine 341 in TM-6 accounts for most of the DPC binding energy and governs conductance

Analysis of the electrophysiological properties of site-directed mutants shows that serine 341 in TM-6 (Figure 1) accounts for most of the binding energy between the channel and DPC. Figure 3C shows data for CFTR in which S341 is mutated to alanine (S341A); the affinity of DPC for the mutant channel is reduced by approximately five-fold compared to wild-type (K_D = 1251 μM). In Figure 4, the K_D for blockade is plotted as a function of voltage. Figure 4B shows that the voltage dependence of the weaker binding for S341A is changed only slightly from the wild-type. In the S341A mutation, Cl^- permeation in the absence of blockers is also changed: the S341A whole-cell currents rectify inwardly (Figure 3C), opposite to wild-type currents. Single-channel measurements (Figure 5) show that the conductance is reduced to ≈ 1 pS for this mutation, although the single-channel kinetics appear qualitatively unchanged. According to topological models like Figure 1, S341 lies just under halfway across the membrane from the cytoplasmic side, a distance corresponding to the electrical location of the DPC binding site (θ = 0.41) predicted from measurements on the wild-type channel. We conclude that S341 in TM-6 is a pore-lining residue.

This importance of S341 is supported by data on S341T, in which a hydroxyl group is conserved on the sidechain. The S341T mutation gives a K_D for DPC binding intermediate to S341A and the wild-type (Table 1) and a smaller degree of inward rectification than S341A (data not shown). We believe that DPC interacts with the -OH of S341, probably through hydrogen bonding of the carboxyl moiety, but that DPC has limited flexibility in its binding configuration with the wild-type channel, since S341T does not fully restore the affinity for DPC to wild-type levels.

The DPC binding site can be moved to TM-12

S1141 in TM-12 has a predicted position analogous to S341 in TM-6 (Figure 1), yet mutation S1141A had no appreciable effects on DPC binding or Cl^- permeation (Table 1). S1141 can, however, form a binding site for DPC when the S341 binding site is removed (S341A) and when the methionine and threonine residues immediately adjacent to S1141 are changed to match the isoleucine and phenylalanine residues immediately adjacent to S341. That is, the triple mutant S341A-M1140I-T1142F binds DPC more tightly than S341A alone, with an affinity close to that of the wild-type channel (Figure 3D, Figure 4). In this triple mutant, the DPC binding site has been removed in TM-6 and recreated in TM-12. This shows that TM-12 also lines the pore.

Residues closer to the extracellular face also affect DPC binding and affect

conductance weakly

Mutations in TM-12 and TM-6 at positions closer to the extracellular membrane face also affected DPC binding, further implicating TM-6 and TM-12 in pore formation. If S341 interacts with the carboxyl group of DPC and the transmembrane domains are α-helices, then K335 in TM-6 and T1134 in TM-12 (Figure 1) are predicted to lie adjacent to a phenyl ring of DPC (Figure 9b). We therefore mutated T1134 and K335 to phenylalanine in order to increase hydrophobicity at these positions. In TM-6, K335F displayed no change in rectification or θ, but slightly weakened DPC binding (Table 1). In contrast, K335E displayed slight inward rectification of unblocked currents, but this mutant had the same DPC affinity as wild-type CFTR (Figure 3F). In TM-12, the T1134F mutation increased DPC affinity to 74 ± 3 μM, but did not change θ (Figure 3E, Figure 4), suggesting that this mutation stabilizes DPC binding at its main site, S341. Hence, residues 335 and 1134 also line the pore of CFTR. The increased binding of DPC on the T1134F mutant was confirmed at the single-channel level, as described below.

T1134F single channels recorded in excised, inside-out patches had a smaller amplitude than wild-type, with conductance $\gamma = 5.8 \pm 0.2$ pS (range 4.1 to 6.4 pS, n = 14), versus $\gamma = 8.0 \pm 0.4$ pS for wild-type (McCarty et al., 1993). This provides further evidence that T1134 lines the pore. As with S341A, however, the T1134F mutant channel kinetics are qualitatively similar to wild-type, with seconds-long openings, uninterrupted at positive voltages and

interrupted by brief closures at negative voltages (Figure 6, Figure 7). Also like the wild-type, T1134F occasionally shows a long-lived subconductance state, with amplitude ≈ 60% of the full conductance. As noted previously for the wild-type channel (McCarty et al., 1993), the subconductance state in T1134F is not blocked by DPC (Figure 6B), as though DPC cannot reach its binding site at S341 when the channel is in this state.

A further test for open-channel block

Application of DPC to the cytoplasmic surface of excised inside-out patches resulted in blocker-induced closures of three- to four-fold longer duration for T1134F than for wild-type, as expected from the increased DPC affinity of the T1134F mutation (Figure 6). The longer residence time of DPC on the T1134F channel enabled us to resolve the kinetics of blockade at several DPC concentrations with V_m = -100 mV. Increasing the concentration of DPC at the cytoplasmic side of excised inside-out patches increased the number of brief flickery closed times, without changing their duration (Figure 7 A-E). The closed times of T1134F due to DPC lengthened to 1.8 ± 0.1 ms (averaged from 20, 50, and 100 μM) and were independent of DPC concentration (Table 2, Figure 7, Figure 8). The channel open time decreased with increasing DPC, such that $1/\tau_o$ increased linearly with DPC concentration. Both effects agree with expectations for an open-channel blocker. In such a scheme, the channel is blocked when DPC binds and unblocked when DPC dissociates:

$$\text{CFTR} \underset{k_{off}}{\overset{k_{on}[DPC]}{\rightleftarrows}} \text{CFTR+DPC (blocked)}$$

where k_{on} is the bimolecular rate constant for DPC binding to CFTR, and k_{off} is the unimolecular rate constant for dissociation of the complex. The parameter k_{off} is $1/\tau_{c,DPC}$ ($= 1/\tau_{c2}$), while k_{on} is the slope of the line of $1/\tau_o$ vs. DPC concentration. From Figure 8, the $k_{on} = 6.4 \times 10^6$ $M^{-1}sec^{-1}$, and k_{off} is 560 sec^{-1}. In an important test of this scheme, we use the kinetic data to predict the equilibrium dissociation constant $K_D = k_{off}/k_{on} = 88$ μM. This calculation agrees very well with the independently measured value of 74 μM obtained in the whole-cell measurements of DPC blockade at V_m = -100 mV.

Note that the unblocked closed times of the T1134F channel, unlike the wild-type, are fit by two time constants; these time constants are nearly equal to those measured during DPC blockade. The higher the concentration of DPC, the more time spent in the long closed states (Table 2).

Other mutations do not affect DPC binding

Several serine or threonine to alanine mutations did not affect DPC binding (Table 1); this is further evidence for the specificity of the residues noted. For most mutants, DPC block was apparent at negative potentials only; exceptions are the blockade of outward currents for T1134F, due to the greatly increased affinity for DPC, and the triple mutation, due to the changed voltage dependence of block. All mutants showed time-independent currents, as did

the wild-type. Wild-type CFTR single channels in symmetrical Cl^- have a linear I-V relation; however, these whole-cell experiments show outward rectification for WT CFTR at strongly hyperpolarizing potentials due to the lower value of cytoplasmic [Cl^-] relative to that in the bath (McCarty et al., 1993; see also Overholt et al., 1993).

Discussion

CFTR is an intriguing molecule, because (1) its topology resembles that of ATP-binding cassette (ABC) transporters, such as the multidrug resistance P-glycoprotein (MDR), the antigen peptide transporters of the major histocompatibility locus, TAP-1 and TAP-2, and bacterial permeases, and yet (2) CFTR is a Cl^- channel, with no other known transported substrate. In addition, cloned chloride-selective ion channels have no common structural motif, such as the tetrameric domain arrangement found in voltage-gated cation channels, or the P-region apparently shared by all K^+ channels. Characterization of the residues of CFTR involved in creating the pore, then, is relevant both to the study of Cl^- channels and to the study of the ABC superfamily.

DPC is an open-channel blocker

Results presented earlier (McCarty et al., 1993) and extended here show that

DPC binds within the pore of CFTR. (1) The block is voltage-dependent; (2) The block is flickery at the single-channel level; (3) The DPC block is enhanced by reduced Cl^- concentration; (4) Mutation of residues within predicted transmembrane domains strengthens or weakens the block. (5) For the T1134F mutation, which has kinetics favorable for detailed study, the rate constant for blocking (inverse of the open time constant) increases linearly with [DPC]; but the rate constant for unblocking is independent of [DPC]. These data agree with the classical kinetic model in which the blockade is governed by a bimolecular forward binding step and by a unimolecular dissociation step (Lester, 1992). It is possible that DPC could reach its binding site in the pore through the lipid phase (McCarty et al., 1993), as demonstrated for the block of sodium channels by some local anesthetics (Hille, 1977). However, the route by which DPC reaches its binding site does not change the conclusions about the nature of the binding site.

Although many observations presented here are consistent with the simple view that DPC is an open-channel blocker at wild-type and mutant CFTR channels, a complication is added by the observations that unblocked T1134F displays an extra closed time constant compared to wild-type, and that this time constant is similar to the residence time of DPC. For the wild-type channel, however, DPC produces closed times much longer than the endogenous closures (McCarty et al., 1993). We believe that the unblocked T1134F channel only coincidentally has a time constant near that of the lifetime

of DPC on the T1134F channel. The extra endogenous time constant may be caused by the insertion of a bulky hydrophobic group into the permeation pathway.

The pore of CFTR is lined by TM-6 and TM-12

We conclude that TM-6 lines the pore because mutation S341A lowers the single channel conductance by a factor of 8, reverses the direction of rectification, and removes most binding of the open-channel blocker DPC. Also in TM-6, mutation K335F slightly reduces DPC block, and mutation K335E gives inward rectification (see also Tabcharani et al., 1993). In TM-12, mutation T1134F strongly increases DPC affinity, as confirmed by single-channel measurements, and significantly lowers the single channel conductance. The sequence M1140I-S1141-T1142F in TM-12 restores DPC binding to the S341A mutant; these effects show that TM-12 also lines the pore. The identification of TM-6 and TM-12 as pore-lining domains is consistent with and extends previous structure-function work on CFTR.

Previous studies of CFTR have found that mutation of positively charged residues in TM-1 and TM-6 (including K335E) give small changes in ionic selectivity (Anderson et al., 1991b), and that naturally occurring mutations of positively charged residues just extracellular to TM-2, or within TM-6 (R347P and R334W) reduce single-channel conductance and alter kinetics (Sheppard et al., 1993). Removal of positive charge at position 347 reduces

multiple-ion occupancy of the pore and lowers single-channel conductance (Tabcharani et al., 1993). Taken together, our results and those of others point to TM-6 as a principal determinant of Cl^- permeation. Indeed, a truncated CFTR construct, including only the first six TM domains, the first nucleotide binding fold, and the R domain, is sufficient to form CFTR-like channels (Sheppard et al., 1994). The conduction pathway may include three Cl^- binding sites on TM-6, controlled directly or indirectly by R334/K335, S341, and R347. The mutations R334W, R347P, and S341A may reduce single-channel conductance by removing a Cl^- binding site. The mutant pore, with only two ion binding sites, would have less mutual repulsion between the Cl^- ions, and, therefore, a lower conductance than the wild-type.

Our study is the first to show an effect on conductance of any putative TM domain other than TM-6 and the first to show any effect on conduction for residues in the C-terminal half of the CFTR sequence. Nonetheless, our TM-12 mutations have no or much weaker effects on permeation than corresponding mutations in TM-6. We conclude that TM-6 and TM-12 make asymmetric contributions to the pore. In earlier studies on the M2 region of nicotinic acetylcholine receptors, analogous mutations in different transmembrane helices at the same presumptive level in the channel had equivalent effects when performed separately and additive effects when performed simultaneously. It was concluded that the ACh receptor pore contains annuli whose properties are averaged from those of the individual side chains

(Leonard et al., 1988; Imoto et al., 1988; Charnet et al., 1990). The asymmetric CFTR channel is apparently not such a featureless annulus.

Role of hydroxylated side chains

Results presented here are the first to implicate serine and threonine residues in Cl^- conduction at CFTR, and they evoke the well-known roles of these hydroxylated residues in the $GABA_A$ and glycine receptor Cl^- channels (Lester, 1992). Indeed, the transmembrane domains of CFTR localized to the pore here are homologous to the amphipathic M2 domains of the $GABA_A$ and glycine receptor Cl^- channels (Figure 10). The abundance of polar serine and threonine residues in the sequences shown implies that sites in the CFTR pore might bind Cl^- by replacing the waters of hydration, a mechanism long proposed for selectivity (Eisenman and Horn, 1983) but recently challenged for K^+ channels (Heginbotham and MacKinnon, 1992; Kumpf and Dougherty, 1993).

Allosteric effects of the mutations?

It remains a formal possibility that the effects of site-directed mutations of CFTR on DPC block are due to propagated allosteric effects, rather than to direct changes in side-chain interaction with DPC. This possibility seems unlikely because of several findings. The mutation that produces the largest effect on DPC block, S341A, also lowers the single-channel conductance from 8

pS to 1 pS and changes the rectification from outward to inward. Only the most tortuous of arguments would conclude that mutation of a residue actually located outside the pore propagates allosterically to give all three effects. Furthermore, S341 lies ~40% through the proposed TM sequence, the electrical distance of the DPC binding site predicted by whole-cell measurements on wild-type CFTR (McCarty et al., 1993), in support of the direct physical identity between the mutated residues and the DPC binding site. The possibility that the effects of S341A are allosteric is also rendered less likely by the intermediate effect on both drug block and rectification of replacing S341 with another hydroxylated residue, threonine. The presumed scenario of a non-specific effect of S-to-A being propagated extensively while the same non-specific effect of S-to-T also propagates, but to a lesser degree, seems unlikely. The conservative S341T mutation alone weakens DPC block enough to implicate residue S341 in binding DPC. In addition, other mutations of hydroxylated residues in TM-6, namely T338A and T339A, affect neither DPC block nor rectification (Table 1). This argues against the proposal that any alteration in sequence within TM-6 causes non-specific effects, and is further evidence for the specificity of the S341A mutation. Similarly, in TM-12, mutation T1134F strengthens DPC binding and also reduces single-channel conductance from 8 pS to <6 pS. DPC binds at the same electrical position, 40% of the way through the membrane, in the T1134F mutant as in the wild-type, evidence that T1134F makes no gross mutations in the binding site.

Control mutation T1134A has insignificant effects on DPC binding, as does mutation S1118A, in TM-11 at a position homologous to T1134. In the absence of atomic-scale structural data on CFTR, the simplest interpretation of our data is that the effects of the mutants are due to differences in direct side-chain interactions with DPC and the Cl^- permeation pathway.

A proposed α-helical model of the pore

The data presented support a model (Figure 9B,C) in which the pore of the CFTR channel is made up of TM-6 and TM-12, with contributions from other, as yet unidentified transmembrane domains. In addition, multiple contacts made by DPC within the pore indicate that both TM-6 and TM-12 line the pore and are α-helical. The data show that positions 1134 and 1141 both interact with DPC. If the 8-residue span of TM-12 including these residues is α-helical, positions 1141 and 1134 are two turns of the helix (10.8 Å) from each other and on the same side. They would then interact with moieties separated by the longest axis of the DPC molecule (9 Å), presumably the carboxyl group and the distal phenyl ring. An extended structure, for instance, a β strand, would place positions 1134 and 1141 too far apart to interact simultaneously with a DPC molecule. Mutations at positions 335 and 341 also independently weaken DPC binding without changing the binding site; hence, we conclude that the intervening span of TM-6 also has an α-helical structure.

The relative orientation of the side chains on the phenylalanines of

K335F and T1134F may explain the opposite results of phenylalanines placed at these nearly equivalent positions. In our model of TM-12, the phenyl ring of T1134F points directly into the pore and lies along and perpendicular to the second phenyl ring of DPC. This proximity may stabilize DPC binding by bringing the π electron cloud of one phenyl group next to the positive charge of the plane of carbon atoms of another group. In TM-6, the K335F mutation slightly decreased DPC binding affinity; Figure 9C shows how a phenyl ring at position 335 would lie parallel to and farther away from the second phenyl ring of DPC, destabilizing DPC binding at S341.

The interaction between Cl^- and DPC

How would lowered external Cl^- affect the voltage dependence of DPC block? If external chloride occupies a binding site at the DPC binding site or nearby, it could destabilize DPC binding by steric and/or electrostatic effects. Lowering of external Cl^-, resulting in reduced occupancy of the external Cl^- site, would stabilize DPC binding. An analogy is found for Ba^{2+} block of Ca^{2+}-activated K^+ channels, where the Ba^{2+} off-rate is raised and the voltage dependence of internal Ba^{2+} block is changed, even to reversal, by raising external K^+ (Neyton and Miller, 1988). Our data suggest that an interaction between DPC and Cl^- occurs at or near S341, for mutations here affect both DPC block and Cl^- binding. The triple mutation could reduce θ by similarly affecting local concentrations of Cl^- within the pore. Residues whose

mutations change θ, like S341, would be sites of competition between Cl^- and DPC. Mutations affecting DPC affinity alone, with no effect on θ, like K335 or T1134, would be interacting with DPC directly without influencing competition with Cl^-.

Implications for substrate specificity in ABC transporters

Our results also shed light on functional aspects of ABC transporters. The MDR is the closest known homolog to CFTR. MDR mediates the efflux of amphiphilic cytotoxic drugs in an ATP-dependent manner (Germann et al., 1993), but some experiments suggest that it may also be a volume-regulated Cl^- channel (Valverde et al., 1992). Photoaffinity labeling of MDR has shown that regions close to or in TM-6 and TM-12 contain drug binding sites (Greenberger, 1993). This suggests that the permeation pathway localized here for CFTR may occur in MDR as well. MDR has a rather broad substrate specificity, perhaps because the permeant substrate makes most of its contacts with only one helix, as found here for Cl^- through CFTR. It will be of interest to determine whether the individual residues governing Cl^- and drug permeation through MDR have positions analogous to those reported here.

Other ABC transporters, such as STE6 in yeast and the mammalian endoplasmic reticulum peptide transporters, have considerably higher substrate specificity than does MDR (Germann et al., 1993). We suggest that such specificity can arise if several helices make simultaneous asymmetric

contact with the permeant substrate. It is not known whether TM-6 and TM-12, two helices that line the CFTR permeation pathway, also subserve permeation in other ABC transporters. Such similarity of structure and function would further bridge the narrowing conceptual gap between transporters and channels.

Experimental Procedures

Molecular Biology

The full coding region of CFTR in pSP64 (McCarty et al., 1993) was excised by digestion with *Pst I* and *Sac I* and transferred into the corresponding *Pst I* and *Sac I* sites of pAlter (Promega), which contains a deficient ampicillin resistance gene. Site-directed mutants were made by annealing an ampicillin repair oligonucleotide and an oligo containing the mutagenic sequence to single-stranded pAlter-CFTR, filling in and ligating with T4 polymerase and ligase, and transforming into BMH 71-18 *mutS* (Clontech) mismatch repair-deficient cells under ampicillin selection. The resulting plasmids, a mixture of pAlter-CFTR plasmids which did and which did not receive both oligos, were transformed into TOP 10 F′ cells. Mutant CFTR colonies were selected for incorporation of a silent restriction site engineered into the mutagenic oligo. All mutants were sequenced in both directions around the mutation. Capped transcripts (2-35 ng) were coinjected with 0.1-0.5 ng of β_2-adrenergic receptor cRNA into *Xenopus* oocytes as previously described (McCarty et al., 1993).

Electrophysiology

Two-electrode voltage clamp data were acquired at room temperature (20 °C) with a GeneClamp 500 and pCLAMP software (Axon Instruments).

The corner frequency was 2 kHz. Recording medium contained (mM): 96 NaCl, 2 KCl, 1 $MgCl_2$, 5 HEPES, pH 7.4 to 7.5. For low Cl^- experiments, the recording medium was the same, with a substitution of 90 mM Na-isethionate for 90 mM NaCl. Recording electrodes (resistance 1-2 MΩ) were filled with 3M KCl. The chamber was connected to ground via two Ag-AgCl pellets connected to the virtual ground bath clamp headstage. Background currents with and without DPC were subtracted from the blocked and unblocked currents shown in the figures. CFTR currents were activated by bath application of 1 μM isoproterenol; activation was maintained at a constant level by reapplication of isoproterenol as needed. For I-V curves, current was averaged over 50 ms from the latter part of each voltage step. For whole cell trials, K_D was calculated from $K_D = I^*(200\mu M) / (I_0 - I)$ for each cell; I, the current with DPC, and I_0, the current in the absence of DPC, were determined empirically at V_m = -100 mV. K_D and θ calculations assume a valence of unity and a single binding site for DPC.

Single channel currents were recorded from manually stripped oocytes injected with 70 ng T1134F cRNA or with 100 ng S341A plus 0.8 ng β_2-AR cRNA; when necessary, channels were activated in cell-attached mode with 5μM forskolin, 100μM IBMX, 100 μM dibutyryl-cAMP and/or 1 μM isoproterenol. Patch pipette solution contained (mM): 150 *N*-methyl-D-glucamine-Cl, 0.5 $MgCl_2$, and 10 TES, pH adjusted to 7.4 with Tris. The intracellular solution for inside-out patches contained (mM): 150 NMDG-Cl, 1.1

$MgCl_2$, 2 Tris-EGTA, 10 TES, and 1 Mg-ATP (from equine muscle, < 1 ppm vanadium), pH 7.4. For the record of wild-type CFTR in Figure 6C, the cytoplasmic solution also contained 10 mM NaF, which did not change the unblocked open- or closed-times (McCarty et al., 1993). When filled with the pipette solution, patch pipette resistances were ≈20 MΩ. Seal resistances ranged from 30 to >300 GΩ. Records were taken with the GeneClamp 500 at 2 kHz and stored on videotape. During acquisition by the Fetchex program of pCLAMP 5.5, currents were filtered at 1 kHz with an 8-pole Bessel filter (Frequency Devices, Inc.), and digitized at 10 kHz. T1134F single-channel traces were amplified at 20 dB/ decade during acquisition. For the S341A mutation, which results in single channels of very low conductance, currents were filtered at 100 Hz and amplified at 20 dB/ decade during acquisition. Events lists were generated by Fetchan version 6.0 and analyzed with pStat 6.0; the simplex maximum-likelihood algorithm was used to fit exponentials to open- and closed-time duration histograms. System dead time was 0.3-0.4 ms. The first bin (from 0 to 1 ms) was excluded from open-time fits, and closed-time fitting began at 0.5 ms. Inward currents (anions passing from the cytoplasmic solution to the external, pipette solution) are shown as downward deflections from the baseline. Statistics are mean ± S.E.M. All other methods and reagents are as previously described (McCarty et al., 1993).

Molecular Modeling

Calculation of DPC structure and display of the models was performed with HyperChem 2.0 (Autodesk, Inc.) running under Windows 3.1. Vacuum structure of DPC was obtained using MM+ energy minimization.

Acknowledgments

We thank H. Davis for expert oocyte preparation, M. Quick and M. Nowak for review of the manuscript, and B. Flatt for initial modeling assistance. This research was supported by the NIH (NRSA to N.A.M. and S.M., and research grant), and the Cystic Fibrosis Foundation.

References

Anderson, M. P., Berger, H. A., Rich, D. P., Gregory, R. J., Smith, A. E., and Welsh, M. J. (1991a). Nucleoside triphosphates are required to open the CFTR chloride channel. Cell *67,* 775-784.

Anderson, M. P., Gregory, R. J., Thompson, S., Souza, D. W., Paul, S., Mulligan, R. C., Smith, A. E., and Welsh, M. J. (1991b). Demonstration that CFTR is a chloride channel by alteration of its anion selectivity. Science *253,* 202-205.

Anderson, M. P., Rich, D. P., Gregory, R. J., Smith, A. E., and Welsh, M. J. (1991c). Generation of cAMP-activated chloride currents by expression of CFTR. Science *251,* 679-682.

Armstrong, C. M. (1971). Interaction of tetraethylammonium derivatives with the potassium channels of giant axons. Journal of General Physiology *58,* 413-437.

Baukrowitz, T., Hwang, T.-C., Nairn, A. C., and Gadsby, D. C. (1994). Coupling of CFTR Cl^- channel gating to an ATP hydrolysis cycle. Neuron *12,* 473-482.

Chang, X. B., Tabcharani, J. A., Hou, Y. X., Jensen, T. J., Kartner, N., Alon, N., Hanrahan, J. W., and Riordan, J. R. (1993). Protein kinase A (PKA) still activates CFTR chloride channel after mutagenesis of all 10 PKA consensus phosphorylation sites. Journal of Biological Chemistry *268*, 11304-11311.

Charnet, P., Labarca, C., Leonard, R. J., Vogelaar, N. J., Czyzyk, L., Gouin, A., Davidson, N., and Lester, H. A. (1990). An open-channel blocker interacts with adjacent turns of α-helices in the nicotinic acetylcholine receptor. Neuron *2*, 87-95.

Cheng, S. H., Rich, D. P., Marshall, J., Gregory, R. J., Welsh, M. J., and Smith, A. E. (1991). Phosphorylation of the R domain by cAMP-dependent protein kinase regulates the CFTR chloride channel. Cell *66*, 1027-1036.

Egan, M., Flotte, T., Afione, S., Solow, R., Zeitlin, P. L., Carter, B. J., and Guggino, W. B. (1992). Defective regulation of outwardly rectifying Cl^- channels by protein kinase A corrected by insertion of CFTR. Nature **358,** 581-584.

Eisenman, G., and Horn, R. (1983). Ionic selectivity revisited: the role of kinetic and equilibrium processes in ion permeation through channels. Journal of Membrane Biology *76*, 197-225.

Gabriel, S. E., Clarke, L. L., Boucher, R. C., Stutts, M. J. (1993). CFTR and outward rectifying chloride channels are distinct proteins with a regulatory relationship. Nature *363*, 263-266.

Germann, U. A., Pastan, I., and Gottesman, M. M. (1993). P-glycoproteins: mediators of multidrug resistance. Seminars in Cell Biology *4*, 63-76.

Greenberger, L. M. (1993). Major photoaffinity drug labeling sites for iodoaryl azidoprazosin in P-glycoprotein are within, or immediately C-terminal to, transmembrane domains 6 and 12. Journal of Biological Chemistry *268*, 11417-11425.

Grenningloh, G., Rienitz, A., Schmitt, B., Methfessel, C., Zensen, M., Beyreuther, K., Gundelfinger, E., and Betz, H. (1987). The strychnine-binding subunit of the glycine receptor shows homology with nicotinic acetylcholine receptors. Nature *328*, 215-220.

Heginbotham, L., and MacKinnon, R. (1992). The aromatic binding site for tetraethylammonium ion on potassium channels. Neuron *8*, 483-491.

Hille, B. (1977). Local Anesthetics: Hydrophilic and Hydrophobic Pathways for the Drug-Receptor Reaction. Journal of General Physiology **69,** 497-515.

Hille, B. (1992). Ionic Channels of Excitable Membranes (Sinauer, Sunderland, MA, ed. 2).

Imoto, K., Busch, C., Sakmann, B., Mishina, M., Konno, T., Nakai, J., Bujo, H., Mori, Y., Fukuda, K., and Numa, S. (1988). Rings of negatively charged amino acids determine the acetylcholine receptor channel conductance. Nature **335,** 645-648.

Jiang, C., Finkbeiner, W. E., Widdicombe, J. H., McCray, P. B., and Miller, S. C. (1993). Altered fluid transport across airway epithelium in cystic fibrosis. Science *262,* 424-427.

Kartner, N., Hanrahan, J. W., Jensen, T. J., Naismith, A. L., Sun, S., Ackerley, C. A., Reyes, E. F., Tsui, L.-C., Rommens, J. M., Bear, C. E., and Riordan, J. R. (1991). Expression of the cystic fibrosis gene in non-epithelial invertebrate cells produces a regulated anion conductance. Cell *64,* 681-691.

Kumpf, R. A., and Dougherty, D. A. (1993). A mechanism for ion selectivity in potassium channels: computational studies of cation-π interactions. Science *261,* 1708-1710.

Leonard, R. J., Labarca, C. G., Charnet, P., Davidson, N., and Lester, H. A.

(1988). Evidence that the M2 membrane-spanning region lines the ion channel pore of the nicotinic receptor. Science *242*, 1578-1581.

Lester, H. A. (1992). The permeation pathway of neurotransmitter-gated ion channels. Annu. Rev. Biophys. Biomol. Struct. *21*, 267-292.

Lopez, G. A., Jan, Y. N., and Jan, L. Y. (1994). Evidence that the S6 segment of the *shaker* voltage-gated K^+ channel comprises part of the pore. Nature *367*, 179-182.

MacKinnon, R., and Miller, C. (1988). Mechanism of charybdotoxin block of the high-conductance, Ca^{2+}-activated K^+ channel. Journal of General Physiology *91*, 335-349.

MacKinnon, R., and Miller, C. (1989). Mutant potassium channels with altered binding of charybdotoxin, a pore-blocking peptide inhibitor. Science **245,** 1382-1385.

McCarty, N. A., McDonough, S., Cohen, B. N., Riordan, J. R., Davidson, N., and Lester, H. A. (1993). Voltage-dependent block of the cystic fibrosis transmembrane conductance regulator channel by two closely related arylaminobenzoates. Journal of General Physiology *102*, 1-23.

Neyton, J., and Miller, C. (1988). Discrete Ba^{2+} block as a probe of ion occupancy and pore structure in the high-conductance Ca^{2+} -activated K^{+} channel. Journal of General Physiology *92*, 569-586.

Overholt, J. L., Hobert, M. E., and Harvey, R. D. (1993). On the mechanism of rectification of the isoproterenol-activated chloride current in guinea-pig ventricular myocytes. Journal of General Physiology **102,** 871-895.

Quinton, P. M., and Reddy, M. M. (1992). Control of CFTR chloride conductance by ATP levels through non-hydrolytic binding. Nature *360*, 79-81.

Rich, D. P., Anderson, M. P., Gregory, R. J., Cheng, S. H., Paul, S., Jefferson, D. M., McCann, J. D., Klinger, K. W., Smith, A. E., and Welsh, M. J. (1990). Expression of cystic fibrosis transmembrane conductance regulator corrects defective chloride channel regulation in cystic fibrosis airway epithelial cells. Nature *347*, 358-363.

Riordan, J. R. (1993). The cystic fibrosis transmembrane conductance regulator. Annual Review of Physiology *55*, 609-630.

Riordan, J. R., Rommens, J. M., Kerem, B.-S., Alon, N., Rozmahel, R., Grzelczak, Z., Zielenski, J., Lok, S., Plavsic, N., Chou, J.-L., Drumm, M. L.,

Iannuzzi, M. C., Collins, F. S., and Tsui, L.-C. (1989). Identification of the cystic fibrosis gene: cloning and characterization of complementary DNA. Science *245*, 1066-1073.

Sheppard, D. N., Ostedgaard, L. S., Rich, D. P., and Welsh, M. J. (1994). The amino-terminal portion of CFTR forms a regulated Cl^- channel. Cell **76,** 1091-1098.

Sheppard, D. N., Rich, D. P., Ostedgaard, L. S., Gregory, R. J., Smith, A. E., and Welsh, M. J. (1993). Mutations in CFTR associated with mild-disease form channels with altered pore properties. Nature *362*, 160-164.

Tabcharani, J. A., Rommens, J. M., Hou, Y.-X., Chang, X.-B., Tsui, L.-C., Riordan, J. R., and Hanrahan, J. W. (1993). Multi-ion pore behaviour in the CFTR chloride channel. Nature *366*, 79-82.

Valverde, M. A., Diaz, M., Sepulveda, F. V., Gill, D. R., Hyde, S. C., and Higgins, C. F. (1992). Volume-regulated chloride channels associated with the human multidrug-resistance P-glycoprotein. Nature *355*, 830-833.

Woodhull, A. M. (1973). Ionic blockage of sodium channels in nerve. Journal of General Physiology *61*, 687-708.

Yellen, G., Jurman, M. E., Abramson, T., and MacKinnon, R. (1991). Mutations affecting internal TEA blockade identify the probable pore-forming region of a K^+ channel. Science *251*, 939-941.

TABLE 1 Affinity and voltage-dependence for block of CFTR variants by DPC

Construct	TM ##	K_D(-100) (μM)	Θ	*n*	I-V Relation Properties
Wildtype		276 ± 14	0.41 ± 0.01	15	Linear; E_{rev} = -8 ± 1 mV
WT Low $[Cl^-]_o$ (10 mM)		181 ± 13*	0.32 ± 0.02*	5	E_{rev} = +48 ± 2 mV
K335E	6	303 ± 14	0.42 ± 0.01	5	Inward Rectification
K335F	6	351 ± 15*	0.42 ± 0.02	4	Linear
T338A	6	220 ± 14	0.36 ± 0.02*	7	Linear
T339A	6	284 ± 47	0.44 ± 0.12	3	Linear
S341A	6	1251± 116*	0.49 ± 0.03*	8	Strong inward rectification
S341T	6	530 ± 80*	0.35 ± 0.09	3	Inward rectification
S1118A	11	243 ± 37	0.40 ± 0.02	5	Linear
T1134A	12	230 ± 20	0.35 ± 0.02*	6	Linear
T1134F	12	74 ± 3*	0.41 ± 0.01	5	Linear
S1141A	12	220 ± 13	0.42 ± 0.03	5	Linear
Triple	6,12	325 ± 26†	0.21± 0.01*†	7	Strong inward rectification

Affinity for DPC was determined empirically at -100 mV, from whole-cell currents measured in the presence of 200 μM DPC, using the same experimental protocol as in Figure 2. Θ is expressed as the fractional electrical distance from the intracellular end of the pore. For these experiments, the slope was calculated from the $K_D(V)$ values over the range of -140 to -60 mV. That Θ approximated the WT value of 0.41 for the mutations in TM6 and TM12 provides evidence that these mutations made no gross perturbation in overall channel structure. Properties of the I-V relation were determined from the average current levels over the final 50 ms of a 75 ms voltage step for WT and all mutants. E_{rev} is the reversal potential, determined empirically from the voltage steps. Triple refers to the S341A-M1140I-T1142F mutant.

TM## Transmembrane domain.

Values given are mean ± S.E.M. for *n* oocytes.

*,† $p < 0.025$ by unpaired t-test compared to WT or mutant S341A, respectively.

TABLE 2 Time constants for block of T1134F single channels by various DPC concentrations

[DPC]	τ_o	τ_{c1}	τ_{c2}	n	Area, τ_{c2}
0	8.4 ± 0.7	0.31 ± 0.02	1.9 ± 0.14	4	0.13 ± 0.01
20	4.6 ± 0.4	0.31 ± 0.05	1.9 ± 0.13	3	0.28 ± 0.05
50	3.2 ± 0.3	0.39 ± 0.03	2.0 ± 0.33	3	0.47 ± 0.07
100	1.3 ± 0.1	0.46 ± 0.02	1.6 ± 0.13	3	0.61 ± 0.07

Time constants are in ms; [DPC] is in μM. Given time constants are averaged from n closed- and open-time histograms such as in Figure 6 and Figure 7. Open-time histograms were fit with a single exponential; closed-time histograms were fit with two. All records taken at V_m = -100 mV from inside-out patches excised into 1 mM ATP plus the given concentration of DPC. [DPC]: the concentration of DPC. τ_o: the open time constant. τ_{c1}: the first closed time constant. τ_{c2}: the second closed time constant. Area, τ_{c2}: the percent of the total closed time due to the second closed time constant. Values given are mean ± S.E.M. for n patches.

Figure 1. **Predicted transmembrane topology of CFTR with location of selected mutation sites.**

1, K335. 2, S341. 3, T1134. 4, S1141. NBF1 & NBF2, nucleotide binding folds 1 and 2. R, R-domain.

Figure 2. **Macroscopic waveforms for DPC blockade of wildtype CFTR.**

Voltage was stepped to test potentials between -140 and +80 mV at increments of +20 mV from a holding potential of -45 mV. CFTR currents were isolated by subtraction of background currents (see Methods). (a) Wild-type CFTR currents. (b) Same cell with 200 μM DPC in the bath. The current traces for -140 mV and -80 mV overlap, as do the currents at -120 mV and -100 mV.

Figure 3. **I-V relations of representative cells for wild-type CFTR and selected mutants, with and without blockers.**

Points for I-V traces are averaged over 50 ms from the latter half of each voltage step, using the voltage protocol in Figure 2. Hollow circles, unblocked CFTR currents. Filled circles, currents with 200 μM DPC. (a) Wild-type CFTR current. (b) Data from another cell. Wild-type current in low external Cl^- solution, showing increased block at hyperpolarized potentials and shifted reversal potential. (c) S341A mutant, showing strong inward rectification and decreased DPC block. (d) Triple mutation (S341A-M1140I-T1142F), showing strong inward rectification and restored DPC block compared to (c). (e) T1134F mutation, showing increased block at all voltages. (f) K335E mutation, indicating inward rectification and unchanged DPC binding affinity.

Figure 4. **Voltage dependence of blocker affinity for wild-type and three mutations of CFTR.**

Hollow circles, wild-type. Filled circles, T1134F. Hollow boxes, S341A. Filled boxes, triple mutation (S341A-M1140I-T1142F). Points are an average from n separate cells (n for each type is given in Table 1). S.E.M. are shown where they exceed the size of the symbols. (A) Fraction of CFTR current remaining after bath application of 200 μM DPC. I_0, current before DPC application. I, current with DPC. Data from individual cells were taken directly from background-subtracted records for each voltage. (B) K_D calculated from $K_D = I^*(200\ \mu M)/(I_0 - I)$ plotted on a semilogarithmic scale. Line shown is the regression line. Slope is proportional to the electrical binding distance, θ. Values for these and other mutants are summarized in Table 1.

Figure 5. **S341A has a low single-channel conductance.**

Currents are from channels in cell-attached mode. Data are filtered at 100 Hz to resolve the openings clearly. The horizontal line indicates the closed level. (a) V_m = +100 mV. (b) V_m = -100 mV.

Figure 6. **The residence time of DPC on the T1134F channel is longer than on the wild-type channel.**

Single-channel records are from inside-out patches excised in 1 mM ATP with V_m = -100 mV, filtered at 1 kHz. Expanded traces at right are taken from the region indicated by the short bar above the unexpanded trace. The horizontal line represents the closed level. (a) Wild-type CFTR, with 200 μM DPC added to the cytoplasmic side of the patch. Open-channel block by DPC causes brief closures. (b) T1134F mutant, with 200 μM cytoplasmic DPC. Note the subconductance state, indicated by an asterisk, which does not show the short DPC-induced closed times. (c) Representative closed-time histogram for the unblocked T1134F channel. (d) Representative closed-time histogram for T1134F with 50 μM DPC added to the cytoplasmic side. Note the greater number of longer closed times with DPC present, as compared to (c). Mean values for time constants are given in Table 2.

Figure 7. **Mean open time decreases with increasing DPC concentration.**

Single-channel traces are shown for T1134F mutants, from inside-out patches excised in 1 mM Mg-ATP plus DPC. A-E: 0, 20, 50, 100, and 200 μM DPC respectively. Patches are clamped at V_m = -100 mV. The horizontal line represents the closed level for each trace. Note that the frequency of brief closures increases with DPC concentration, while the closure duration is unchanged. For 0, 20, 50, and 100 μM DPC, at right are open-time histograms from representative patches, fit with single exponentials. Note that the mean open time decreases with increasing [DPC]. The bin from 0 to 1 ms is not shown. The maximum values for the ordinates in each histogram are: for 0 μM, 675 events detected; 20 μM, 2400; 50 μM, 2600; 100 μM, 7500. Mean values for open- and closed-time constants are given in Table 2. Block by 200 μM DPC produce flickers that were too rapid for quantitative analysis; however, the data show a qualitative trend toward further decreases in open time.

Figure 8. **Further kinetic analysis of the data for DPC blockade of T1134F.**

Hollow circles, $1/\tau$, where τ represents open time. Filled circles, $1/\tau$, where τ represents the second (DPC-induced) closed-time constant within a burst. The horizontal line marks the average of $1/\tau_{c2}$ for 20, 50, and 100 μM DPC. Note that $1/\tau_o$ increases with [DPC], while $1/\tau_{c2}$ is constant, as predicted by the bimolecular scheme given in the text. The DPC off-rate, k_{off}, is given by $k_{off} = 1/\tau_{c2} = 560\ sec^{-1}$. Also $1/\tau_o$ increases with [DPC] at a rate $k_{on} = 6.4 \times 10^6\ M^{-1}sec^{-1}$. The equilibrium DPC dissociation constant $K_D = k_{off}/k_{on} = 88\ \mu M$ at $V_m = -100$ mV.

Figure 9. **Model of DPC binding within the pore of CFTR.**

(a) Structure of DPC in vacuum. (b) Model of DPC interactions with TM-6 (left) and TM-12 (right). TM-6 and TM-12 are modeled as α-helices based on the interactions of DPC with the highlighted residues (see text). Highlighted residues in TM-6 are K335 and S341. Highlighted residues in TM-12 are T1134 and S1141. DPC is shown between the two transmembrane domains; the carboxyl moiety is nearly parallel to and on the other side of the lower phenyl ring, adjacent to S341. External face of the membrane is towards the top of the picture. (c) Same as (b), with mutations K335F and T1134F highlighted. Note that K335F lies parallel to the second phenyl ring of DPC and T1134F lies perpendicular. We do not exclude the possibility that DPC might also bind in the reverse orientation, with phenyl rings extending towards the intracellular side from S341. We assume that transmembrane domains other than TM-6 and TM-12 also contribute to the pore, and would lie in front of and behind the plane of the picture. Red, oxygen; light blue, carbon; dark blue, nitrogen; white, hydrogen; yellow, sulfur.

Figure 10. **Sequence alignment of CFTR TM-6 and TM-12 with the M2 region of the rat glycine receptor alpha subunit.**

Shading indicates similar residues; boxes highlight serine and threonine residues. Numbers label the first (left) and last (right) residues, from N to C terminal, in each transmembrane domain. The N-terminal ends are extracellular for TM-6 and TM-12, intracellular for the glycine receptor M2 (Grenningloh et al., 1987).

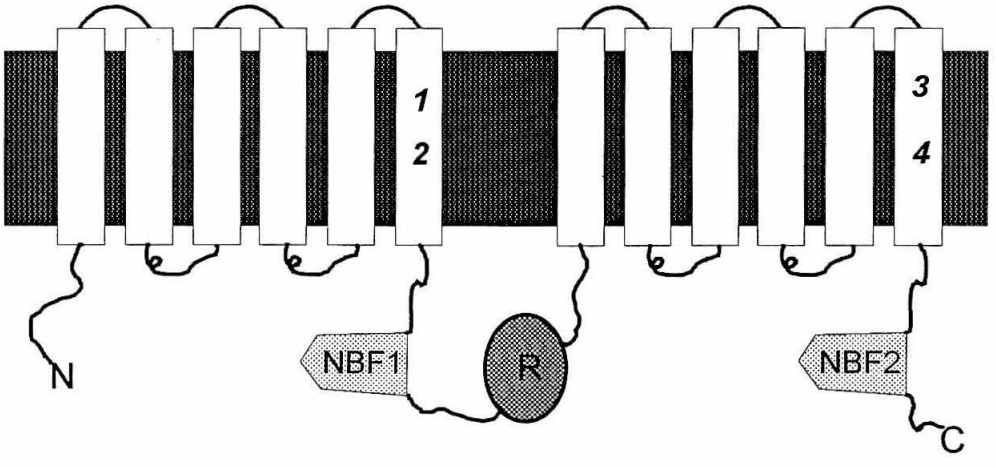

Figure 1

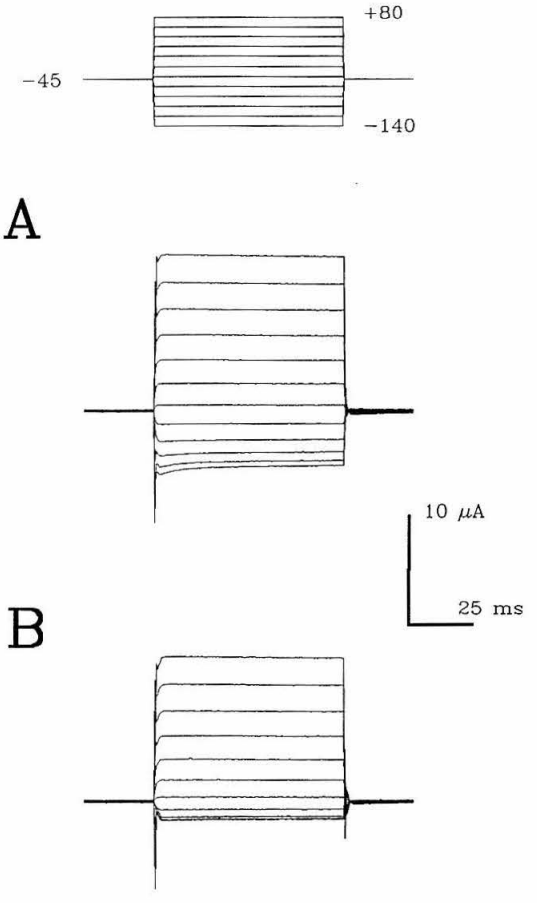

Figure 2

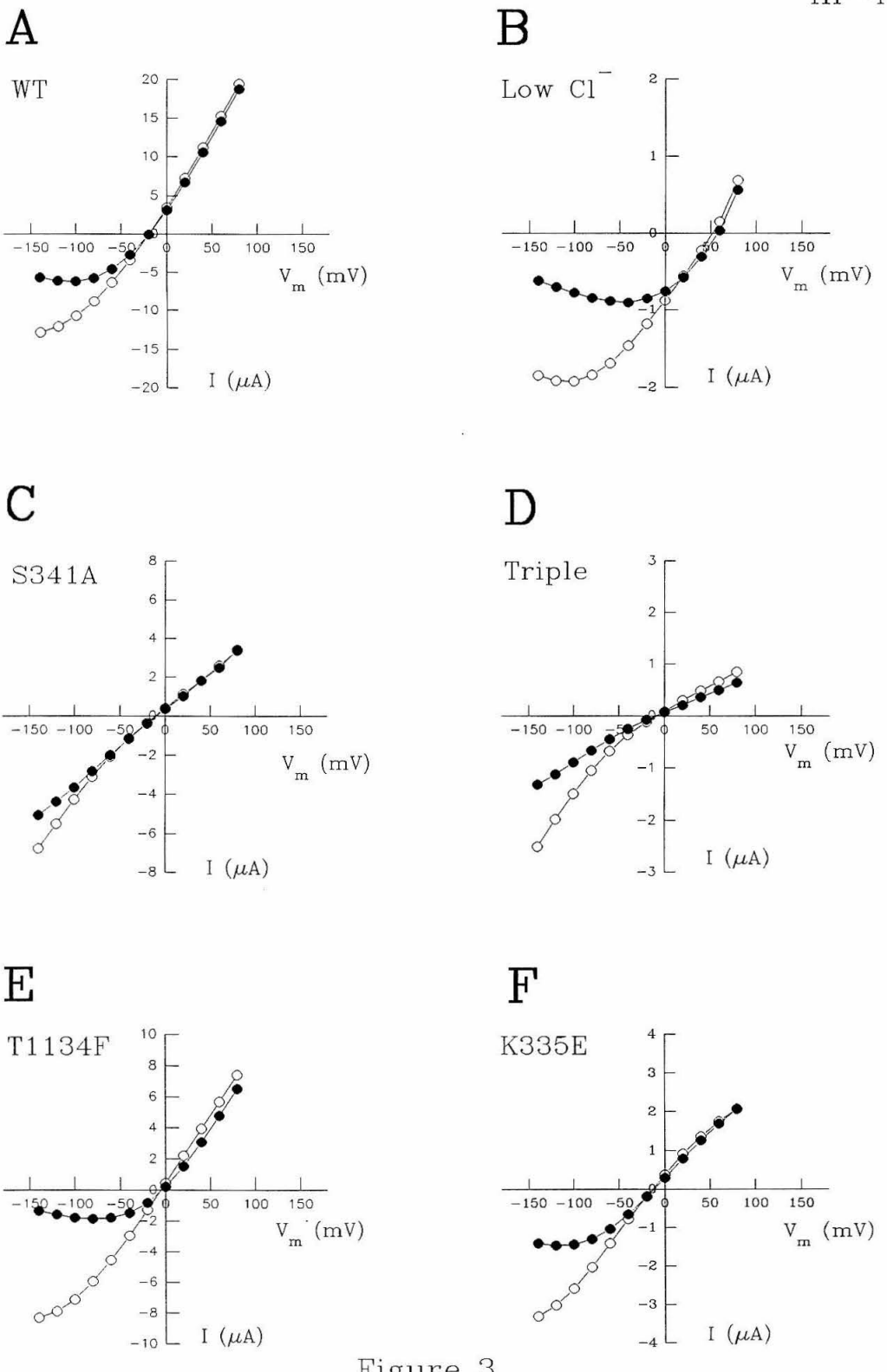

Figure 3

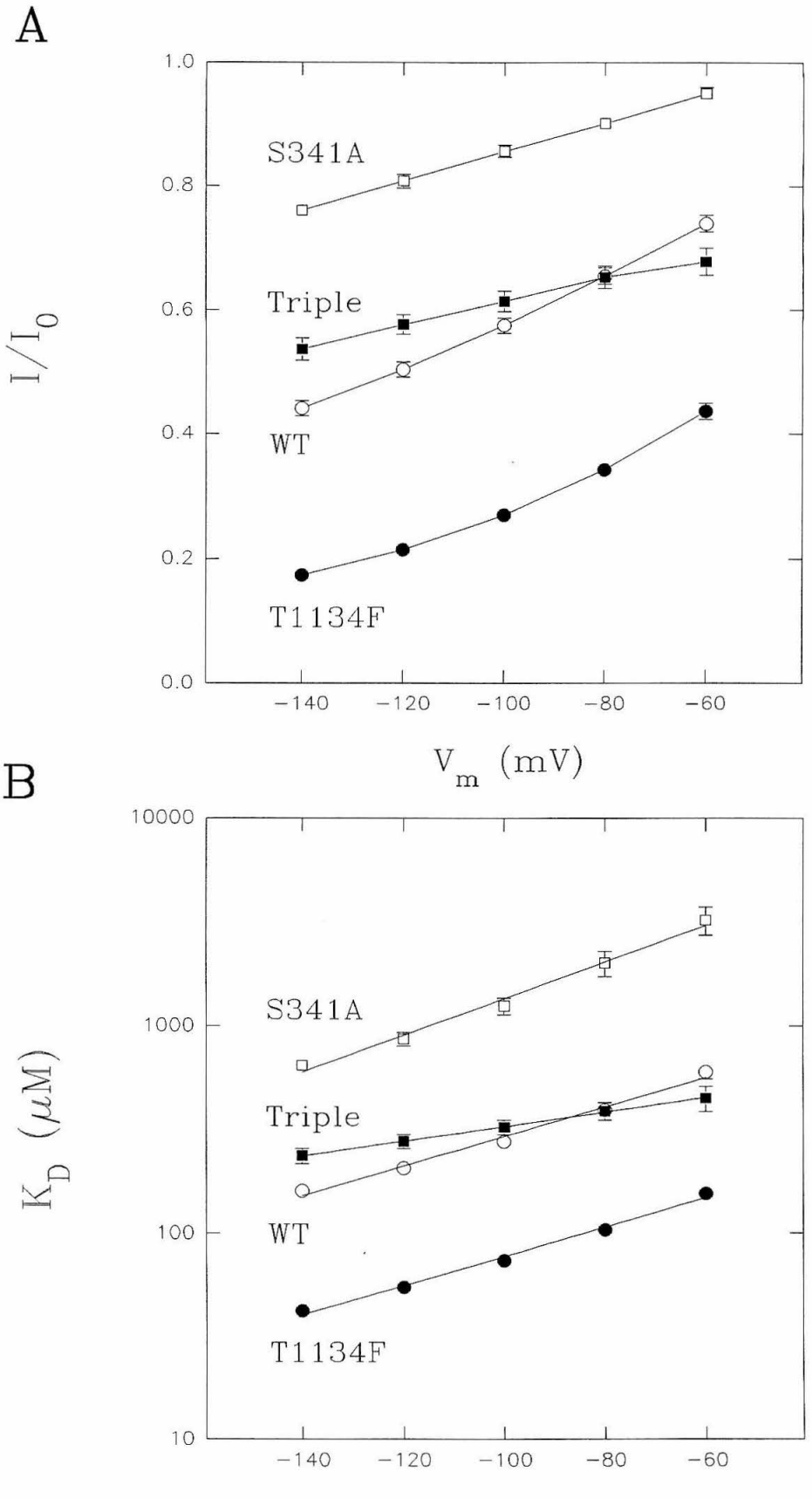
A
1.0
0.8
0.6
0.4
0.2
0.0
I/I0
S341A
Triple
WT
T1134F
−140
−120
−100
−80
−60
Vm (mV)
B
10000
1000
100
10
KD (μM)
S341A
Triple
WT
T1134F
−140
−120
−100
−80
−60

Figure 4

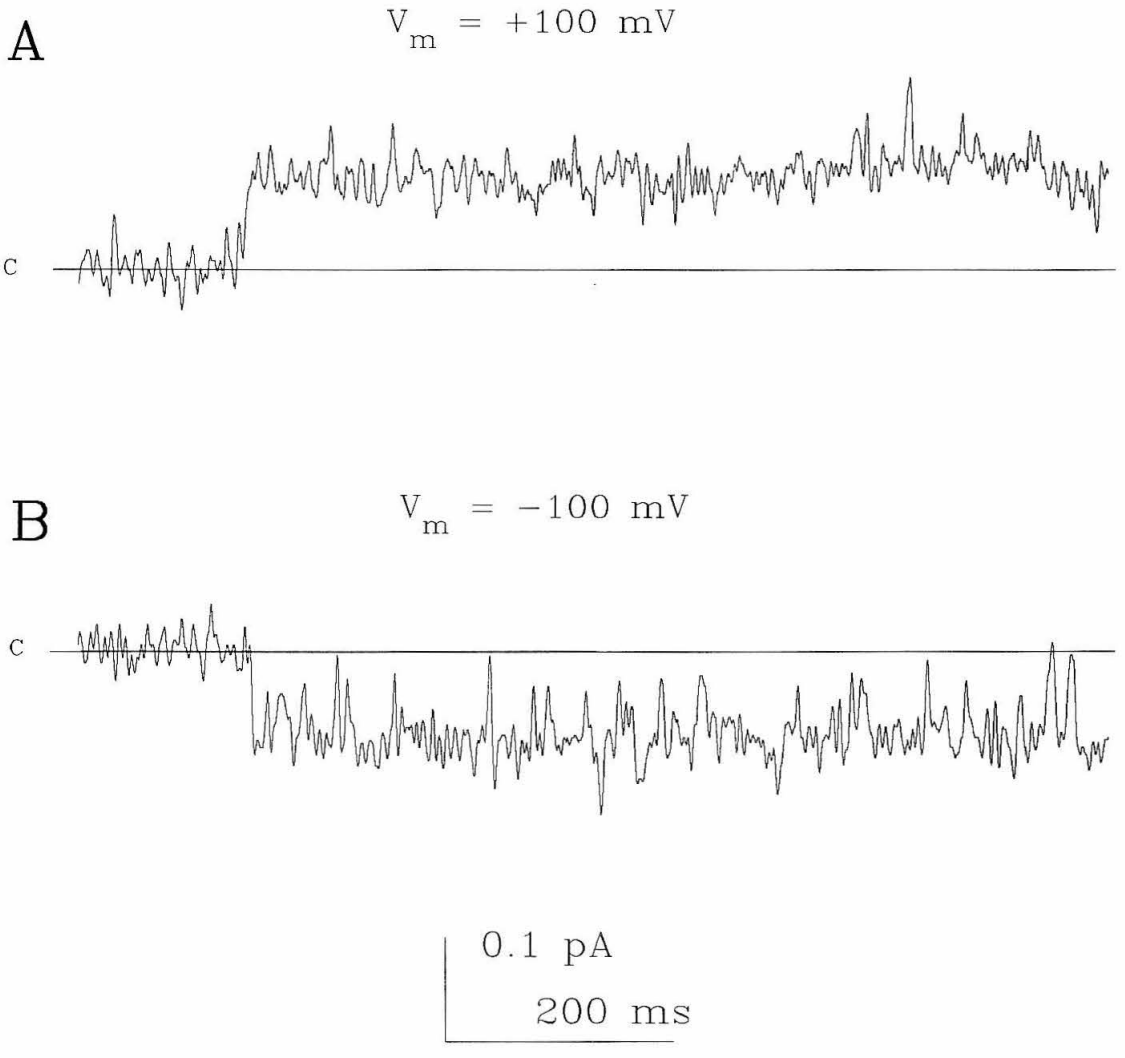

Figure 5

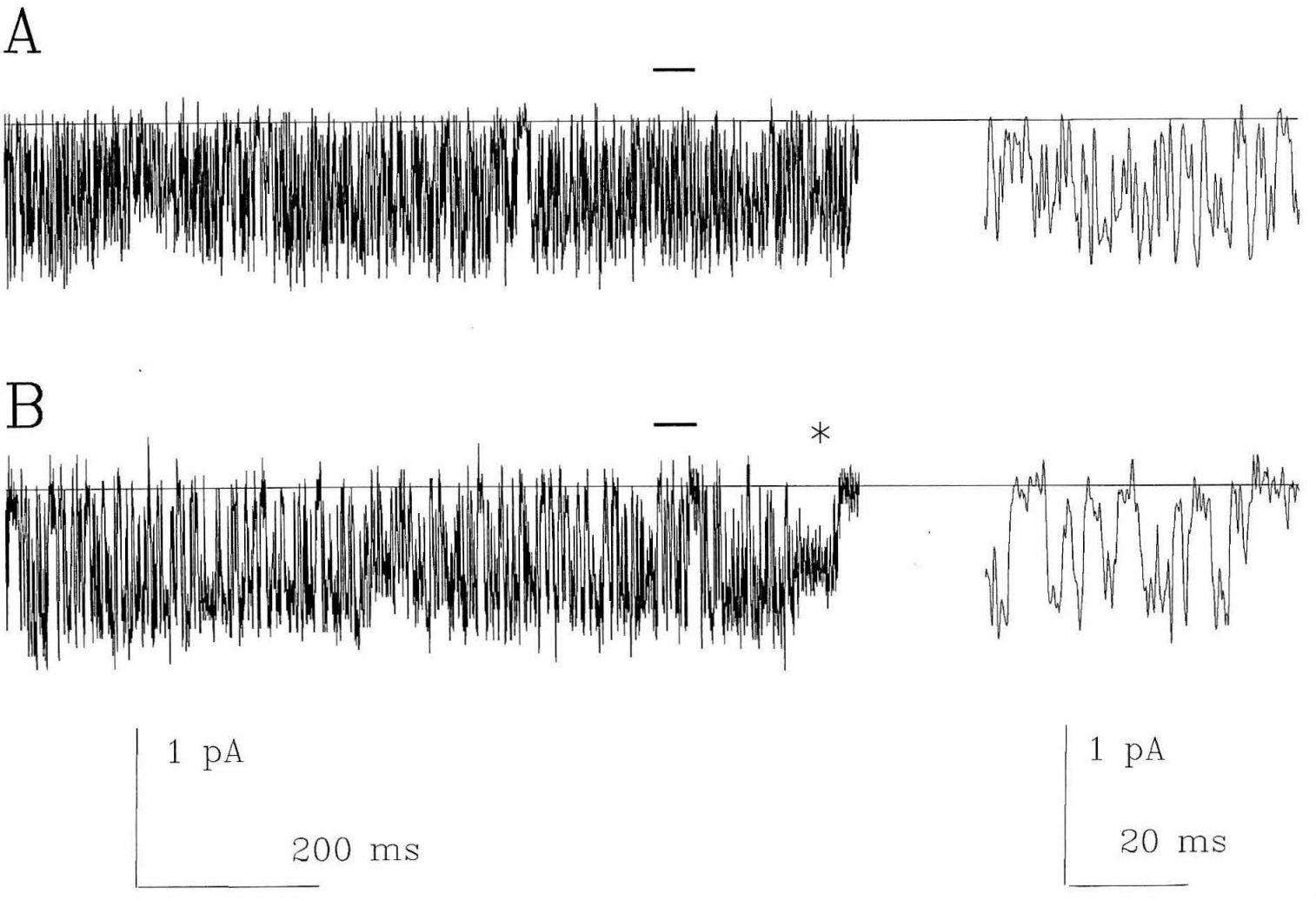

Figure 6 part I

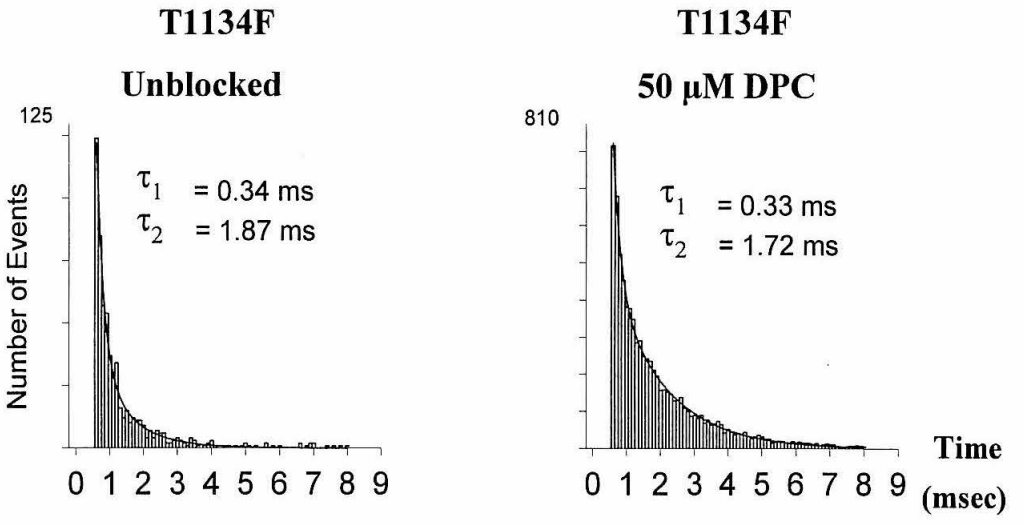

Figure 6 part II

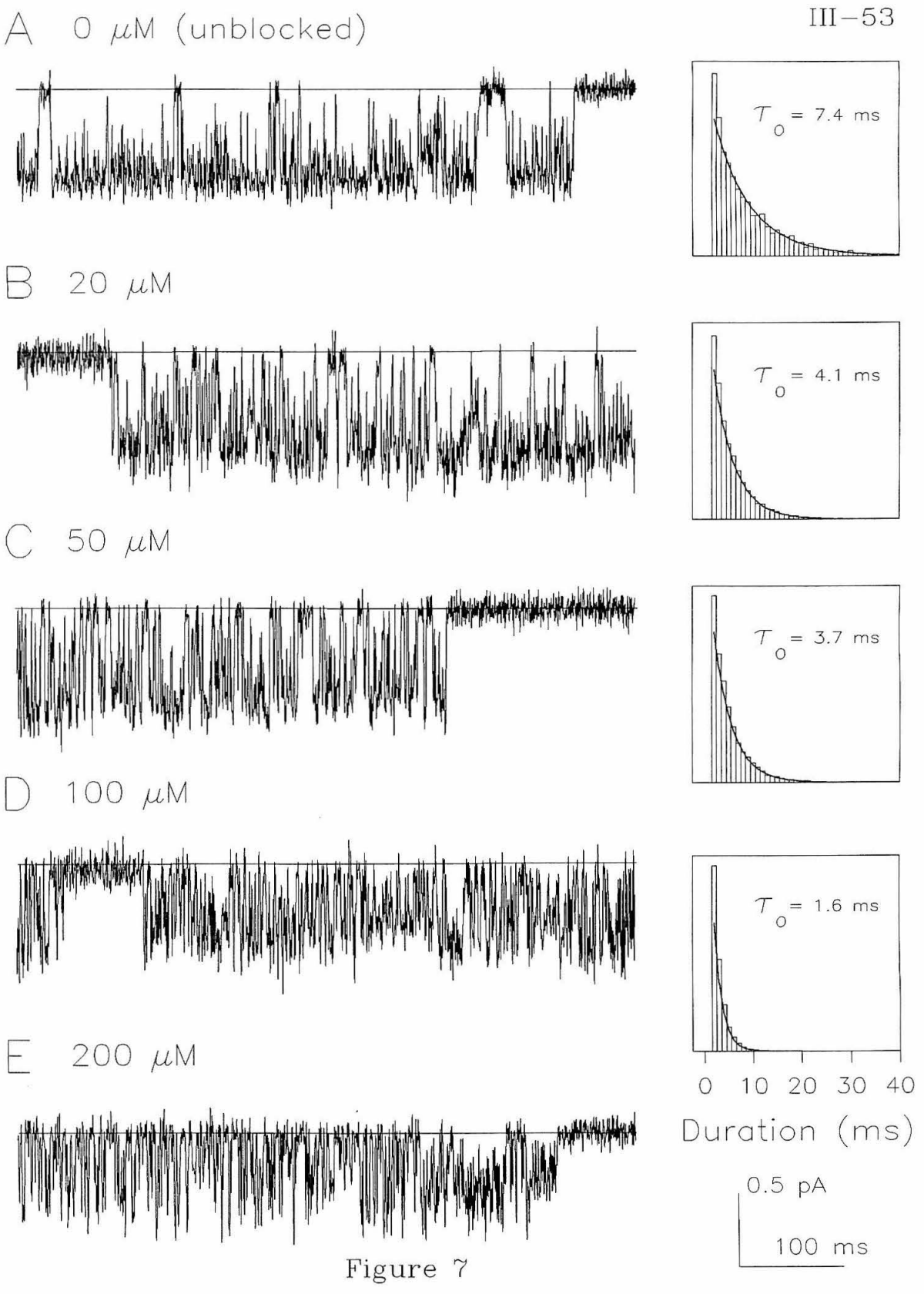
A 0 μM (unblocked)
τ0 = 7.4 ms
B 20 μM
τ0 = 4.1 ms
C 50 μM
τ0 = 3.7 ms
D 100 μM
τ0 = 1.6 ms
E 200 μM
0 10 20 30 40
Duration (ms)
0.5 pA
100 ms

Figure 7

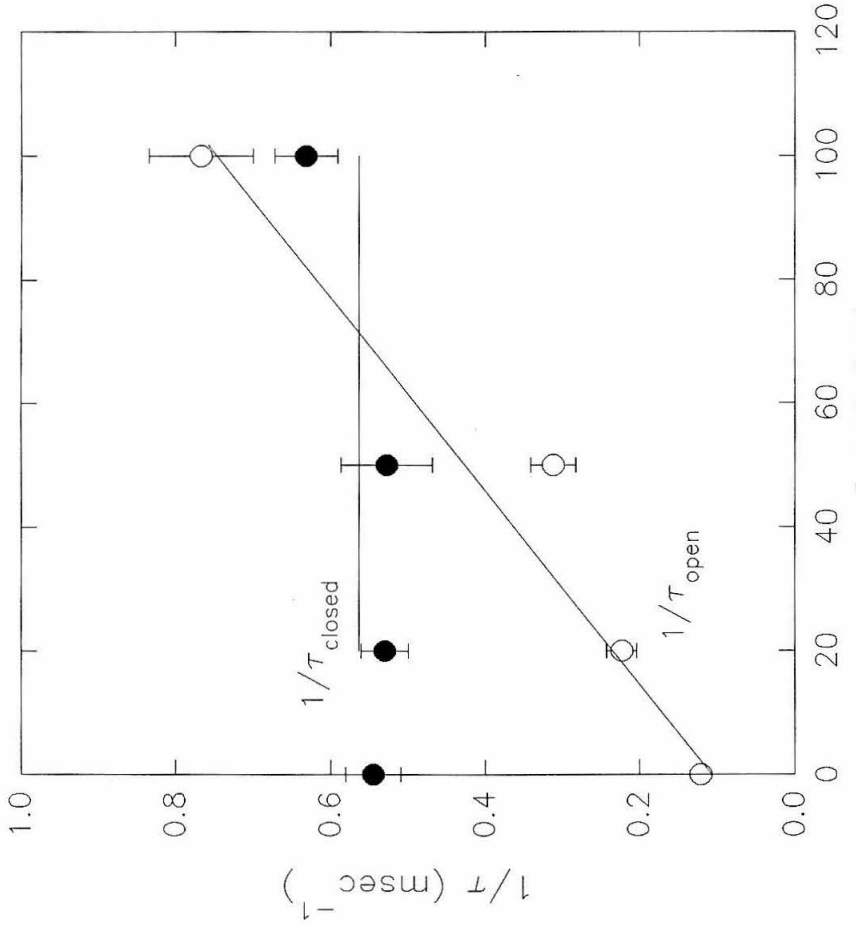
1.0
0.8
0.6
0.4
0.2
0.0
0
20
40
60
80
100
120
1/τ (msec⁻¹)
[DPC] (μM)
1/τ closed
1/τ open

Figure 8

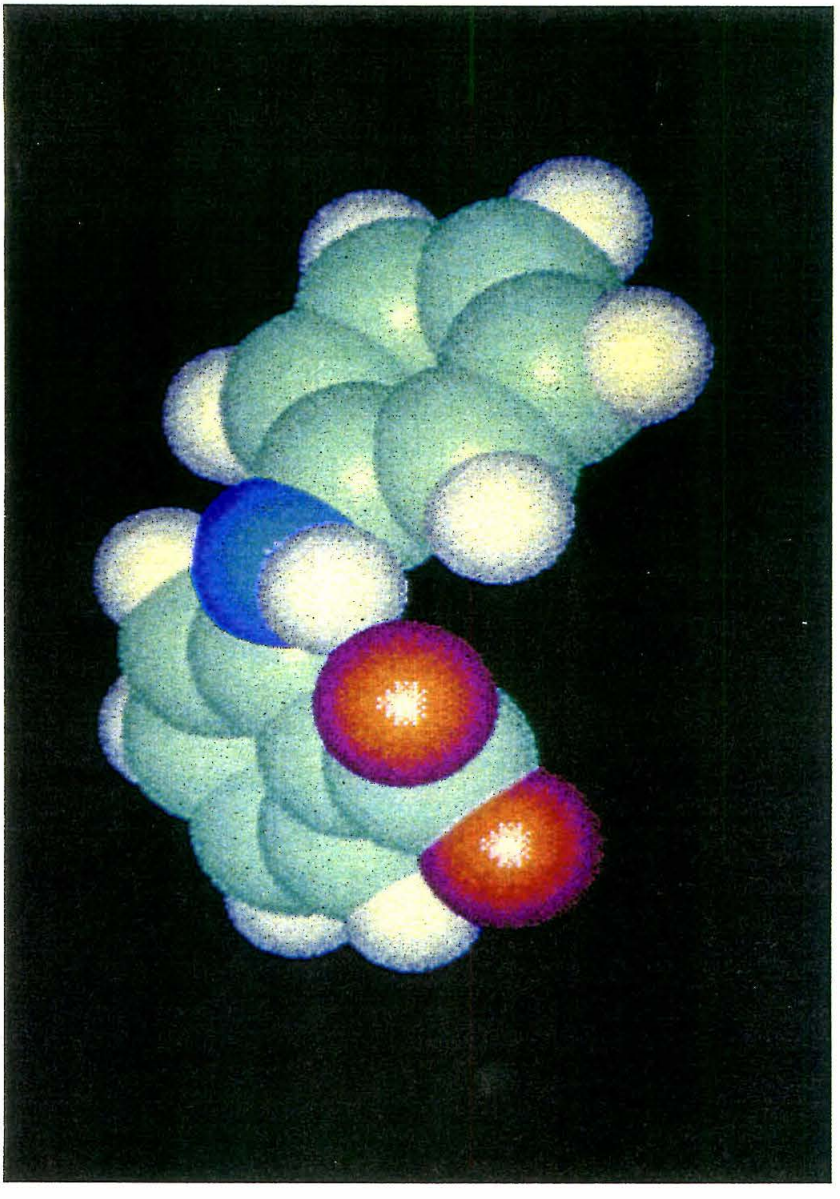

Figure 9 part I

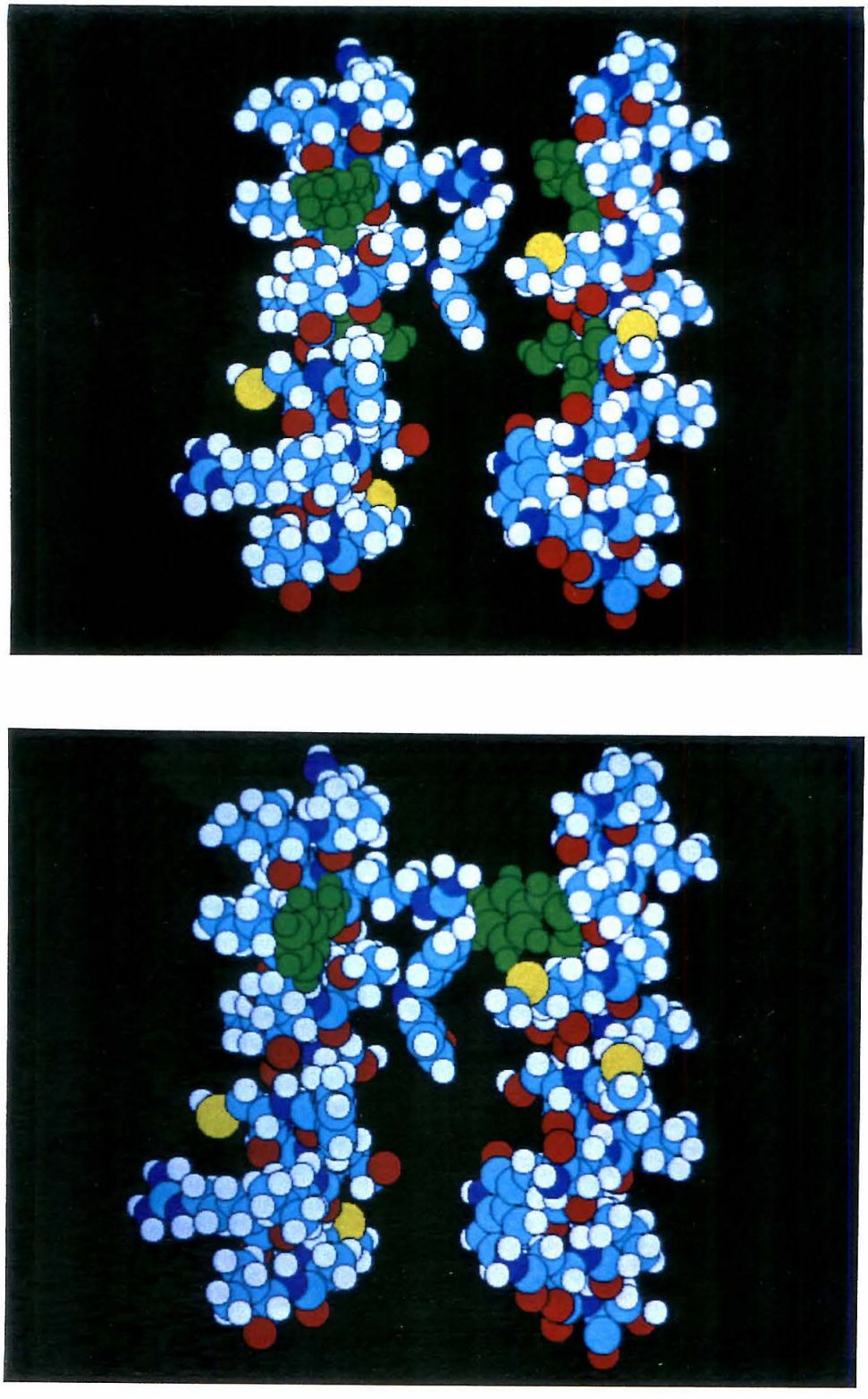

Figure 9 part II

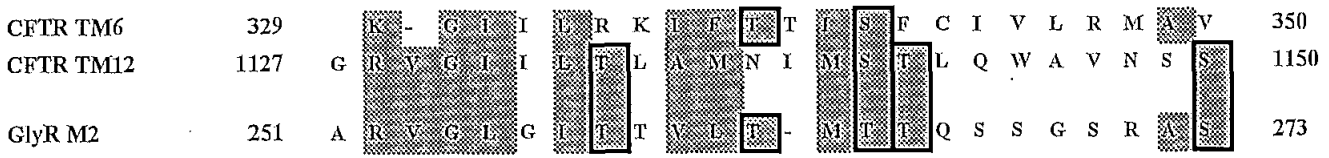
CFTR TM6 329 K - G I I L R K L F T T F S F C I V L R M A V 350
CFTR TM12 1127 G R V G I I L T L A M N I M S T L Q W A V N S S 1150
GlyR M2 251 A R V G L G I T T V L T - M T T Q S S G S R A S 273

Figure 10

Further Mutations

Stefan McDonough, Nael A. McCarty, Norman Davidson, and Henry A. Lester

Division of Biology

California Institute of Technology

Pasadena, CA 91125

FFA on the T1134F mutant

As described earlier, the T1134F mutation has an endogenous closed-time constant approximately equal to the lifetime of DPC on the channel. This fact alone would imply that DPC acts not as an open-channel blocker, as suggested by evidence summarized in chapter 3, but to stabilize an endogenous closed state. On the wild-type channel, however, DPC lengthens the closed times well beyond the endogenous times. And θ, the DPC binding site, is identical for the wild-type and for the T1134F mutant. To be consistent with all the data, a stabilization mechanism suggests that the mechanism of DPC block is totally different for T1134F and the wild-type channels.

Nevertheless, in a further effort to separate the endogenous time constant from the blocker-induced time constant, the effect of FFA on the T1134F channel was assayed. The lifetime of FFA on the wild-type channel is ≈ double that of DPC. Thus, it was hoped that FFA would have a correspondingly higher affinity than DPC for the T1134F channel, and give a clear third time constant to the closed time distribution. This would further prove that the similarity between the endogenous second closed time constant and the DPC-induced closed time constant is coincidental.

T1134F single-channels were excised into 1mM ATP, with 50 μM FFA in the pipette, and held at V_m = -100 mV (see Figure 1; all methods exactly as in chapters 2 and 3). Unfortunately, FFA blocks T1134F more poorly than it blocks the wild-type channel (n = 3). The off-rate is slightly less than for the

wild-type channel (τ_{c2} = 1.6 ± 0.04 msec; WT τ_{c2} = 1.41 ± 0.12 msec), but the on-rate is significantly lower (τ_o = 4.3 ± 0.2 msec; WT τ_o = 2.4 ± 0.1 msec). The model of blocker binding in chapter 2, Figure 9, applied to FFA, would place the trifluoromethyl group of FFA next to T1134. It is not surprising, therefore, that FFA cannot access its binding site on the T1134F mutant as easily as on the wild-type channel. Although this result failed to separate the endogenous and the blocker-induced time constants of T1134F, it further implicates T1134 as a pore-lining residue.

Mutations in transmembrane domain 11

It is extremely unlikely that only two TM domains, 6 and 12, form the pore of a monomeric CFTR. More likely, CFTR is a multimer, or else other transmembrane domains contribute to the monomeric pore. A multimeric pore could also involve TM domains other than 6 and 12. To address the possibility of additional pore-lining TM domains, the same strategy was used as for the "triple" mutation in TM-12 that restored DPC binding to the S341A mutant. In TM-12, the I-S-F sequence could bind DPC in the absence of S341. The same approach was taken with TM-8 and TM-11: the mutations V922I-A923S-D924F ("trip-8") and F1111-I1112S-A1113I ("trip-11") were subcloned into the pAlter-CFTR/S341A cassette using *Nco-I* and *Hpa-I* restriction enzymes. The resulting constructs are termed "trip-8/ S341A" and "trip-11/ S341A." Below is a sequence alignment of TM-6 with TM-8 and TM-11.

	extracellular	intracellular
TM-6	N-^{330} G I I L R K I F T T ***I S F*** C I V L R M A V^{350}-C	
TM-11	C-^{1123}G T T L I ***S*** I F T V ***A I F*** F I V F I M E I^{1103}-N	
trip-11	C-^{1123}G T T L I S I F T V ***I S F*** F I V F I M E I^{1103}-N	
TM-8	N-^{912} S Y Y V F Y I Y V G ***V A D*** T L L A M G F F^{932}-C	
trip-8	N-^{912} S Y Y V F Y I Y V G ***I S F*** T L L A M G F F^{932}-C	

Trip-8/ S341A did not express, though RNA of the proper length was synthesized and injected (data not shown). Trip-11/ S341A did express; whole-cell currents showed the inward rectification characteristic of S341A (Figure 2). The DPC block, however, was intermediate to wild-type and S341A, giving an inconclusive result. At V_m = -100 mV, K_D = 583 ± 30 μM, and θ = 0.26 ± 0.02 (n = 5; see chapter 3, Table 1 for comparison to wild-type, S341A, and S341T). Note that this K_D is similar to that of S341T; this may indicate that in the trip-11/ S341A mutation, DPC can access a binding site in TM-11, but that the serine of the new binding site (presumably I1112S) is not perfectly situated to bind DPC. In addition to the inconclusive value for the K_D, the low value for θ implies that the voltage-dependence of DPC block has been weakened. In the absence of a strong change in affinity, this further complicates interpretation. Another mutation was constructed to test the involvement of TM-11.

In TM-12, the T1134F mutation gave a significant increase in DPC

binding affinity, yet no change in the binding site θ. Therefore, an analogous mutation, S1118F, was constructed in TM-11. Intriguingly, the S1118F mutation gave voltage-dependent current relaxations, the only mutant constructed to do so (Figure 3). The S1118F mutation also changed the voltage-dependence of DPC block, while the overall affinity of S1118F for DPC was roughly unchanged from wild-type: K_D (-100 mV) = 266 ± 13 μM, θ = 0.27 ± 0.01. If TM-11 is α-helical, mutation S1118F would place three phenylalanine residues in close proximity to each other, at positions 1107, 1111, and 1118. To see if these three phenylalanines were responsible for the current relaxations, the double mutation S1118F-F1111S was constructed. Unfortunately, this mutation also displayed current relaxations of approximately the same time constants (Figure 3). Note that currents from the S1118A mutation (see Chapter 3, Table 1) were time-independent. This suggests that it is the presence of phenylalanine, not absence of serine, that causes the relaxations. The basis for the current relaxations is still unclear.

The site-directed mutations constructed in TM-8 and TM-11 did not give conclusive data about pore-lining domains in addition to TM-6 and TM-12. However, some effects were seen, and the S1118F mutation is the only CFTR mutation ever reported to display time-dependent currents. Further experiments might investigate the single-channel basis of the relaxations, or test the oligomerization state of CFTR by fusing the cytoplasmic N- and C- terminii to make an artificial dimer.

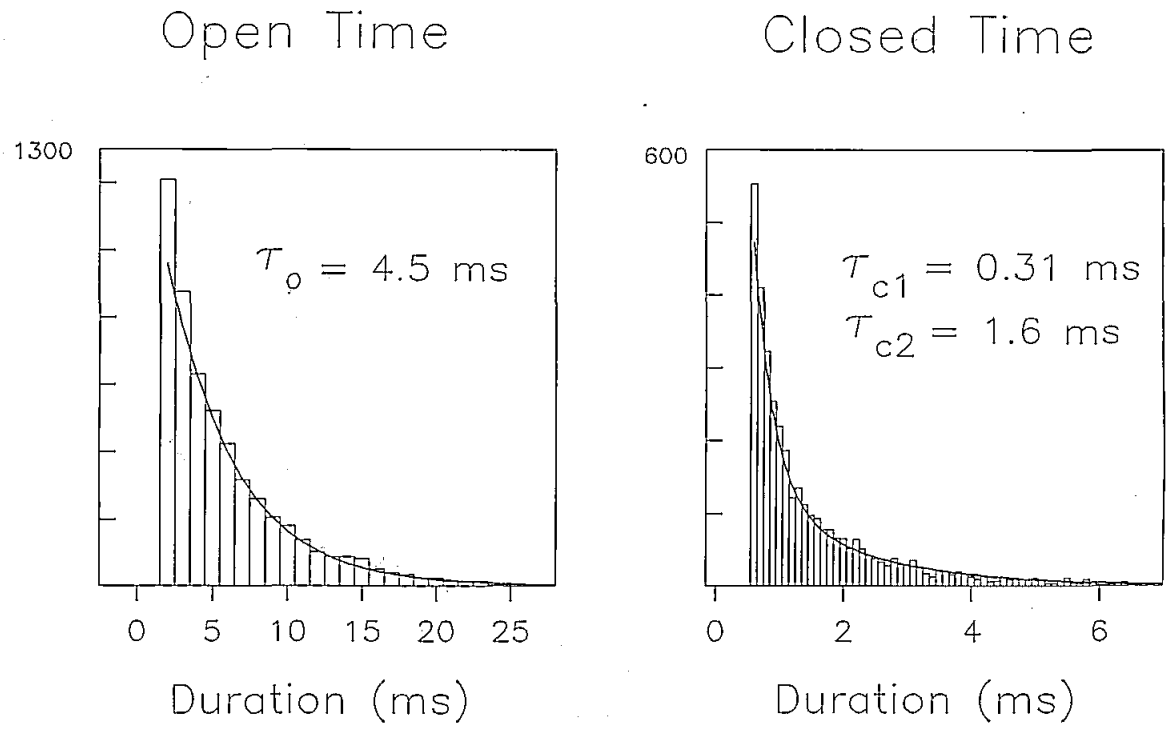
Open Time
1300
τ_o = 4.5 ms
0
5
10
15
20
25
Duration (ms)
Closed Time
600
τ_{c1} = 0.31 ms
τ_{c2} = 1.6 ms
0
2
4
6
Duration (ms)

Figure 1

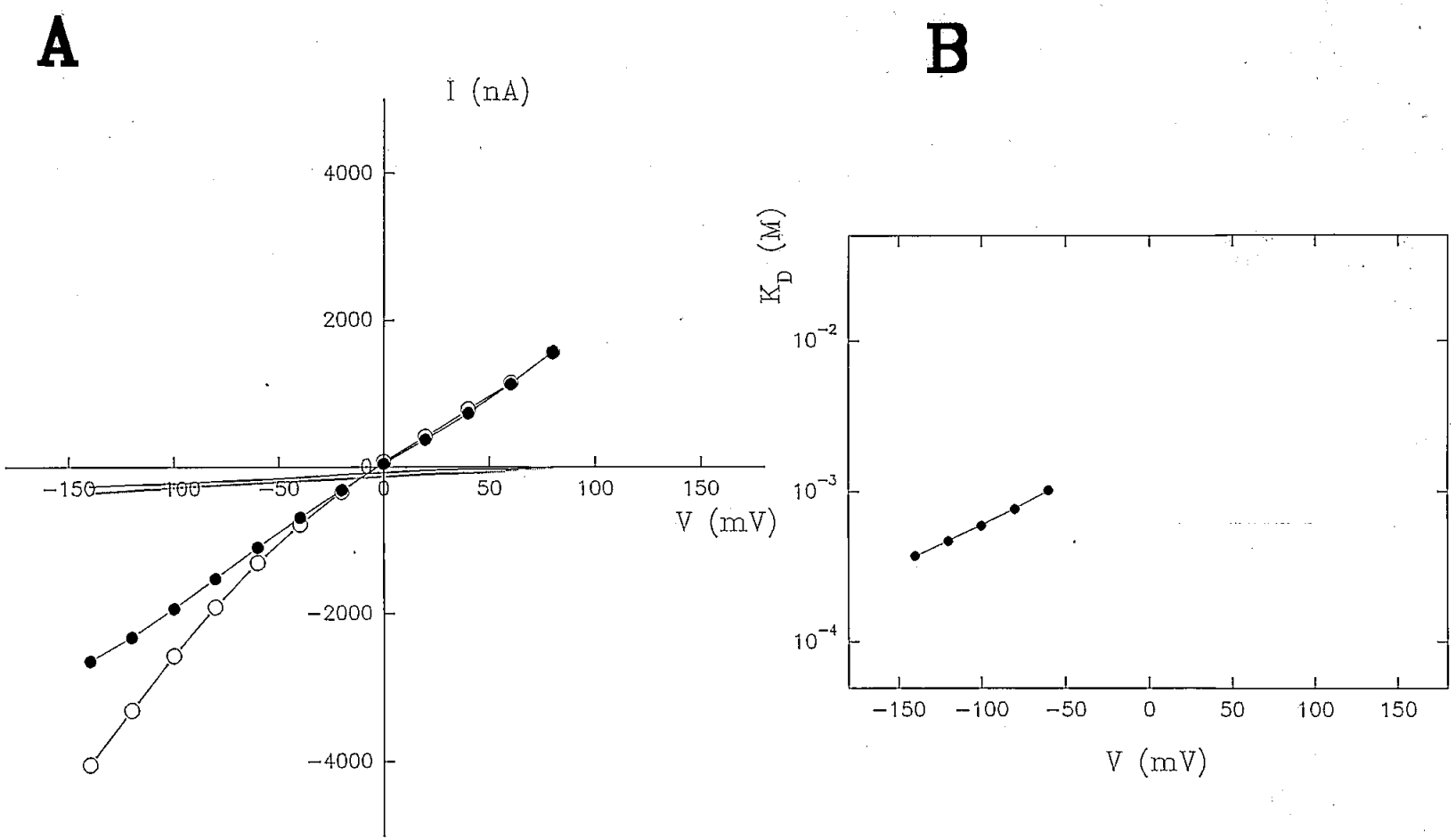
A
I (nA)
4000
2000
-2000
-4000
-150
-100
-50
0
50
100
150
V (mV)
B
K_D (M)
10^{-2}
10^{-3}
10^{-4}
-150
-100
-50
0
50
100
150
V (mV)

Figure 2

S1118F

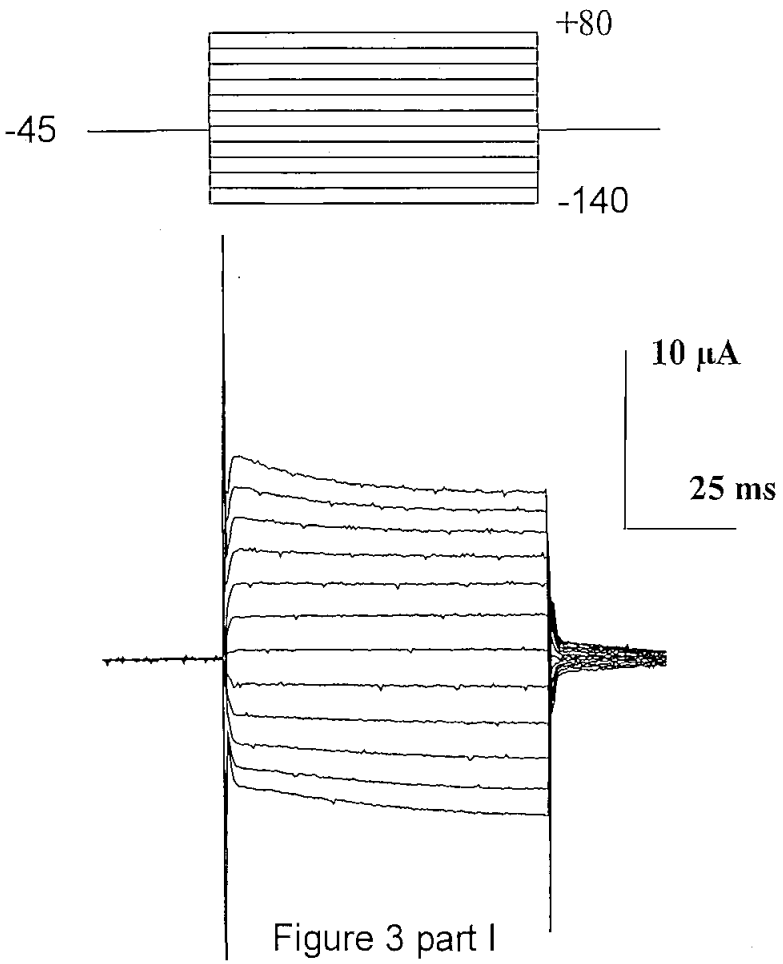

Figure 3 part I

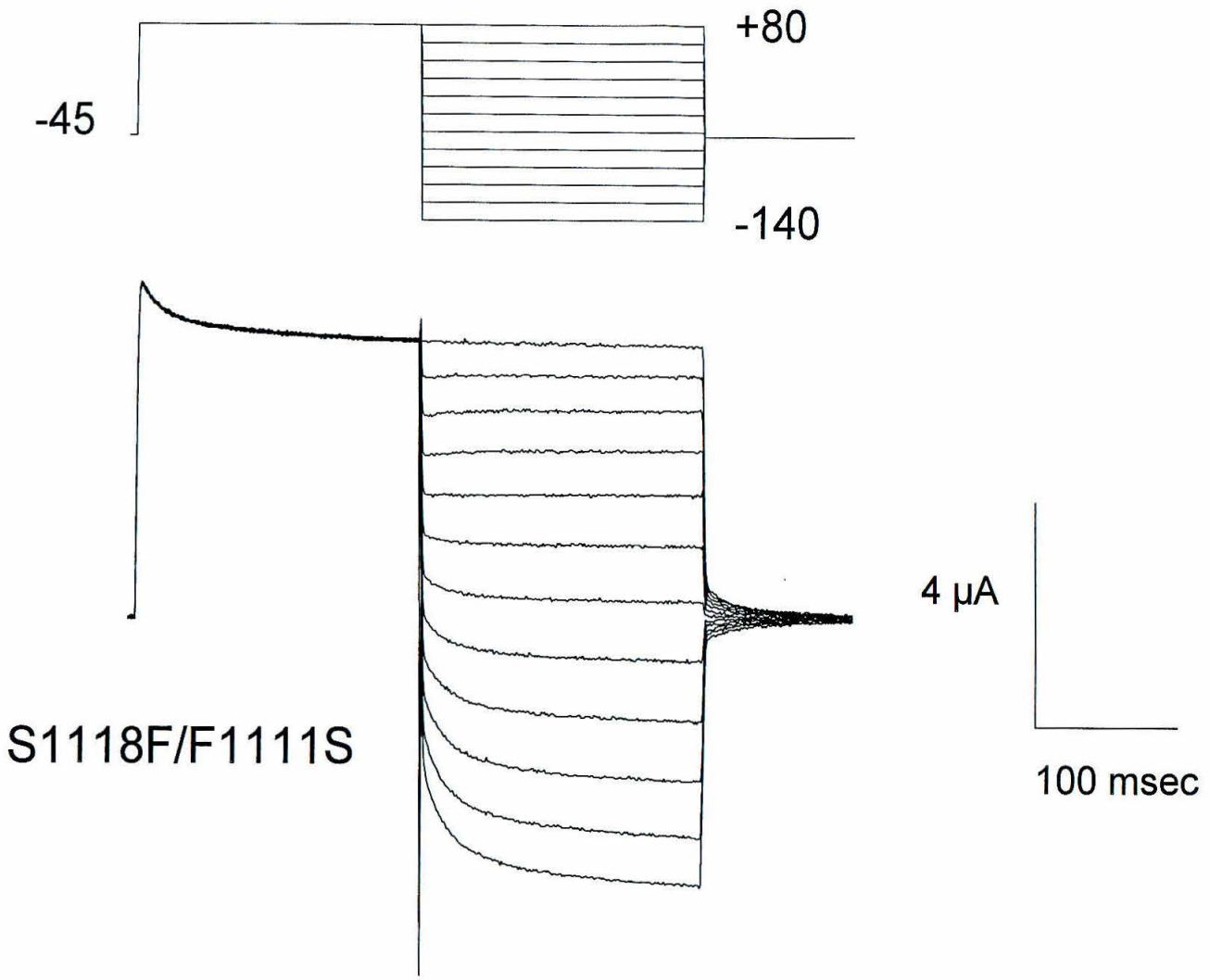

Figure 3 part II